SGC-180025

GCOM-C "SHIKISAI"
Data Users Handbook

First Edition

December, 2018

Preface

As the global environment change has become a worldwide concern such as global warming-up progress in recent years, the studies related to climate change prediction are promoted in order to keep environment where future people are able to lead their lives. For elucidating global climate change, weather forecasting, water circulation mechanisms, JAXA (Japan Aerospace Exploration Agency) is promoting “GCOM (Global Change Observation Mission)” which aims to verify the effectiveness by constructing systems that enable long-term continuous global-scale observations and by utilizing their data to the climate change studies, weather forecasting, and fishing industry.

GCOM is consisting of the two series of observation satellites: Global Change Observation Mission-water (GCOM-W) and Global Change Observation Mission-climate (GCOM-C). GCOM-W “SHIZUKU” was launched on May 18, 2012, and is now continuing observation operation with AMSR2 (Advanced Microwave Scanning Radiometer 2) on board. Subsequently, GCOM-C “SHIKISAI” was launched on December 23, 2017, and the initial checkout operation for three months after launch was completed and is continuing observations SGLI (Second-generation Global Imager) on board.

SGLI mounted on GCOM-C is the succession sensor of the Global Imager (GLI) mounted on ADEOS-II (MIDORI II) and is the imaging radiometer which measures the radiation from near-ultraviolet to thermal infrared region (380 nm-12 μm) in 19 channels. Global observation of once for approximately every two days is possible at mid-latitude near Japan by observation width at ground greater than 1,000 km. In addition, SGLI realizes high resolution than the similar global sensor and has a polarized observation function and a multi-angle observation function.

The observation data by SGLI is transmitted to JAXA/Tsukuba Space Center via online after downlinked to ground stations (JAXA domestic stations in Japan and Svalbard Station) and data processing and provision is performed. 28 types of geophysical variable data set (vegetation/ biomass, sea surface temperature, ocean-color, aerosol, cloud characteristics, snow-ice characteristics, etc.) covering land, atmosphere, ocean and cryosphere are generated by the SGLI global observation data.

JAXA performs Initial calibration and validation of SGLI observation data, and Level1 products (radiance) and Level2 & Level3 products (geophysical variable) will be released to the public via Globe Portal system (G-Portal：https://gportal.jaxa.jp/gpr/) in December 2018.

This handbook intends to provide the necessary information for using GCOM-C/SGLI product. We hope that effectiveness of these data are demonstrated in fishery and weather prediction, as well

as contribute to solve the global environmental change mechanism and climate change impact, monitoring of global environmental change and environmental preservation.

December 2018
Japan Aerospace Exploration Agency
GCOM Project Team

GCOM-C "SHIKISAI" Data Users Handbook
Contents

List of Tables and Figures

Chapter 1**Introduction**

Melting glacier and ice sheet in polar region, extraordinary high temperature and super typhoon that take a heavy toll of lives, expansion of infectious diseased areas such as dengue fever…today, the global warming has been seriously progressing and changes in the global environment that have never been experienced are observed. The average global temperature has risen by about 1°C over the past 30 years, and concerns are being raised about a further rise in the future. However, it is difficult to forecast the future climate and current temperature projections for the year 2100 are uncertain and vary in a range of approximately 2°C. The reasons for uncertainty in the forecasts are that the sensitivity and the mechanism of the climate system are still unknown. "Radiation budget" and "carbon cycle" are the factors that have a particularly large impact on climate.

Through continuous and long-term observations of radiation budget and carbon cycle, we can derive quantitative relationships between the fluctuations of these elements and climate change, making it possible to predict their impact on the climate.

GCOM-C (Global Change Observation Mission – Climate "SHIKISAI"), the climate change observation satellite developed by JAXA(Japan Aerospace Exploration Agency), conducts long-term global observations of geophysical variables related to the global climate system across 28 items including aerosol and vegetation over 4 areas of atmosphere, land, ocean, and cryosphere. The data will be used to contribute to higher accuracy of global warming prediction.

1.1 **Purpose of This Document**

This document provides users who obtain SGLI products publically released by JAXA with the information needed to make effective use of these products. It also gives information related to various products including standard products, GCOM-C satellite, the onboard sensor, and the ground system.

1.2 **Scope of This Document**

This document provides overview of the information necessary for the users including descriptions of the satellite, the sensor, the ground systems, the products and the data providing service. This document includes information that users need to access the data providing service in order to obtain data sets. The document is comprised of five chapters and an annex:

Chapter 1 Introduction
Chapter 2 Overview of GCOM-C/SGLI
Chapter 3 Overview of GCOM-C Ground System

Chapter 4 SGLI Products

Chapter 5 Data Providing Service

Annex — List of Abbreviations, Related Information, SGLI Product Formats

1.3 **Overview of GCOM-C/SGLI Mission**

SGLI (Second-generation Global Imager) is the sensor mounted on GCOM-C satellite. This chapter gives the descriptions of the GCOM concept as a background to the measurement sensor, followed by the descriptions of SGLI.（Source: GCOM-C Climate Change Observation Satellite (Briefing document), (Japanese)）

1.3.1 **GCOM Concept**

The Global Change Observation Mission (GCOM) project was launched for the purpose of conducting global and long-term observations of the earth's environment from space. Its main role is to observe water circulation and climate change, and monitor the earth's health from space. GCOM consists of two series of satellites: GCOM-W (Global Change Observation Mission – Water "Shizuku") and GCOM-C (Global Change Observation Mission – Climate "Shikisai"). The GCOM-C, equipped with the Second-generation Global Imager (SGLI) – a multi-band optical imaging radiometer, conducts observations of clouds, aerosols (atmospheric dust), ocean color, vegetation, snow/ice, and other properties. The GCOM-W, equipped with the Advanced Microwave Scanning Radiometer 2 (AMSR2), conducts observations of precipitation, water vapor, ocean wind speeds, sea surface temperature, soil moisture content, snow depth, and more.

A global and long-term observation by GCOM is expected to help monitor and elucidate the mechanism behind water circulation and climate change. Figure 1-1 shows the development and operation schedules for JAXA earth observation satellites, and Figure 1-2 shows the mission of JAXA's climate and environment observation satellites.

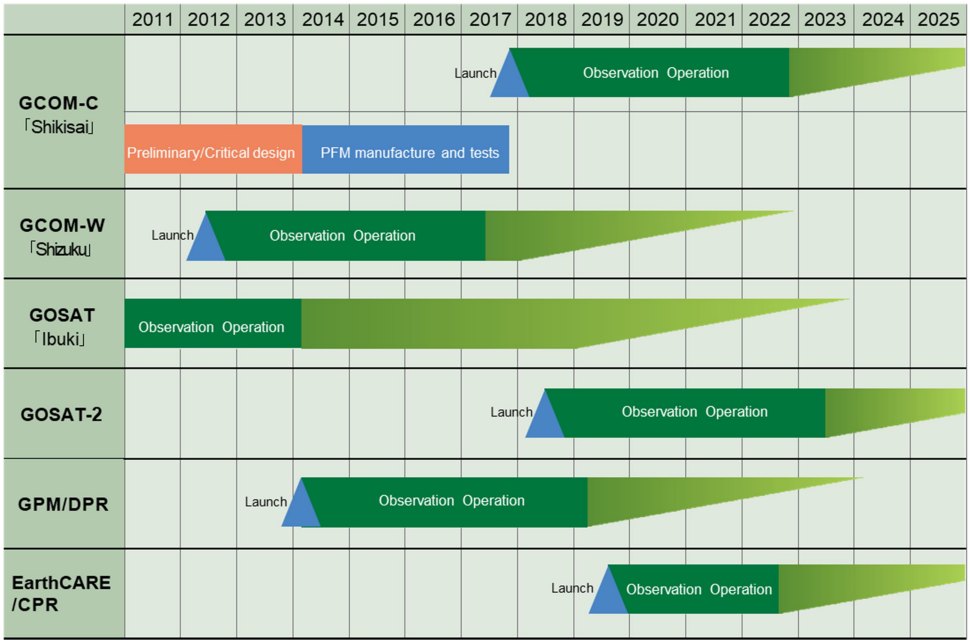

Figure 1-1 Development and Operation Schedule for JAXA Earth Observation Satellite

Because of the earth's massive size, it is difficult for one country to act alone in conducting observations needed to grasp the trends in global environmental changes. Therefore, a coordinated international framework called the Global Earth Observation System of Systems (GEOSS) has been established, under which participating countries are administering their space programs for monitoring the climate and the environment. GCOM is the mission that contributes to GEOSS.

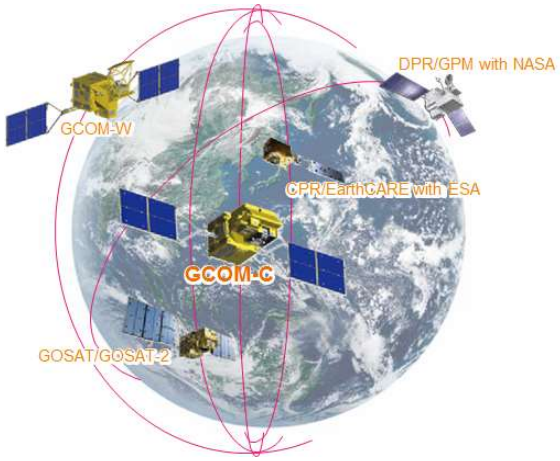

Figure 1-2 Mission of JAXA's Climate and Environment Observation Satellite

1.3.2 **Overview of SGLI Mission**

1.3.2.1 **Radiation Budget: Observation of Aerosol and Cloud**

This section describes the observation of aerosol and cloud in relation to the radiation budget. Aerosol is a collective term for fine solid particles floating in the atmosphere. Aerosols and clouds have a major influence on climate change, but the extent of the influence in regard to global warming is still uncertain. GCOM-C contributes to improve the precision of climate change forecast through its highly accurate, long-term observation of aerosol and cloud.

There are various types of aerosols such as "soot" produced by fossil fuels or forest fire, "sulfuric acid (sulfate)" derived from the emitted gas of fossil fuels, volcanic explosion or marine plankton, "marine salt and yellow sand" blown by wind, and "volcanic ash" and "pollen." PM2.5, which recently became a big topic as it was brought from China in high density and has negative impact on human health, is also a type of aerosol. Those extremely small floats, aerosols, are greatly affecting the global environment in the form of global warning and acid rain.

One of the impacts is "direct effect" that lowers the ground surface temperature as aerosols scatter or absorb the sunlight directly. When the Mt. Pinatubo in Philippines erupted in 1991, a huge amount of microparticulated volcanic ash and volcanic gas became aerosols and formed a "Parasol" that shut off the sunlight. As a result, for over two years, the temperature was lowered by about 0.5 °C globally. At the same time, it is known that the sulfuric acid aerosol carried to the stratosphere destroyed a significant volume of the ozone layer. In this way, aerosol itself has very strong impact.

Another impact is "indirect effect" that aerosols become condensation nucleuses when cloud is formed by moisture. Moisture in the atmosphere becomes water or ice as the temperature decreases and forms cloud particles. At the time, the larger the number of aerosols to be nucleuses, the larger the volume of small cloud particles. When clouds are formed from an equivalent volume of moisture, the cloud color becomes whiter and brighter as the contained cloud particles becomes smaller, and accordingly, the sunlight coming into the earth is reflected well and thus the ground surface temperature is lowered. Just as described, aerosols have the effect to impact on the climate change through cloud formation.

The aerosol direct and indirect effects have a major influence on climate change, but the extent of influence in regard to global warming is still uncertain. This is because expert opinion is still divided on whether clouds, which are changed in characteristic as global warming progresses, will cause the acceleration or deceleration of global warming.. The long-term observation of aerosols and clouds is necessary to get accurate quantification of the influence of aerosols.

In addition to the visible and near-infrared radiometer of other conventional satellites, GCOM-C also combines proprietary near-ultraviolet and polarization observation functions that can provide highly accurate observations of aerosols emitted from human activity,

volcanoes, forest fires and other terrestrial events. All these features will enable long-term global observation of aerosols.

Figure 1-3 shows the aerosol optical thickness observed from NASA's Terra/Aqua satellite in October 2015. The redder the map, the thicker the optical thickness. In Indonesia, a large amount of smoke produced by the large-scale open burning performed every fall causes serious air pollution in neighboring nations (center of the figure). Most of the aerosol emitted through human activity is generated on land and terrestrial aerosol was difficult to observe with a high level of accuracy with conventional satellites.

Figure 1-4 is a bar graph showing the extent of the effect of global warming and cooling caused by greenhouse gases, aerosols and other factors as reported by the IPCC. The estimation of the influence of aerosol still includes a great extent of uncertainty.

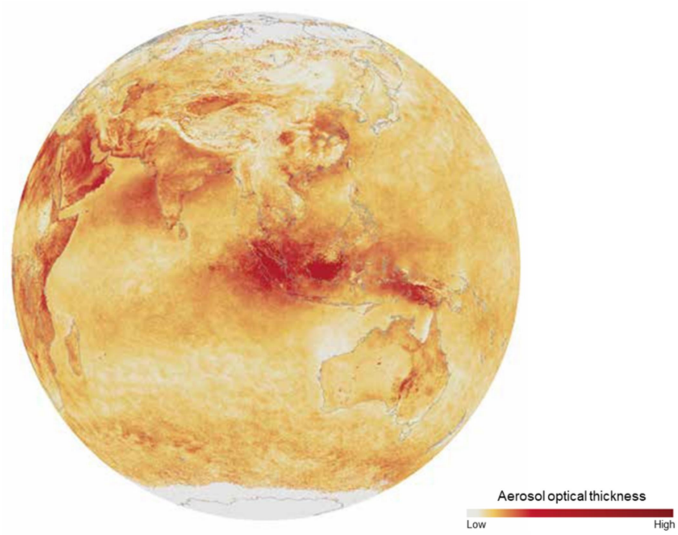

Figure 1-3 Optical Thickness of Aerosol Observed by Terra/Aqua

*Terra/Aqua data was processed at JAXA

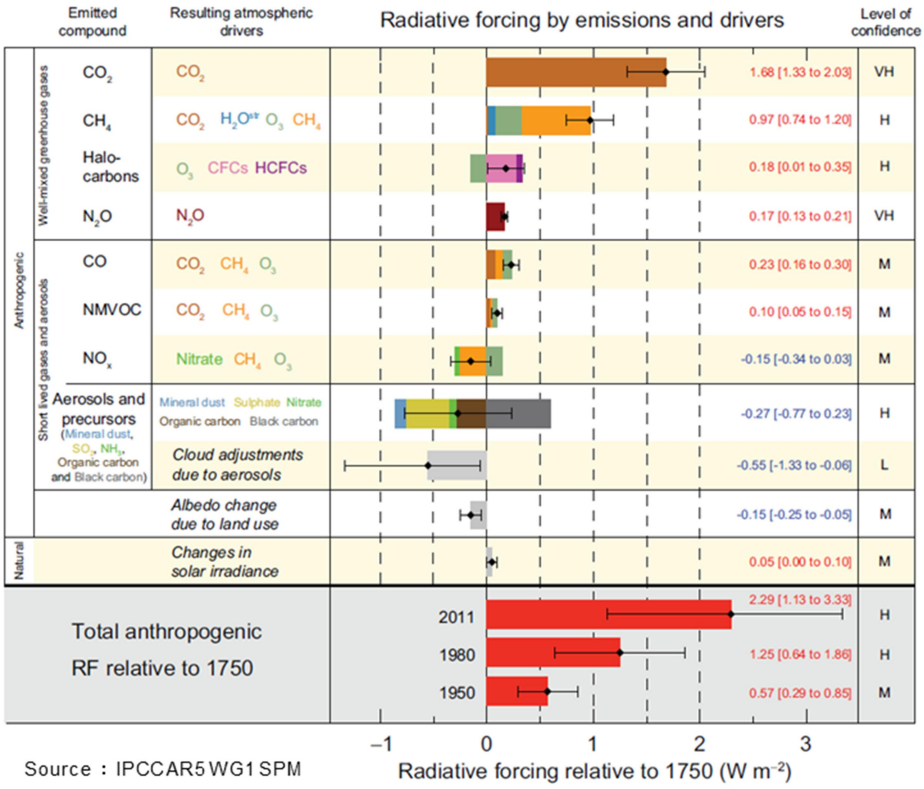

Figure 1-4 Estimated value- and factor-based aggregation of radiative forcing (Source: IPCC AR5 WG1 SPM)

1.3.2.2 **Carbon cycle: Observation of vegetation and sea surface temperature**

This section describes the observation of vegetation and sea surface temperature in relation to the carbon circulation. CO_2 is regarded as the primary contributor to global warming. Although vegetation and sea surface temperatures are said to greatly add to the concentration of carbon dioxide to the atmosphere, accurately estimating the extent of absorption of both factors is a major difficulty. GCOM-C observes global vegetation, temperature distribution and their changes over a long period of time to understand the absorption and emission mechanism of CO_2 and contributes to improve the prediction accuracy of climate model.

The CO_2 concentration in the atmosphere has been greatly increased in the last few decades. Although CO_2 concentration has been fluctuating between 200 and 300 ppm over the past tens of thousands of years, the fluctuation was very gradual. This is because the balance between the CO_2 emission from breathing of animals and plants and decomposition of their carcasses and the CO_2 the absorption by plant photosynthesis and dissolution into the sea controlled the rapid change of CO_2 concentration in the atmosphere.

Today, CO_2 emission has been increased dramatically by human activities, and the aforementioned balance is corrupting. At least a half of CO_2 emission from human activities has been absorbed by plants and marine, but as the volume of CO_2 emission is extremely

large, CO_2 concentration has been increased by 40% comparing to 1750s when industrial revolution was started. Such rapid increase of CO_2 concentration has never been seen before in earth's history.

In the future, when global warming is accelerated, if the volume of CO_2 absorption by plants and marine can be predicted, the influence of global warming on vegetation and marine on global warming can be understood. However, regarding plants, leaves absorb CO_2 by photosynthesis but other parts emit CO_2 by breathing for day and night. Further, absorption and emission of CO_2 changes depending on the climate conditions such as temperature and rain fall, CO_2 concentration in the atmosphere, and species or age of trees. Therefore, it is extremely difficult to accurately estimate the change of forest distribution in the future and how the change influences the volume of CO_2 absorption.

In addition, the volume of CO_2 absorbed by ocean from the atmosphere is fluctuated by the CO_2 concentration in the atmosphere and sea surface. Especially, factors that influence CO_2 concentration of the sea surface are various including sea surface temperature and creature activities. For instance, if the water temperature rises, just like warmed soda, CO_2 in sea water cannot be dissolved completely and it will be released to the atmosphere. As biological activities increase, CO_2 concentration becomes lower as phytoplanktons consume CO_2. If global warming is accelerated, in the future, higher temperature of sea water disturbs the dissolution of CO_2 strongly and thus marine absorption of CO_2 is predicted to be decreased. However, when other various factors such as the effect of marine acidification caused by the absorbed CO_2 on the marine ecology are considered, accurate estimation of absorption volume is also a very difficult task.

GCOM-C leverages its mid- to high-resolutions of 250 m, 500 m, and 1 km and high frequency observation capability to observe vegetation and sea surface temperatures globally. In particular, GCOM-C can use its multi-angle observation feature to collect data on vegetation roughness which is expected to greatly improve the accuracy of land cover classification of coniferous forests, broad-leaved forest, grasslands, deserts and other terrains across the globe.

Figure 1-5 shows the vegetation index (land) and sea surface temperature (ocean) observed by Terra/Aqua in August 2017. The vegetation index is a proxy for vegetation distribution and productivity: it is shown that the value is high in the Amazon and low in the Sahara. Also, the North Atlantic Current is apparent from the observation of sea surface temperature that is flowing from the Gulf of Mexico to the western coast of Europe.

Figure 1-6 shows the balance of CO_2 emissions (red) and absorptions (blue) in the atmosphere as reported by IPCC. Comparing to the estimation of CO_2 volume emitted by using fossil fuels and cement production, there is still great uncertainty regarding the estimation of CO_2 volume that can be absorbed through land-sea ecosystems.

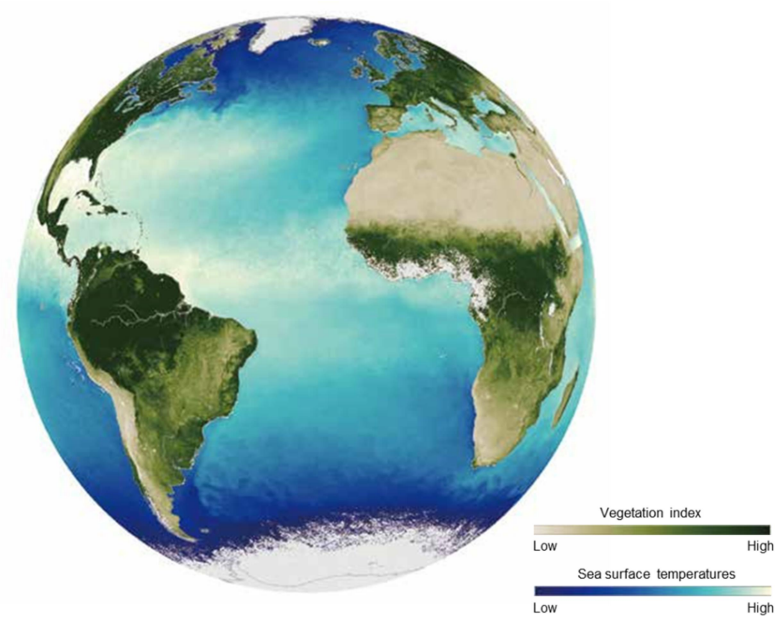

Figure 1-5 Vegetation Index and Sea Surface Temperature observed by Terra/Aqua

*Terra/Aqua data was processed at JAXA

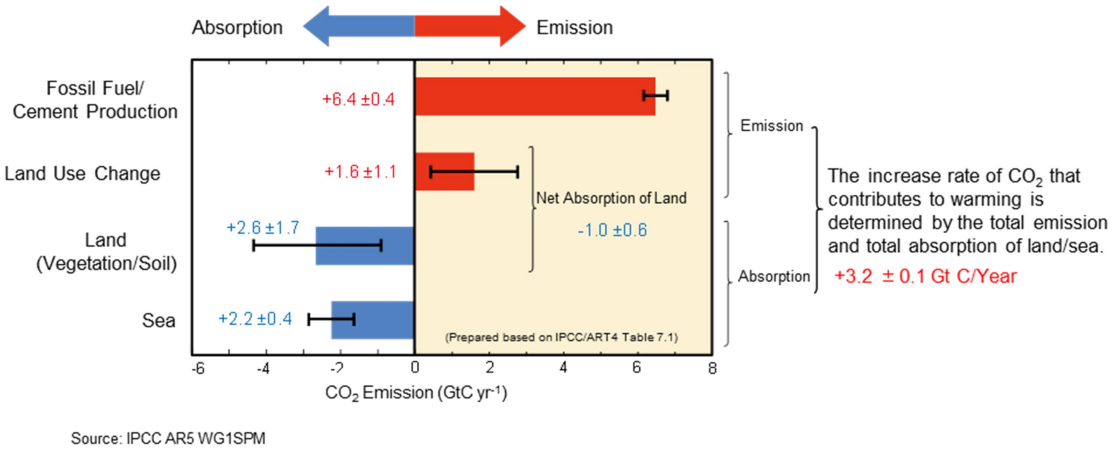

Figure 1-6 Balance of CO2 Emissions and Absorptions (Source: IPCC AR5 WG1 SPM)

1.3.2.3 **Use of Observation Data**

GCOM-C is used to observe various global environments that are affected by climate change in conjunction with other factors such as aerosol, sea surface temperatures, vegetation, snow and ice, solar radiation, and phytoplankton. Data collected by GCOM-C will not only play a role in future climate projection, but will also bring many benefits to our daily lives.

(1)to (4) shows the samples of GCOM-C/SGLI data use. For other data use, please refer to JAXA/EORC (https://suzaku.eorc.jaxa.jp/GCOM_C/monitor/gallery/index_j.html).

(1) Example of Data Use 1 - Fishery -

Seafood is an important part of daily diets in many countries. GCOM-C is used for wide-area observation of sea surface temperatures that greatly affect the ecosystems of marine life including plankton, which is the first link in the food chain. Conducting science-based analysis of the collected data and using the results to help fisheries search for productive fishing ground will lead to more stable catches. Helping us enrich our diet is also another important role of GCOM-C.

Figure 1-7 shows color composite images of the periphery of Tsushima Straits at 11:10 AM on January 1st, 2018 (JST: Japan Standard Time) (center image) and the coastal area and offshore of Kanto region at 10:28 AM on January 6th, 2018 (JST) (right image) which were observed at a resolution of 250 m (the map on the left shows where the images are taken). SGLI equipped with a channel for marine observation is able to observe dark sea surface at a high sensitivity so that it is able to capture the slight difference in the color generated due to the concentration difference of suspended matters and plankton. As shown in Figure 1-7, enabling to observe the sea color of coastal sea areas in detail, it is expected to be useful for predicting fisheries and understanding red tide occurrence status.

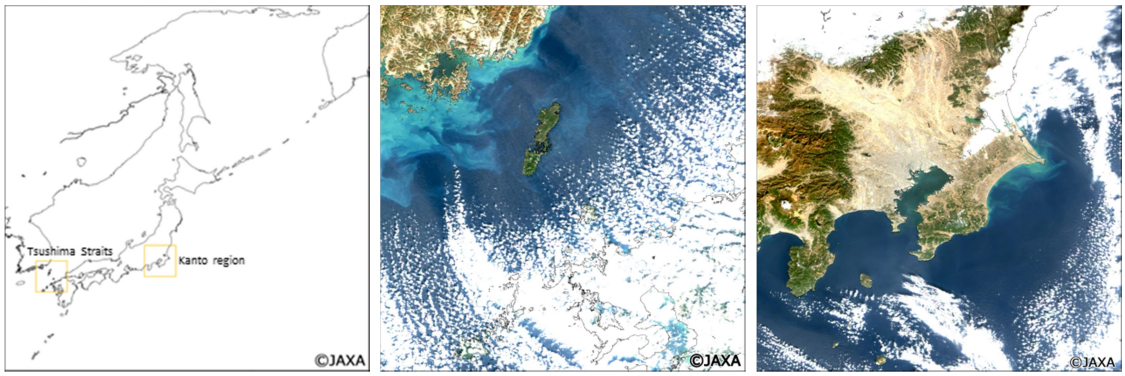

Figure 1-7 Sea Color around Japan Observed by SGLI

Color composite images of the periphery of Tsushima Straits at 11:10 AM on January 1st, 2018 (JST) (center image) and the image at the right side shows the coastal area and offshore of Kanto region at 10:28 AM on January 6th, 2018 (JST) (right image). The reflectance of each channel, VN7, VN6, ad VN4 is assigned to RGB.

(2) Example of Date Use 2 – Agriculture –

Data collected by GCOM-C regarding the distribution of cultivated land around the world, crop history, and agricultural climate (solar radiation, land surface temperature, etc.) can be used to determine the growing conditions and production volume of crops. GCOM-C, for example, can collect global crop information regarding wheat, soybeans and other produce which Japan retains mainly through imports, and this information can be used to conduct risk analysis and evaluations to help establish strategies to manage Japan's food supply. The provision of rice crop information of Asian countries to applicable organizations is also expected to contribute to the stabilization of the global food supply.

GCOM-C is able to observe a wide range of wavelength from near-violet to thermal infrared and tells the thermal condition of ground surface according to the observation of thermal infrared wavelength range. The left figure of Figure 1-8 shows the image of ground surface temperature estimated from the thermal infrared band (wavelength 10.8μm, 12.0 μm) observed around 10:40 on August 1st, 2018. The white color areas in the image indicate clouds. The right figure of Figure 1-8 shows the image of vegetation, and the darker the green color, the more the vegetation. Comparing the ground surface temperature with the vegetation, it is shown that the daytime temperature is extremely high in big cities such as Tokyo, Nagoya, Kyoto and Osaka, and on the contrary, the daytime temperatures in forest areas are relatively lower.

The wavelength range of thermal infrared can be observed even during nighttime as the observation objective is the radiation (thermal release) from the earth. In addition, compared to conventional thermal infrared observations by earth observation satellites, the capability of observation at high spatial resolution of 250 m and high frequency is one of the most significant characteristics of GCOM-C.

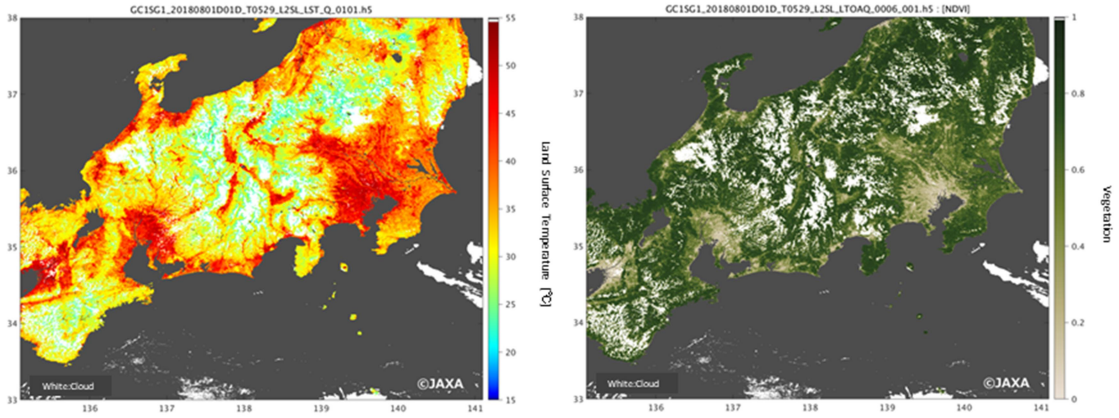

Figure 1-8 Land Surface Temperature (left) and Vegetation (right) Based on SGLI Data

The land surface temperature observed around 10:40 on August 1st, 2018. The white color areas in the image indicate clouds (edge of cloud or thin cloud may not be detected as cloud). Note that, as of August 2018, the accuracy of ground surface temperature is under verification as it is in the initial calibration verification period before data release. The right image shows the vegetation (NDVI).

(3) Example of Data Use 3 - Oceanographic Condition and Weather -

The use of GCOM-C to collect sea surface temperature images at a high resolution of 250 m, and the use of polarization, multi-angle, and near ultraviolet observations to obtain high-accuracy terrestrial aerosol data, can contribute to improving the accuracy of ocean climate information, numerical forecasting, and yellow dust prediction models. GCOM-C can also be used to monitor water quality around coastal and basin areas, and the collected data can be provided to fisheries to help identify occurrences of and reduce damage caused by red tide, blue-green algae, blue tide and other phenomena.

Figure 1-9 shows the image of observation around Japan on March 29th, 2018. The left figure shows a color composite image that the observation data of SGLI's red (VN08: 673.5 nm), green (VN05: 530 nm), and blue (VN03: 443 nm) channels are respectively assigned to RGB so that the colors appear just as seen by human eyes. In the image, the areas with thick yellow sands appear more yellow-brown than other areas (yellow arrows in the left image of Figure 1-9). The right figure shows a false-color composite image in which blue (VN03: 443 nm), violet (VN02: 413 nm) and near-ultraviolet (VN01: 380 nm) observation data are assigned to RGB. The existence of aerosols on land and the contrast with clouds and sea surface become clearer, and the contract between yellow sands and other type of aerosols can be distinguished more clearly. In the right figure, it can be seen that aerosols are spread to northern Kyushu and Chugoku areas. In addition, volcanic smoke extending to the north east from the periphery of Sakurajima and smoke probably caused by the forest fire at the top of the image can be seen.

GCOM-C plans to quantify aerosol quantities and properties with high precision on a global scale using a characteristic function of polarization observation in addition to many observation channels.

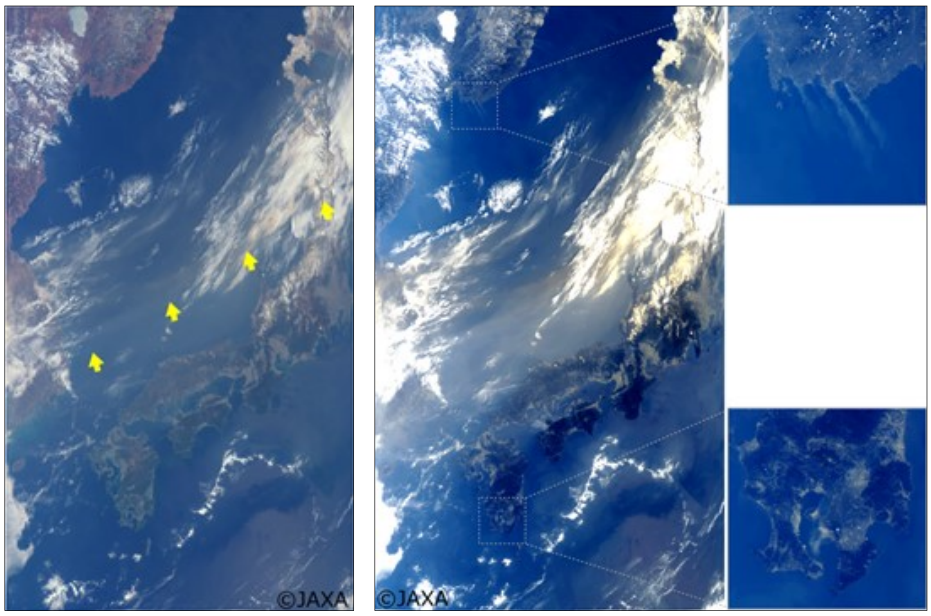

Figure 1-9 Color Composite Images of Areas around Japan Based on SGLI data

The color composite images prepared from the observation data of March 29th, 2018. In the left figure, red (VN08: 673.5 nm), green (VN05: 30 nm), blue (VN03: 443 nm) are, and in the right figure, blue (VN03: 443 nm), violet (VN02: 413 nm), near-ultraviolet (VN01: 380 nm) are assigned to RGB respectively.

(4) Example of Data Use 4 - Volcano and Forest Fires -

Not only are volcanic eruptions damaging the environment, the smoke emitted from the eruptions can also cause serious disruptions to our everyday lives such as causing flight cancellations. Forest fires also cause enormous physical damage to natural resources and man-made structures, and breathing in the smoke can have serious health effects. These factors are turning into an important global issue. GCOM-C can be used to observe infrared and ultraviolet radiation that is unseen to the naked eye, and the infrared scanner can detect the state of volcanic activity and the areas where forest fires are occurring, and the ultraviolet scanner can detect smoke emitted from volcanic activity or fires. This information can be used to reduce damage caused by volcanoes and forest fires and help to achieve greater safety and security in our everyday lives.

On February 19th, 2018, Mt. Sinabung in northern part of Sumatra, Indonesia was erupted. Figure 1-10 shows the image of volcanic smoke around the mountain peak captured by GCOM-C at 250 m resolution in visible – thermal infrared wavelength band around 3:40 (world time) at the date. The top image of Figure 1-10 shows the true-color composite with RGB wavelength bands of SGLI, and the light-brown matters around the center are considered to be volcanic ashes. The bottom left image of Figure 1-10 shows the thermal infrared (11 μm wavelength) brightness temperature image, and since the volcanic ashes reaching the upper atmosphere emit infrared radiation close to the temperature at the altitude, it is possible to estimate the level of altitude that the volcanic ashes reach by the observed

infrared brightness temperature. In addition, the bottom right figure of Figure 1-10 shows the brightness temperature difference (brightness temperature of 11 μm minus that of 12 μm) image. As the absorption band of silicate minerals consisting volcanic ashes is around 10 μm, observation of brightness temperature difference between 11 μm and 12 μm enables to distinguish volcanic ashes from water cloud and ice cloud even during night time without sunlight. The area of volcanic ashes shows strongly negative brightness temperature difference indicating that there exist volcanic minerals characteristic of volcanic ashes.

Volcanic ashes spread up in the air not only disturb the operation of aircrafts but also, from the long-term view, affect the climate change as the sunlight is blocked. GCOM-C is expected to observe these phenomena globally.

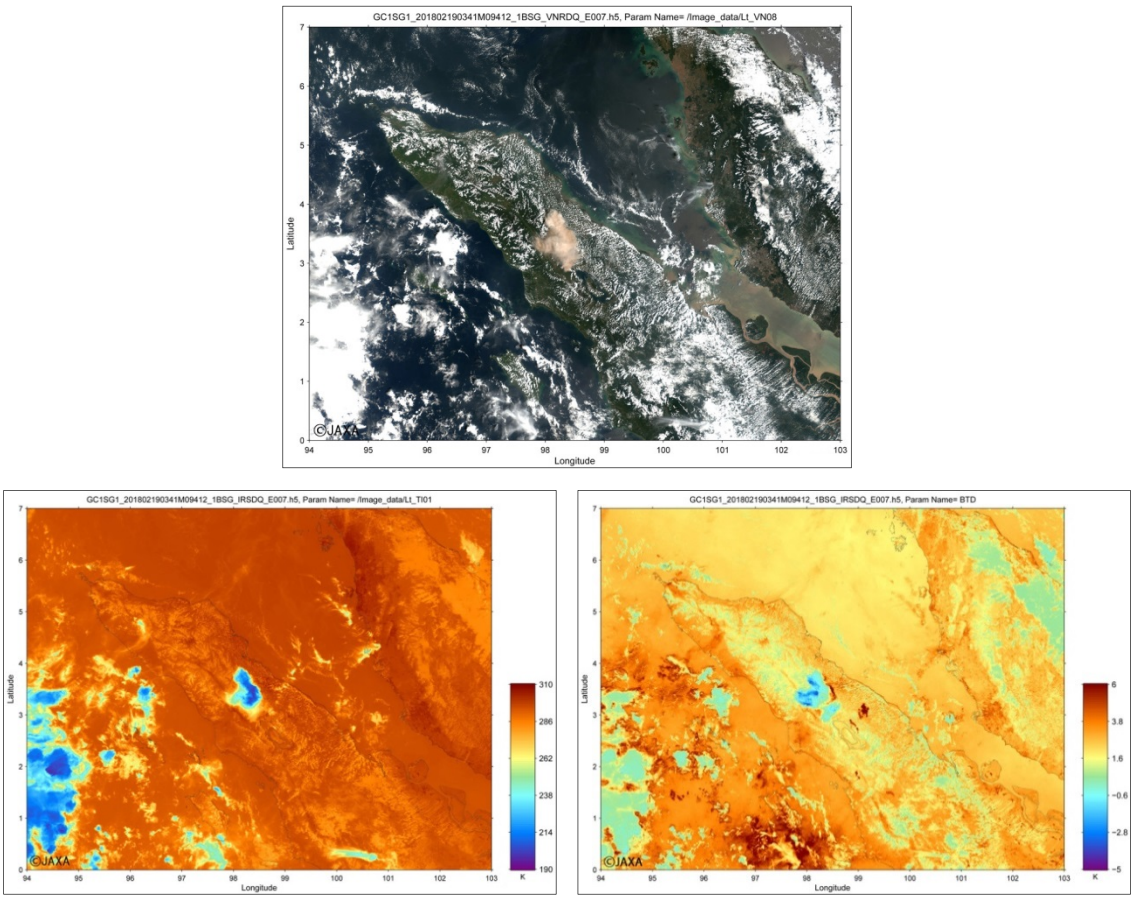

Figure 1-10 Volcanic Smoke of Mt. Sinabung in Sumatra, Indonesia Observed by SGLI

The top image shows the true color composite with RGB wavelength band, the bottom left shows the thermal infrared (11 μm wavelength) brightness temperature, and the bottom right shows the brightness temperature difference (brightness temperature of 11μm minus that of 12 μm) image.

Chapter 2 **Overview of GCOM-C/SGLI**

GCOM-C conducts long-term and continuous global observation and data collection to elucidate the mechanism behind fluctuations in radiation budget and carbon cycle needed to make accurate projections regarding future temperature rise. At the same time, cooperating with research institutions having a climate numerical model, it contributes to reduction of errors in temperature rise prediction derived from the climate numerical model and improvement of accuracy of prediction of various environmental changes.

SGLI, the sensor mounted on GCOM-C, is an optical imaging radiometer that conducts multi-band observation in the range from near-ultraviolet to thermal infrared region (380 nm to 12 μm). It realizes high resolution than GLI (Global Imager) and has a polarized observation function and a multi-angle observation function. The polarized observation function enables to observe the land aerosols that have been conventionally difficult to capture and improves the accuracy of estimation of parasol effect by aerosols. In addition, the multi-angle observation function enables to monitor the long-term fluctuation of vegetation biomass and improves the measurement accuracy of vegetation production volume. Through those observations, while improving the accuracy of prediction of temperature rise by the climate numerical model, the global forest carbon stock is monitored.

2.1 **Overview of GCOM-C**

GCOM-C that incorporates SGLI, a succession machine of GLI, as mission equipment inherits observations that have been done by ADEAOS (ADvanced Earth Observing Satellite) series of various physical amounts determining the global climate. In addition, although the land aerosols and vegetation biomass observations are essential for high-accuracy climate numerical model, they have not been accurately observed. Thus, focusing on those observations, further enhancement of observation functions is being promoted.

Figure 2-1 and Table 2-1 show the appearance and main specifications of GCOM-C respectively. Table 2-2 shows the overview of functions of the satellite bus subsystems.

● GCOM-C proto-flight model
(under proto-flight test)

● Launch Configuration

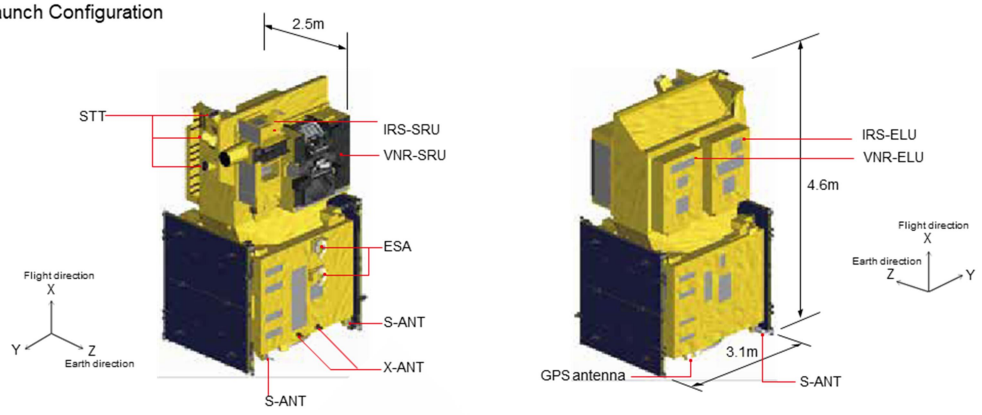

● On-orbit satellite configuration

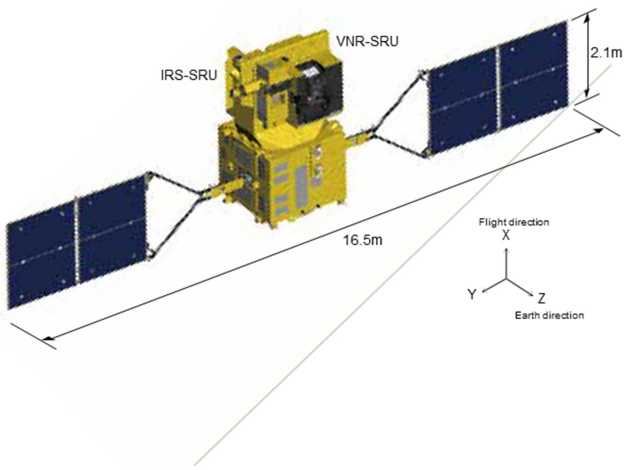

SGLI	Second generation GLobal Imager
VNR-SRU	VNR Scanning Radiometer Unit
VNR-ELU	VNR Electronic Unit
IRS-SRU	IRS Scanning Radiometer Unit
IRS-ELU	IRS Electronic Unit
ESA	Earth Sensor Assembly
S-ANT	S-band Antenna
STT	Star Tracker
X-ANT	X-band Antenna

Figure 2-1 Appearance of GCOM-C

Table 2-1 Main Specifications of GCOM-C

Launch	Launch vehicle	H-ⅡA
	Launch site	Tanegashima Space Center
	Launch date	December 23, 2017
Orbit	Sun-synchronous sub-recurrent Orbit（frozen orbit）	
	Altitude（above the equator）	798km
	Inclination	98.6°
	Local sun time at descending node	10:30±15min.
Weight	Launch mass	Approx. 2060kg （including the propellant）
Shape	Box shape with two solar array paddles	
	Satellite body section	Approx. 2.5m×2.5m×4.6m
	Solar array paddle（after deployment）	Approx. 7.1m×2.1m
Life	Design life	5 years
	Probability of survival	0.8 min., 5 years after launch
Power generated	4,000W min.（End of life）	
Mission equipment	Second-generation Global Imager Visible and Near Infrared Radiometer InfraRed Scanning radiometer	

Table 2-2 Satellite Bus Subsystems

Satellite Bus Subsystem	Function
Mission Data Handling Subsystem（MDHS）	MDHS subsystem transmits observed data to the ground. After the data obtained by SGLI is digitalized using the mission data coder, it is stored in the mission data recorder (MDR) and simultaneously converted to X-band frequency (8 GHz band) and transmitted to the ground.
Telemetry, Tracking and Command Subsystem (TT&C)	TT&C subsystem processes commands received from the ground and transmits satellite status data to the ground. The system deciphers commands received from the S band frequency (2GHz) and transmits the processed telemetry data to the ground.
Attitude and Orbit Control Subsystem (AOCS)	AOCS controls the attitude and orbit of the satellite. The attitude is controlled by the reaction wheel assembly based on the data from star trackers. The orbit is controlled by using thrusters. GPS is used to determine the position of the satellite.
Electrical Power Subsystem (EPS)	EPS uses power generated by the solar array paddle subsystem to supply power to each component and charge the batteries, and supplies power from the charged batteries during eclipse. For enhanced fault tolerance, EPS is equipped with an independent two bus power system.
Solar Array Paddle Subsystem (PDL)	PDL generates power for the satellite from sunlight. During orbit, the paddle drive mechanism (PDM) rotates the solar array paddles (PAD) so that the solar panel surface is always directed towards the sun.
Deployment Monitor Subsystem (DM)	DM is equipped with floodlights which enables the camera to monitor the deployment and rotation of the solar array paddles even when in eclipse.
Reaction Control Subsystem (RCS)	RCS subsystem uses thrusters to generate propulsion. The propellants are stored in the propellant tank and supplied to the thrusters during the mission.
Structure Subsystem (STR)	STR is comprised of the Mission Module equipped with the SGLI components and star trackers and the Bus Module equipped with bus components. It is also equipped with a mechanical interface compatible with the H-IIA launch vehicle.
Thermal Control Subsystem (TCS)	TCS subsystem controls the temperature of each satellite component from the launch phase to the end of the mission. The TCS offers passive thermal control through MLI, OSR and other components, as well as active thermal control through heat pipes. The heater can be turned on and off by the heater control circuit.

2.2 **Second-generation Global Imager（SGLI）**

SGLI is an optical sensor with 19 spectral channels that can measure light intensity, with high accuracy and wide range, from near-ultraviolet to thermal infrared (380 nm to 12 μm) radiation reflected or emitted from the earth. Using SGLI to conduct global and long-term observations of clouds, aerosols, ocean color, vegetation, snow and ice, and other components can help elucidate the mechanism behind fluctuations in radiation budget and carbon cycle needed to make accurate projections regarding future temperature rise.

SGLI is the next generation model of Ocean Color Temperature Scanner (OCTS) on board the Advanced Earth Observing Satellite (ADEOS), and the Global Imager (GLI) installed on the ADEOS-II. SGLI consists of two radiometer components: Visible and Near Infrared Radiometer (VNR) and InfraRed Scanning radiometer (IRS). Some of the improvements made over the GLI includes its higher spatial resolution (from 1 km to 250 m), and the polarized and its multi-angle observation capabilities for observing on-land aerosol and other components. Table 2-2 shows the appearance of SGLI. Table 2-3 shows the SGLI channel specification and Table 2-4 to Table 2-6 show SGLI sensor performance pre-launch on the ground test. Figure 2-3 shows the relationship between geophysical variables of climate change factors and SGLI observation wavelengths, and Figure 2-4 and Figure 2-5 show the total wavelength characteristics of each band. The wavelength characteristics are available at JAXA/EORC (http://suzaku.eorc.jaxa.jp/GCOM_C/data/prelaunch/index.html).

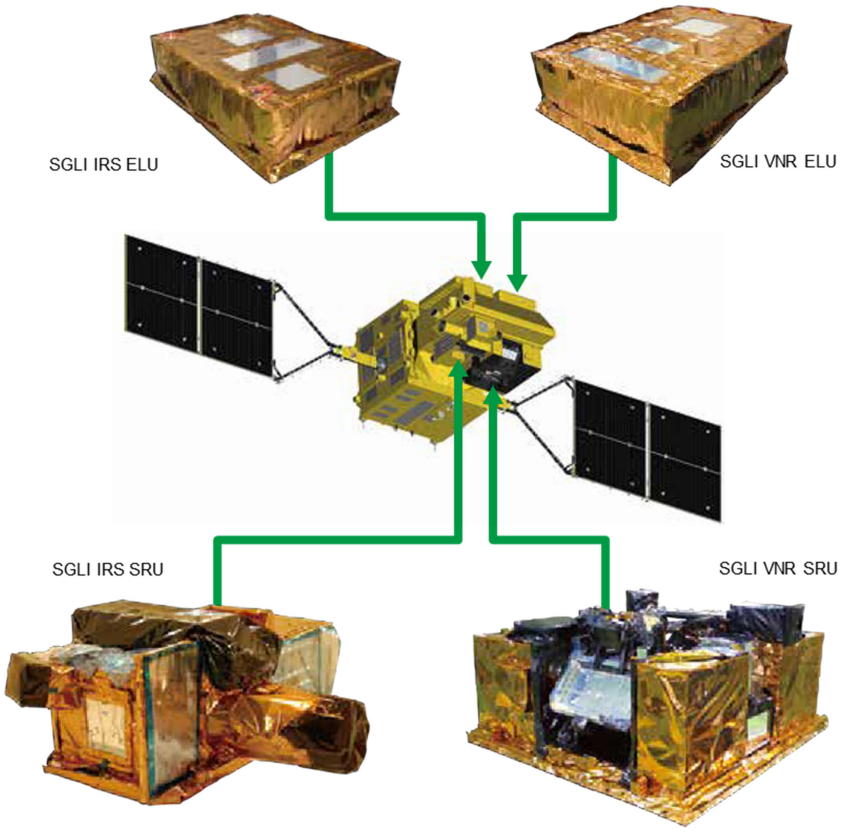

Figure 2-2 Appearance of SGLI

Table 2-3 SGLI Channel Specification

SGLI channels						
CH	λ	λΔ	L_{std}	L_{max}	SNR at Lstd	IFOV
	VN, P, SW:nm T:μm		VN, P, SW: W/m2/sr/μm T: Kelvin		VN, P, SW: SNR T: NEΔT	m
VN1	380	10	60	210	250	250/1000
VN2	412	10	75	250	400	250/1000
VN3	443	10	64	400	300	250/1000
VN4	490	10	53	120	400	250/1000
VN5	530	20	41	350	250	250/1000
VN6	565	20	33	90	400	250/1000
VN7	673.5	20	23	62	400	250/1000
VN8	673.5	20	25	210	250	250/1000
VN9	763	12	40	350	1200	250/1000
VN10	868.5	20	8	30	400	250/1000
VN11	868.5	20	30	300	200	250/1000
P1	673.5	20	25	250	250	1000
P2	868.5	20	30	300	250	1000
SW1	1050	20	57	248	500	1000
SW2	1380	20	8	103	150	1000
SW3	1630	200	3	50	57	250/1000
SW4	2210	50	1.9	20	211	1000
T1	10.8	0.7	300	340	0.2	250/500/1000
T2	12.0	0.7	300	340	0.2	250/500/1000

λ: Wavelength L_std: Standard radiance SNR: Signal to Noise ratio
λΔ: Wavelength width L_max: max radiance IFOV: Instantaneous Field Of View
NEΔT: Noise Equivalent Temperature Difference

Table 2-4 VNR Sensor Performance

Band		Center Wave length	Band width	Signal Level		SNR at Lstd
				Lstd (Spec.)	Saturation Level	
		nm		W/m2/str/μm		-
VNR-NP (3telescope)	VN01	379.9	10.6	60	240-241	624-675
	VN02	412.3	10.3	75	305-318	786-826
	VN03	443.3	10.1	64	457-467	487-531
	VN04	490.0	10.3	53	147-150	858-870
	VN05	529.7	19.1	41	361-364	457-522
	VN06	566.1	19.8	33	95-96	1027-1064
	VN07	672.3	22.0	23	69-70	988-1088
	VN08	672.4	21.9	25	213-217	537-564
	VN09	763.1	11.4	40	351-359	1592-1746
	VN10	867.1	20.9	8	37-38	470-510
	VN11	867.4	20.8	30	305-306	471-511
VNR-PL	PL01_+60	672.2	20.6	25	295	609
	PL01_0				315	707
	PL01_-60				293	614
	PL02_+60	866.3	20.3	30	396	646
	PL02_0				424	763
	PL02_-60				400	752

Table 2-5 SWIR Sensor Performance

Band		Center Wave length	Band width	Signal Level		SNR at Lstd
				Lstd (Spec.)	Saturation Level	
		nm		W/m2/sr/μm		-
SWIR	SW1	1.05	21.1	57	289.2	951.8
	SW2	1.39	20.1	8	118.9	347.3
	SW3	1.63	195.0	3	50.6	100.5
	SW4	2.21	50.4	1.9	21.7	378.7

Table 2-6 TIR Sensor Performance

Band		Center Wave length	Band width	Signal Level	NEdT at Tstd
				Tstd (Spec.)	
		nm		K	K
TIR	T1	10.785	756	300	0.08
	T2	11.975	759	300	0.13

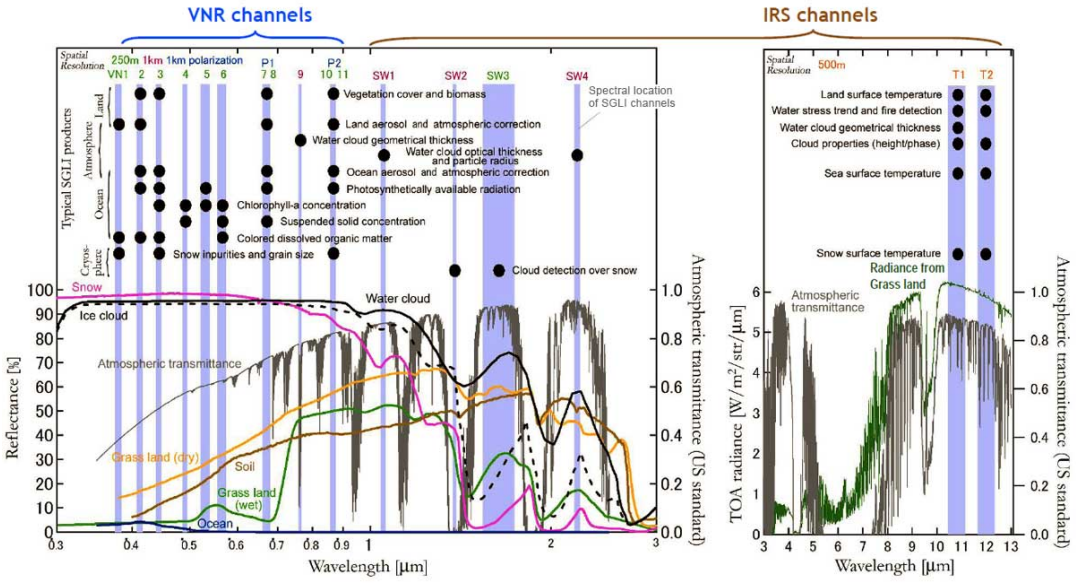

Figure 2-3 Relationship between Geophysical Variables of Climate Change Factors and SGLI Observation Wavelengths

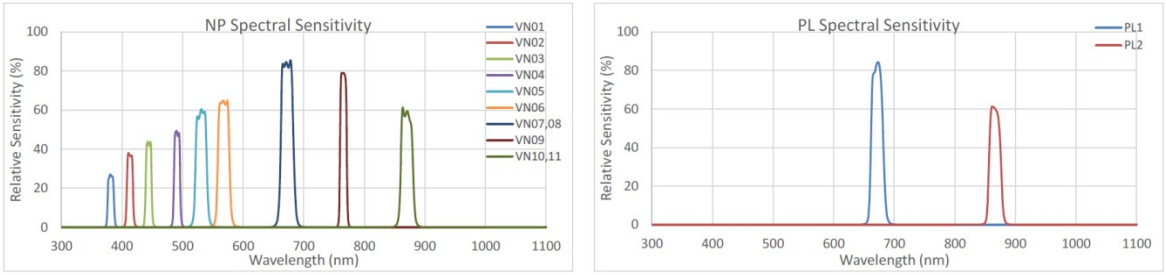

Figure 2-4 VNR Response Function

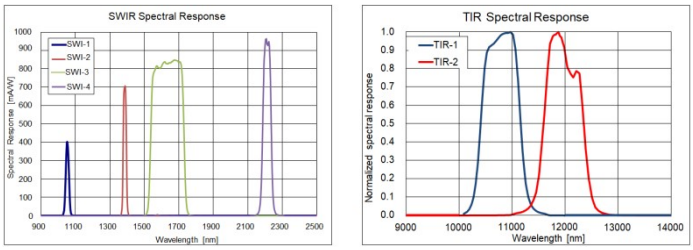

Figure 2-5 IRS Response Function

2.2.1 **SGLI Principle of Operation**

SGLI consists of two radiometer components: Visible and Near Infrared Radiometer (VNR) and InfraRed Scanning Radiometer (IRS). Figure 2-6 shows the observation image of SGLI. SGLI is able to conduct observation once in two days around Japan (latitude 35°). The observation width of SGLI VNR is 1,150 km, and that of SGLI IRS is 1,400 km.

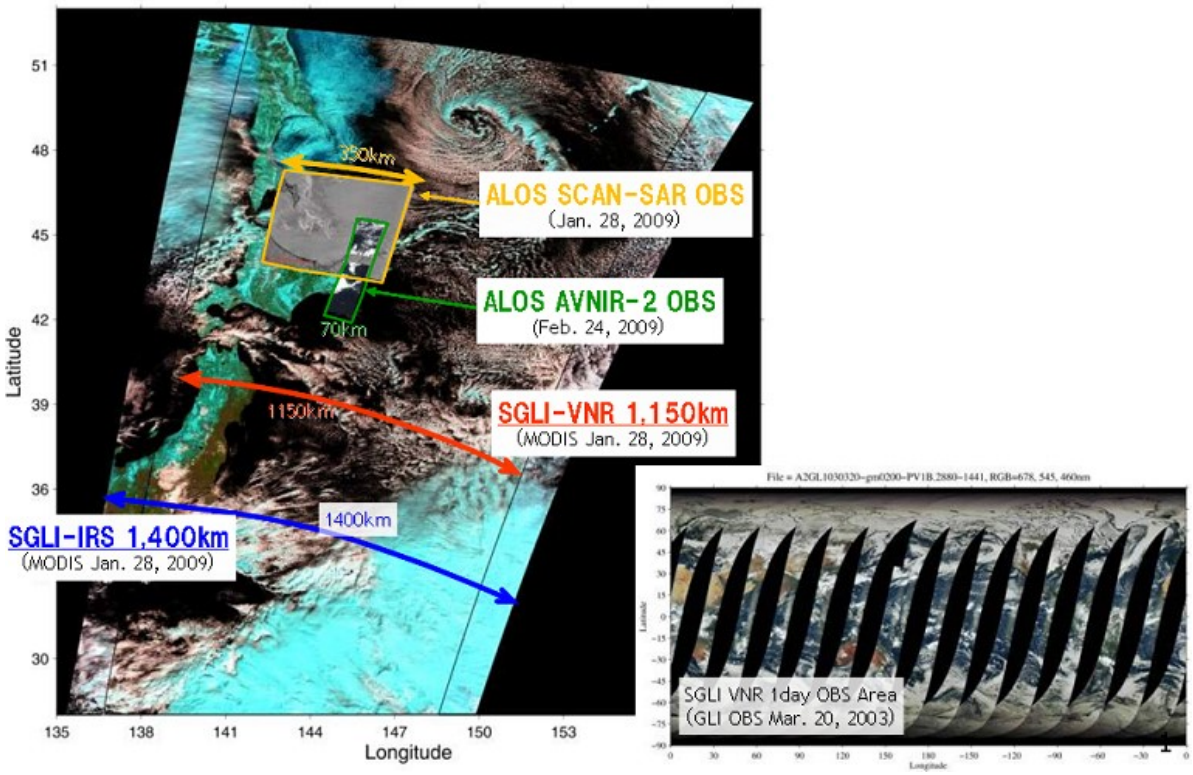

Figure 2-6 Observation Image of SGLI

ALOS is the observation satellite by Advanced Land Observing Satellite "Daichi." Also, MODIS is an optical sensor (moderate resolution imaging spectrometer) developed by NASA/GSFC and mounted on NASA's earth observation satellite Terra/Aqua.

The VNR is comprised of the optical unit (SRU : Scanning Radiometer Unit) and the electrical unit (ELU : Electronic Unit). The optical unit is comprised of a non-polarized light observation

sensor (NP sub-unit: 380 nm to 868.5 nm, 11 channels) that scans areas in the nadir direction, and a polarized light observation sensor (PL sub-unit: 673.5 nm, 868.5 nm, 2 channels) that can provide multi-angle observations by switching to azimuth angles ranging from +45° to -45°. The sensor's detector employs a charge-coupled device (CCD), and is an electrical scanning method (pushbroom scanner method) radiometer that does not require mechanical scanning.

The non-polarized (NP) observation sensor has three telescopes having 24° field of view each in the different directions, accordingly with a scanning width of 70° in total (approximately 1,150 km). NP sensor observes the wavelength of 11 channels extracted inside of the sensor in the resolution of 250 m on land and in coastal areas, and in the resolution of 1 km in oceanic regions.

The polarized (PL) sensor has two telescopes for 673.5 nm and 868.5 nm and performs polarization observation in three angles, 0° and ±60°. PL sensor is mounted on the tilting mechanism that can be set at any degree in the range of ±45° in forward/backward of along-track direction. For forward view of +45° and backward view of -45°, a scanning width of approximately 1,150 km can be observed in the resolution of 1 km. Figure 2-7 shows the tilting mechanism of PL observation and Figure 2-8 shows VNR SRU. The ELU has the function to monitor and control the SRU and then edits and outputs the detected signals.

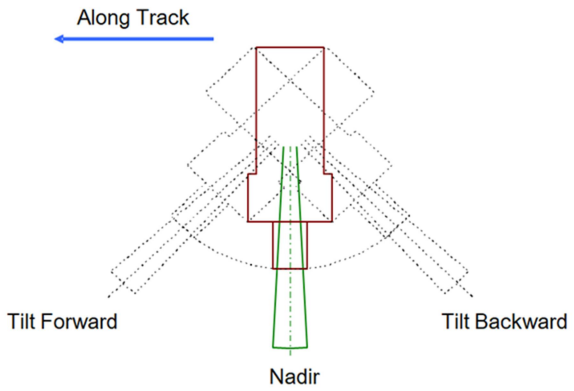

Figure 2-7 Tilting Mechanism of PL Observation

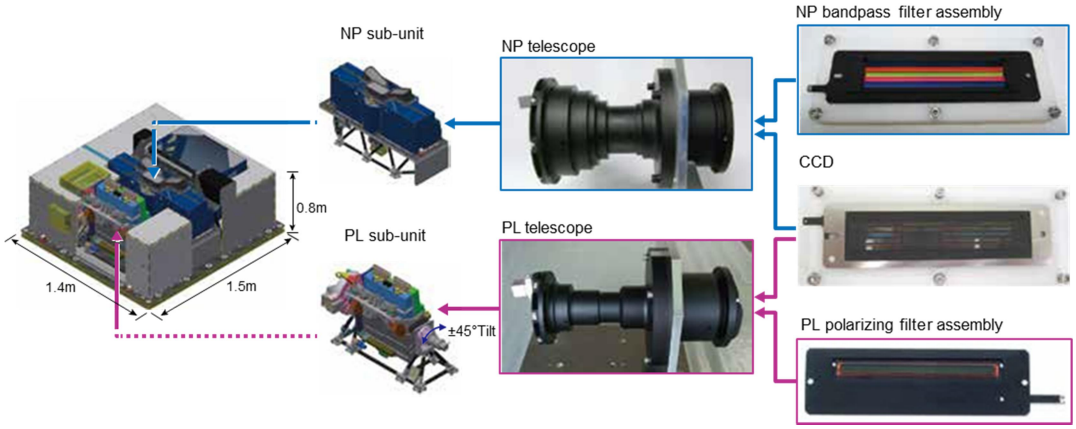

Figure 2-8 VNR SRU

IRS is comprised of the optical unit and the electrical unit. The optical unit divides the light reflected from the earth into the spectral regions of Short Wavelength Infrared (SWI: 1.05 μm to 2.21 μm, 4 channels) and Thermal Infrared (TIR: 10.8 μm, 12.0 μm, 2 channels) by a dichroic mirror via Ritchey-Chretien type optical system and leads the light into the respective detectors. The InGaAs detector is used for the short wavelength infrared, and the Photo Voltaic (PV)-type HgCdTe detector is used for the thermal infrared. The InGaAs detector is cooled to -30 °C using a Peltier element, and the HgCdTe detector is cooled to 55 K using the Stirling cooling system.

To avoid influence from the incident angle dependence of the scan mirror reflectivity, the IRS scanning method employs the mechanical scanning method (whisk-broom method) in which the scan mirror is set at an angle of 45 degrees with respect to the rotation axis. Using this scanning method, the IRS scans the earth's surface once every 0.74 s, and observes approximately 80° width (1,400 km) in one scan. Figure 2-9 shows IRS SRU. In the same way as for VNR, ELU monitors and controls SRU unit then edits and outputs the detected signals.

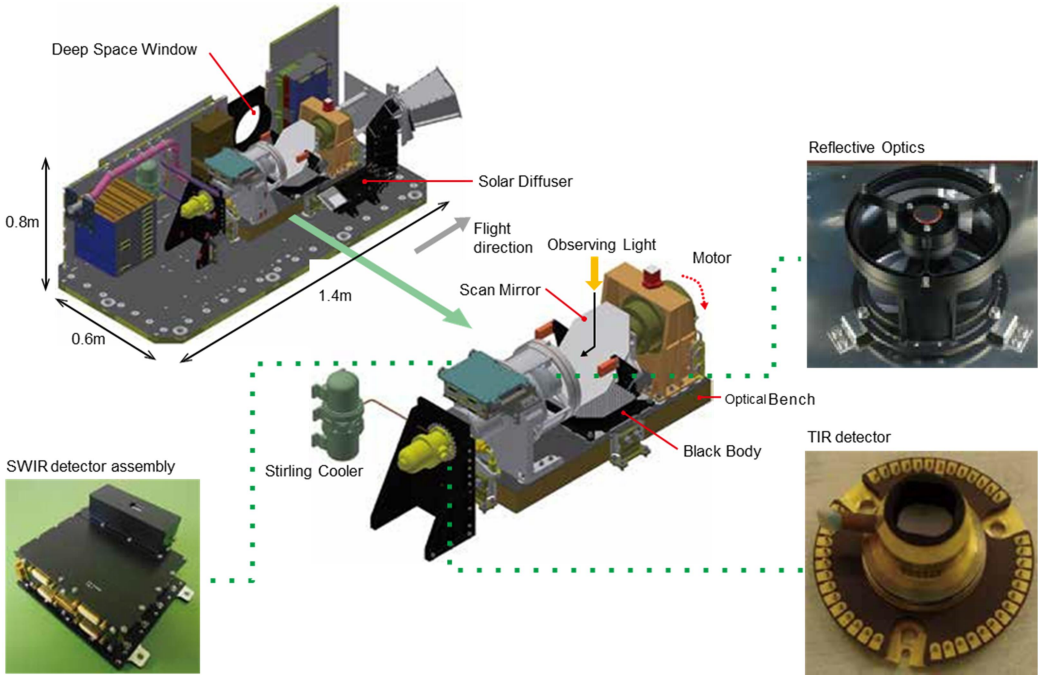

Figure 2-9 IRS SRU

2.2.2 **SGLI System Configuration**

The 11-channel observation wavelengths of VNR-NP sensor are extracted by positioning spectral filter strips on the focal plane of the 11-line CCD (length of approximately 80 mm). The spectral filter is composed of two filters to enable suppression of response at out-of-band wavelengths. VNR-PL is observed the polarization at -60°, 0°, and 60°angles to calculate the Stokes parameters I, Q, and U. PL's three polarized angles are extracted by positioning polarizing filters, composed of three polarizer strips in each angle on the focal plane of the 11-line CCD. Figure 2-10 shows the channel array in VNR-NP, and Figure 2-11 shows the array of polarizing direction of VNR-PL.

In CCD of VNR, the pixel number of a line is 6000 each telescope. In NP, 4 pixels in CT direction and 4 pixels in AT direction are added, that is, 16 pixels are digitally added at on-board to make one pixel corresponding to 250 m. On the other hand, in PL, 7 pixels in CT direction x 7 pixels in AT direction = 49 pixels are digitally added at on-board to make one pixel corresponding to 1 km.

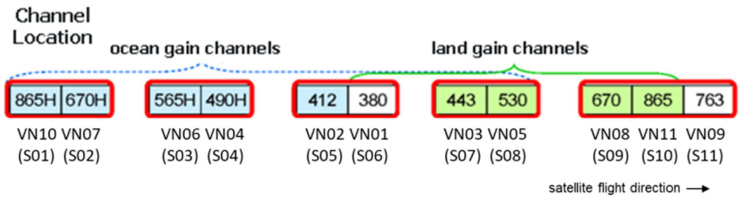

Figure 2-10 Channel Array in VNR-NP

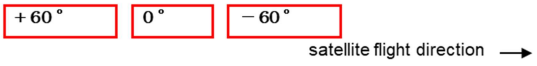

Figure 2-11 Array of Polarizing Direction of VNR-PL

IRS employs mechanical scanning method using 45° mirror, and the scan mirror rotates at the constant rate of 740 ms to leads the observing light to IRS internal. Figure 2-12 shows the definition of IRS scanning angle and view.

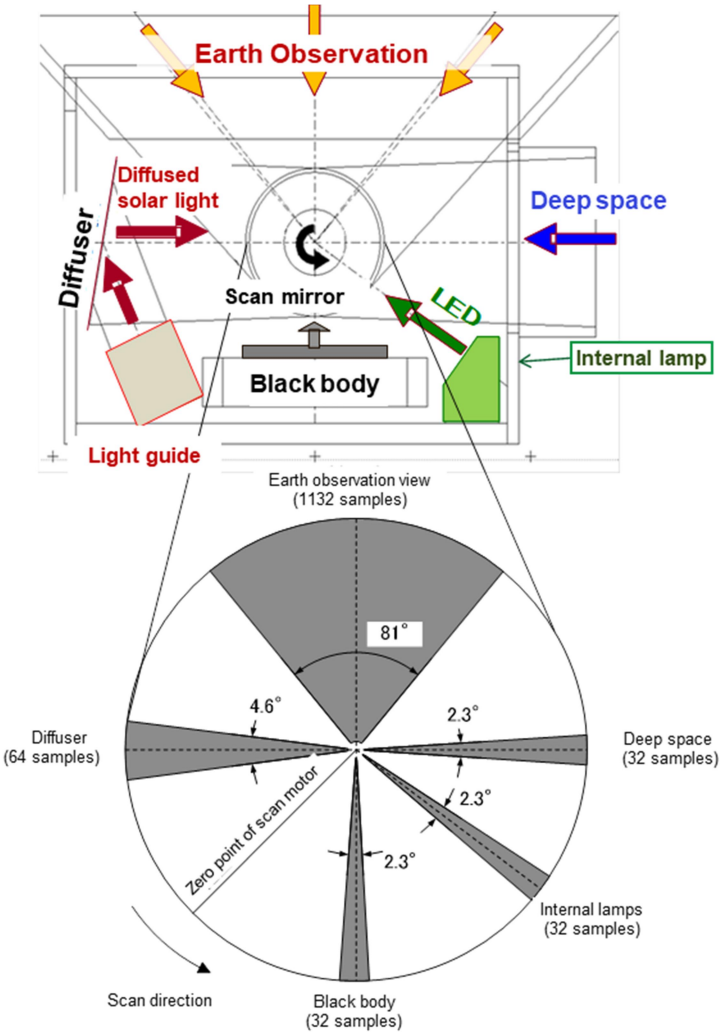

Figure 2-12 Definition of IRS Scanning Angle and View

The number of samples is the number of DSP output samples.

2.2.3 **Calibration Concept**

SGLI evaluates the health check and the trend by evaluating the data obtained through on-orbit calibration and calibration maneuver conducted periodically. Table 2-7 shows SGLI calibration types.

Table 2-7 SGLI Calibration Types

	On-orbit calibration					Calibration maneuver		
	Solar diffuser calibration	Internal lamp calibration	Dark image calibration	Black body calibration	Deep space calibration	Lunar calibration maneuver	Solar angle correction maneuver	90-deg yaw maneuver
VNR	○	○	○	-	-	□	△	△
SWIR	○	○	○	-	◇	□	△	-
TIR	-	-	-	◇	◇	□	-	-

○ : Once in 8 days ◇: Each scan □: Once in a month △: Once in a year

2.2.3.1 **VNR Calibration**

VNR has the radiometric calibration function using solar light, internal lamps, and lunar light, and also has an electrical calibration function. For the calibration employing the solar light and internal lamps (white LED and infrared LED), the light reflected from the expanded diffuser is used. By facing the diffuser in the nadir direction of the non-polarized light observation sensor, and using the tilting device to face the polarized observation sensor toward the diffuser, the reflected light from the diffuser can be received and calibrated by each sensor.

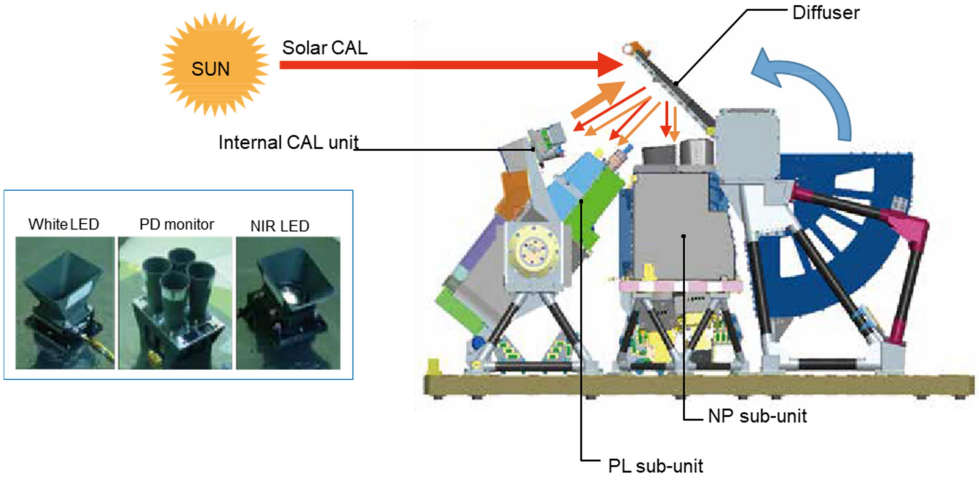

Figure 2-13 VNR Solar Diffuser and Internal Lamp Calibration

2.2.3.2 **IRS Calibration**

Figure 2-14 shows IRS calibration functions. IRS collects ground observation data in a scan range of 80° from it's one 360° rotation of the scanning mirror, and acquires data of the calibration sources (solar light, internal lamps, black body and deep space) from angles outside the observation range. For the short wavelength infrared channel (SWIR), the radiometric calibration is conducted using the solar light, internal lamp (LED with wavelength of 1.6 μm, halogen lamp) and lunar light. In addition, for the thermal red channel, every two-point calibration is conducted for each scanning using the data obtained by observing the black body (high temperature calibration source) and deep space (low temperature calibration source).

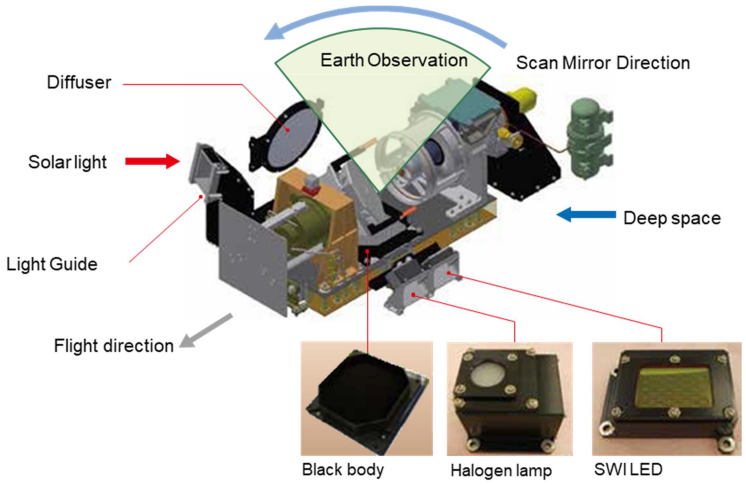

Figure 2-14 IRS Calibration Features

2.2.3.3 **Calibration Maneuver**

In GCOM-C, the maneuver is performed to obtain data to calibrate the sensor.

(1) Lunar Calibration Maneuver

In SGLI lunar calibration pitch maneuver, the lunar observation images captured by maneuvering GCOM-C attitude around the pitch axis are used as radiometric calibration data to evaluate sensor input and output properties, inter-band relative sensitivity, and dark signal noise. The moon that reflects solar light is stable light source and is suitable as a long-term calibration light source. Until the end of observation operation, the lunar calibration pitch maneuver is performed approximately every 29 days that is the synodic period of the moon and sun. In addition, observation is conducted when the Phase Angle is around 7°. The channels to be calibrated are all VNR observation channels and all IRS observation channels.

(2) Solar Angle Correction Maneuver

The earth is circling around the sun and due to the earth's elliptical orbit and orbit inclination, the yaw axis (solar β angle) changes gradually. The solar angle correction yaw maneuver of SGLI calibrates the yaw axis direction in solar calibration by maneuvering the attitude of GCOM-C around the yaw axis. The channels to be calibrated are all VNR observation channels and IRS-SWIR channel.

(3) 90-deg Yaw Maneuver

SGLI 90-deg yaw maneuver uses the terrestrial target of homogeneous reflectance, which captured by maneuvering GCOM-C's attitude by about 90° around the yaw axis, as radiometric calibration data to evaluate the PRNU (Photo Response Non-Uniformity). Rotating the satellite around the yaw axis, maneuver is conducted so that different CCD pixels

are able to observe almost same terrestrial target. The channels to be calibrated are all VNR observation channels.

2.2.4 **Observation Operation**

The basic observation pattern of SGLI and overview of observation operation of SGLI are respectively shown in Table 2-8 and Figure 2-15. The daytime observation is performed at all 19 channels. The resolution for land and coastal observation is 250 m or 500 m (thermal infrared only), and the resolution for open ocean observation is 1 km. In addition, the nighttime observation is conducted in the land region of shortwave infrared channel (SWIR) and global region of thermal infrared channel (TIR). Regarding the start up and end timing of VNR and IRS SWIR observation in the terrestrial daytime observation, it turns ON earlier than the end of shade period on ground for twilight observation, and turns OFF after the start of shade period. In VNR polarized tilt observation, the normal observation sequence is tilt forward for north side and tilt backward for south side considering the solar position. In addition, each sensor's observation is turned ON and OFF independently. Note that the aforementioned patterns are basic observation patterns, and the actual observation operation will be planned considering the data volume to be downlinked.

Table 2-8 SGLI Basic Observation Pattern

Basic observation modes		VN-NP	VN-P		SW1-2, 4	SW3	T1-2	Mbit/s
1	Day-land/coast-T250	250m	1km	+45° −45°	1km	250m	250m*	23.407
2	Day-land/coast-T500						500m	20.922
3	Twilight-land/coast-T250	1km	1km	+45° −45°	1km	250m	250m*	7.273
4	Twilight-land/coast-T500						500m	4.788
5	Day-offshore/polar	1km	1km	+45° −45°	1km	1km	1km	2.612
6	Night-land-T250	OFF	OFF		1km	250m	250m*	5.360
7	Night-land-T500						500m	2.875
8	Night-coast-T250	OFF	OFF		OFF	OFF	250m*	3.353
9	Night-coast-T500						500m	0.868
10	Night-offshore/polar	OFF	OFF		OFF	OFF	1km	0.246

*: 250m mode is limited by downlink data volume per a path

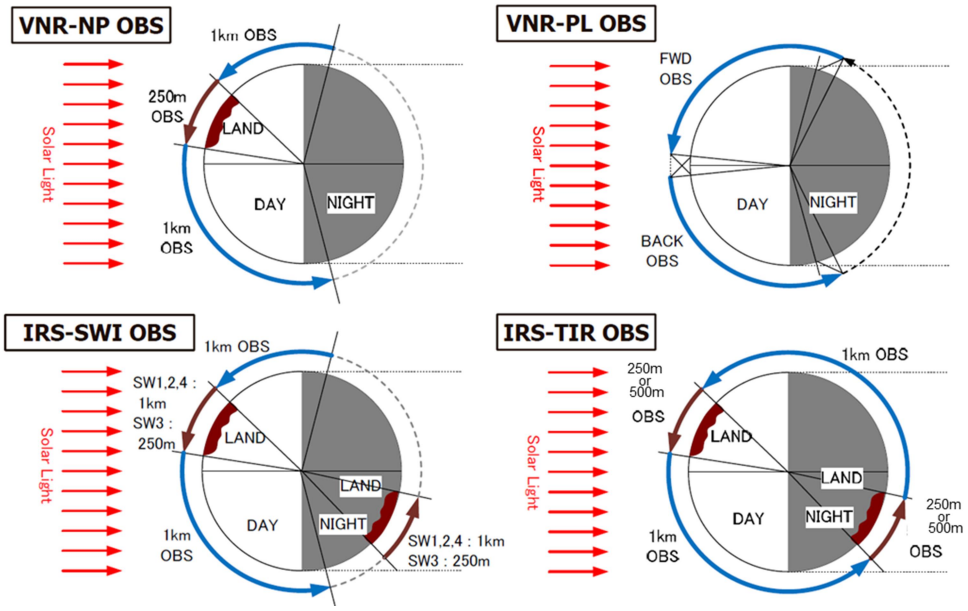

Figure 2-15 Overview of SGLI Observation Operation

Chapter 3 **Overview of GCOM-C Ground System**

3.1 **Overall System**

GCOM-C ground system consists of three systems: "satellite control system," "mission operation system," and "research system." The satellite control system mainly provides satellite operation. The mission operation system processes and provides data. The research system develops algorithms and conducts validations.

Figure 3-1 shows the overview of GCOM-C ground system. The tracking network system uses the ground network system to receive telemetry, send commands and operate ranging. In addition, it receives X-band data at the receiving and recording equipment of domestic and international stations, demodulates the observation data, and generates ASD (APID Sorted Data). As the foreign station, Svalbard station (northern latitude of 78 degrees) offered by a Norwegian company, Kongsberg Satellite Services AS (KSAT), is used.

The satellite control system establishes mission operation plans and satellite operation plans and processes the telemetry/commands coming through the tracking network and Svalbard station.

The mission operation system processes the X-band observation data received at the receiving and recording equipment of domestic and foreign stations. In the data processing, Level0, Level1 and Level2 & Level3 processing are performed using ASD as input, and data storage control are provided. In addition, it processes near-real time products and provides them to alliance organization.

The research system receives the Level1 and Level2 & Level3 products from the mission operation system and verifies the algorithms and parameters for processing and correction.

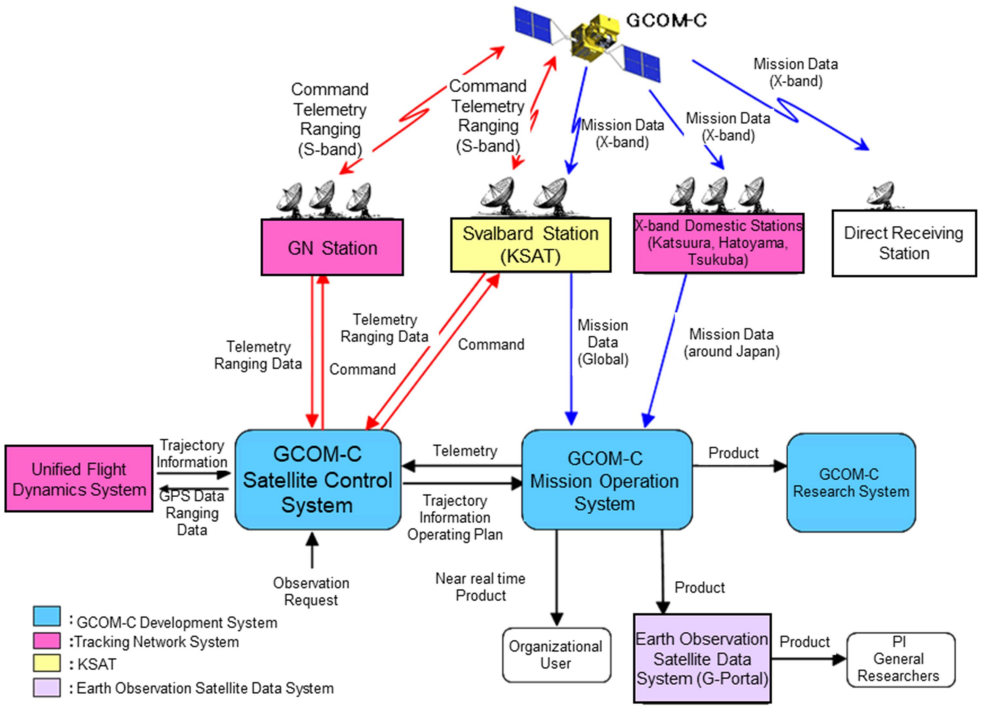

Figure 3-1 GCOM-C Ground System

3.2 **Satellite Control System**

Telemetry and command operation of satellite is principally performed using the ground network system (GN station) of JAXA. Telemetry data of satellite are stored in a data recorder in orbit, and received at Svalbard station (KSAT) in each orbit cycle. The data is then sent to the satellite control system at Tsukuba Space Center to check the satellite condition at the invisible zone in orbit.

3.3 **Mission Operation System**

GCOM-C mission operation system consists of "GCOM-C data processing function" that processes mission data downlinked from a satellite to a ground station at X-band and "GCOM information system function" that stores and controls the processed GCOM-C data, products and satellite operation information and transmits data inside and outside of the system. It also provides near-real time products to alliance organization. The outlines of the data processing system and information system are described below:

(1) Data Processing Function

(a) Process Control Function

The function to control GCOM-C data processing in general including development of processing plans, status management, control of functions unique to the processes based on the plans (calling out of external functions etc.), and load control of processing computer.

(b) Process Individual Function

The function to perform processing individual to GCOM-C/SGLI (Level1 processing and Level2 & Level3 processing) based on the processing plan provided by the processing control function.

(2) Information System Function

(a) System Control Function

The function to manage the system configuration for the entire mission operation system.

(b) Data Transmission Function

The function to provide data for inside and outside of the mission operation system.

(c) Data Storage Function

The function to store operation information related to the data and products generated by the data processing function.

(d) System Monitoring Function

The function to monitor the performance of the mission operation system.

3.4 **Receiving and Recording Equipment**

The receiving and recording equipment (X-band stations) for GCOM-C operation comprise Katsuura station, Hatoyama station, Tsukuba station, and KSAT (Svalbard station). Katsuura station, Hatoyama station and Tsukuba station in Japan generally receive the real time visible signals. Svalbard station receives the global observation data.

Katsuura station, the primary domestic station, is the equipment to receive and record the observation data at domestic antenna and provides ASD to the mission operation system. The main purpose of Katsuura Station's regular X-band operations is the reception and transfer of real time observation data as well as real time HK telemetry data. Hatoyama station and Tsukuba station are positioned as a backup domestic station and serve as the backup domestic station when the primary Katsuura Station is offline because of contention with other satellites or for regular maintenance operations.

On the other hand, the KSAT/Svalbard station operates S-band TT&C (telemetry, command), generates the ASD of X-band observation data and HK telemetry data and transmits them to the GCOM-C mission operation system. The main purpose of the KSAT/Svalbard Station's normal X-band operations is the reception and transfer of stored observation data recorded on the satellite's data recorder as well as stored HK telemetry data. Table 3-1 summarizes the satellite operations at each ground station.

In addition to the above, real time observation data will be distributed directly from the satellite by X-band transmissions to ground stations (domestic and international direct receiving stations) that require direct receiving. Transmissions to domestic and international direct receiving stations are operated on the basis of an agreement between JAXA and the corresponding domestic or international institution.

Table 3-1 Ground Station Satellite Operation

Station	TT & C Operations (S-band)		Mission Data Transfer Operations (X-band)			
	Command Ranging	Real time/Stored Telemetry	Stored Telemetry	Stored Observation Data	Real time Telemetry	Real time Observation Data
Katsuura Station (X-band)	–	–	○	○	○	○ (Japan and vicinity)
Hatoyama Station/Tsukuba Station (X-band)	–	–	○	○	○	○ (Japan and vicinity)
KSAT/Svalbard Station (S/X-band)	○*1	○	○	○	○	(○) (North Pole and vicinity)
JAXA New GN Station (S-band)	○	○	–	–	–	–

*1 Svalbard Station undertakes ranging operations only when necessary.

3.5 **Ground System Operation**

3.5.1 **Processing by Mission Operation System**

Observation data received at the KSAT/Svalbard Station and domestic stations (Katsuura station, Hatoyama station and Tsukuba station) are transferred as ASD to the mission operation system at the Tsukuba Space Center where the data undergo Level0, Level1 and Level2 & Level3 processing. The orbit and attitude information used in Level1 processing is based on the use of the onboard GPS receiver's orbit and attitude values contained in the sensor packet's payload correction data (PCD).

3.5.2 **Delivering Products to Alliance Organizations**

SGLI Level1 products and physical variables products (Level2) generated by the Level2 & Level3 processing, for Japan and vicinity, and for global are provided in near-real time to the alliance organization within the delivery time requirements from observation to product delivery (near-real time processing requirements). Table 3-2 and Table 3-3 show the currently defined near-real time products. The details of those products are provided in Chapter 4.

The number of alliance organizations and products subject to near-real time delivery may expand in the future.

Table 3-2 Near-real time Products (Japan and Vicinity)

Delivered Product	
SGLI Near-real time Product	1) Level1B 2) Sea surface temperature (Level2) 3) Chlorophyll-*a* concentration (Level2) 4) Normalized water-leaving radiance (Level2)

Delivered Product	
	5) Snow and Ice cover extent (Level2)

Table 3-3 Near-real time Products (Global)

Delivered Product	
SGLI Near-real time Product	1) Level1B 2) Sea surface temperature (Level2) 3) Snow and Ice cover extent (Level2) 4) Snow and ice surface temperature (Level2) 5) Land surface temperature (Level2)
	6) Aerosol over ocean (Level2) 7) Aerosol over land (near-ultraviolet) (Level2) 8) Aerosol over land (polarization) (Level2)

Chapter 4 **SGLI Products**

4.1 **Product Definitions**

SGLI products including Level2 & Level3 products are in HDF5 format and consist of Group, Dataset, and Attribute. For the definitions of HDF5 format, please refer to the HDF Group (http://www.hdfgroup.org).

4.1.1 **Process Level Definitions**

Table 4-1 shows the definition of processing level of SGLI products.

Table 4-1 Definition of SGLI Products

Processing Level	Description
Level-0	Uses ASD as input. Data set after sorting the previous data set based on the time and packet sequence count in the ASD and applying loss processing.
Level-1A	Granule scene radiance products after the following processing using Level-0 data as input. ・Delete duplicate packet. Interpolate lost packets in the mission data with dummy packets ・Edit and cut out of scenes (include overlap data) ・Radiometric correction ・Geometric correction ・Append information of lost packet and quality information
Level-1B	Granule scene radiance products after the following processing using Level-1A product as input. ・Radiometric correction ・Geometric correction and resampling to Level-1B reference coodinates ・Append geometric information per wavelength band and calibration information Or low-resolution resampling products derived from high-resolution Level-1B products.
Level-2	Granule scene, global, and tile (*1) data of geophysical variables derived from Level-1B or Level-2 products including global and tiled mosaic products with the spatial resolutions of 250m and 1km for scene and tile products, and 4km(1/24deg.) for global products. *1: Tiles are defined as 10 degrees square at the equator on the Sinusoidal grid.
Level-2 statistics	Temporal (8-day and 1-month) statistics or cloud-free mosaic of Level-2 tile products with the same spatial coverage and resolution.
Level-3	Spatial (1/12deg. And 1/24deg.) and temporal (1-day, 8-day and 1-month) statistics of Level-2 products with the global spatial coverage.

4.1.2 **Process Flow**

Figure 4-1 shows the processing flow of Level1 product and Level2 product. The left side of Figure 4-1 is the upstream of the process, and the arrows indicate main input data of the process. In addition, Figure 4-2 shows the processing flow of Level2 and Level3 products. Using Level2 products as input, Level2 statistic product and Level3 temporal statistic, spatial statistic products are generated. The types of products are described in 4.1.3 , 4.1.4 , and

4.1.5 . The overview of Level2 & Level3 algorithms are provided in 4.3

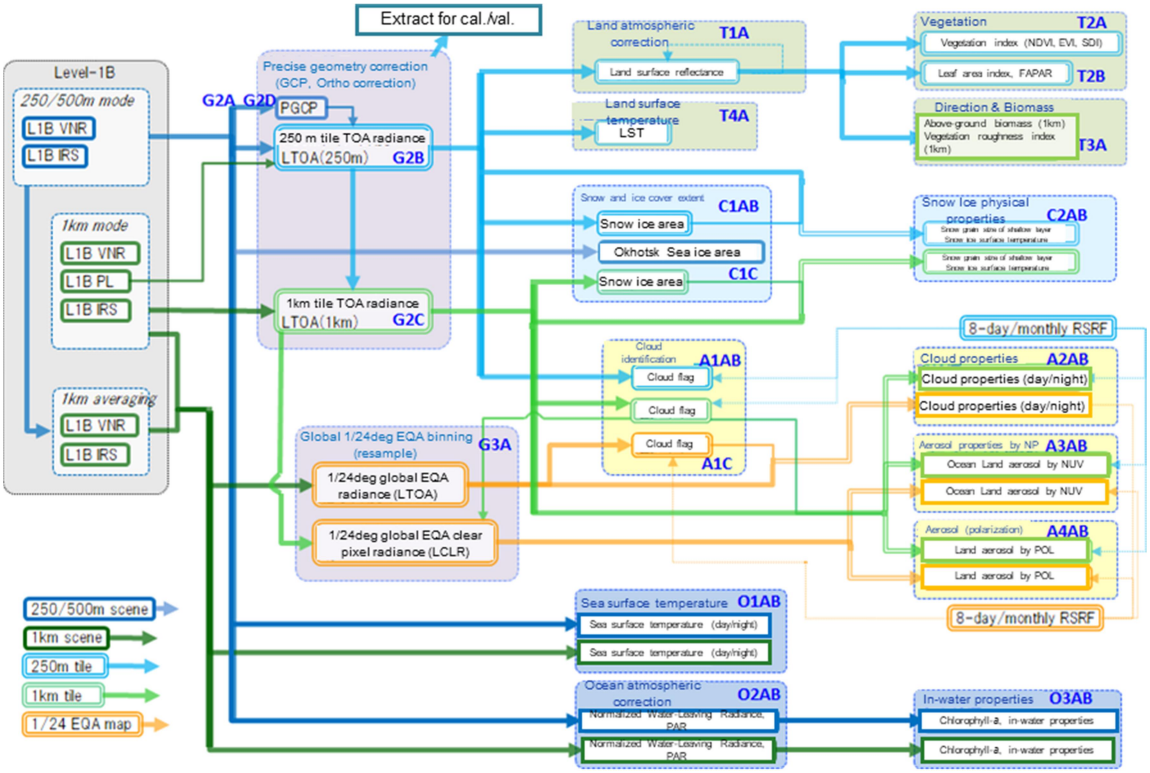

Figure 4-1 SGLI Level1 and Level2 Processing Flow

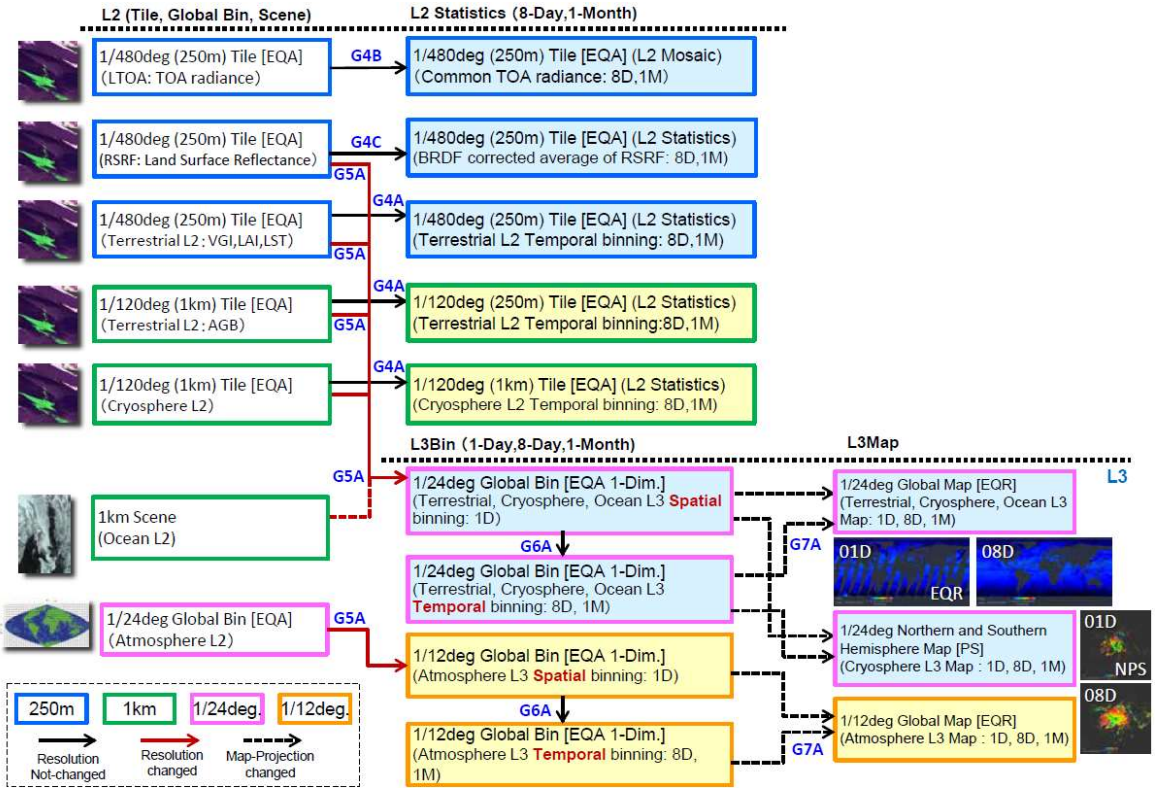

Figure 4-2 SGLI Level2 and Level3 Processing Flow

4.1.3 **Leve-1 Product**

Level1 product is generated for each sensor of VNR-NP, VNR-PL, and IRS (SWIR + TIR). In addition, according to the difference of processing performed to the observation data as shown in Table 4-1, they are divided into Level1A and Level1B. For Level1B product generated at high resolution, Level1B product obtained by resampling it to 1 km resolution is generated too.

4.1.3.1 **Level1A Product**

The brief information stored in Level1A product is shown below. Please refer to Product Format Description for more details.

(1) Stored Data

Observation DN value is stored for each band as image data. Please refer to 4.2.2.2 for the algorithm to convert to radiance. The geometry is not corrected, and the observation position of ground of pixel is varied each band. Therefore, the latitude/longitude information of 10 pixels interval in each band is appended. However, there is no interval in AT direction of IRS. The stored geometric information is the center position of the pixel.

(2) Image Dataset Size

(a) VNR-NP

[telescope (Left, Nadir, Right) x line x pixel]= [3 x line* x 1500 (250 m) or 375 (1 km)]

*line value varies depending on the file.

(b) VNR-PL

[line x pixel]= [line* x 857 (1 km)]

(c) IRS-SWIR

[line x pixel]= [line* x 4584 (250m) or 1146 (1 km)]

(d) IRS-TIR

[line x pixel]= [line* x 4584 (250 m) or 2292 (500 m) or 1146 (1 km)]

4.1.3.2 **Level1B Product**

The brief information stored in Level1B product is shown below. Please refer to Product Format Description for more details.

(1) Stored Data

The top of atmosphere radiance SI (Scaled Integer) after radiometric correction is stored as

16-bit image data. However, the upper 2 bits are the flag to identify the stray light correction information and thus the conversion to actual radiance should be done carefully.

The geometries are projected to L1B reference coordinates (see 4.2.2.4) commonly for VNR-NP and IRS, and the ground observation position in each band are same. Therefore, as geometric information, latitude, longitude, solar azimuth angle and solar zenith angle of 10 pixels interval are stored commonly for band. On the other hand, since the precise satellite position in observed pixels is varied depending on band, the satellite azimuth angle and the satellite zenith angle are stored by 10 pixels interval for each band. The stored geometric information is the center position of the pixel.

In addition, QA flag corresponding to the observation image is appended to Level1B product.

(2) Image Dataset Size

(a) VNR-NP

[line x pixel]= [line* x 5000 (250 m) or 1250 (1 km)]

*line value varies depending on the file.

(b) VNR-PL

[line x pixel]= [line* x 1000 (1 km)]

(c) IRS-SWIR

[line x pixel]= [line* x 5000 (250 m) or 1250 (1 km)]

(d) IRS-TIR

[line x pixel]= [line x 5000 (250 m) or 2500 (500 m) or 1250 (1 km)]

(3) Conversion from SI Value to Top of Atmosphere Radiance

To convert SI value to top of atmosphere radiance $[L]_{ch,l,p}$, extract the lower 14 bit of SI value ($[SI]_{ch,l,p}$) and calculate as follows using $slope$, $offset$ values stored to Level1B product. In addition, because of the sensor specification, band that is saturated depending on the observed target exists. Here, *l* indicates line and *p* indicates pixel.

$$[L]_{band,l,p} = [slope]_{band} \times [SI]_{band,l,p} + [offset]_{band}$$

(4) Conversion from SI Value to Top of Atmosphere Reflectance (solar zenith angle non-correction)

Regarding VNR and SWIR, to convert SI value to top of atmosphere reflectance $[R]_{ch,l,p}$, extract the lower 14 bit of SI value ($[SI]_{ch,l,p}$) and calculate as follows using $slope\_reflectance$, $offset\_reflectance$ values stored to Level1B product.. The solar-earth

distance is corrected for $[R]_{ch,l,p}$, but $\cos\theta_{solar\_zenith}$ is not corrected. In addition, Table 4-2 shows the average solar irradiance F_0 of each band normalized at 1AU.

$$[R]_{band,l,p} = [slope\_reflectance]_{band} \times [SI]_{band,l,p} + [offset\_reflectance]_{band}$$

Table 4-2 Average Solar Irradiance F_0 (at 1AU)

Band*1	F0[W/m^2/um]*2	Band*1	F0[W/m^2/um]*2
VN01	1092.1436	VN10	956.2323
VN02	1712.1531	VN11	956.5352
VN03	1898.3185	PL01	1503.605
VN04	1938.4602	PL02	956.8333
VN05	1850.9604	SW01	646.5213
VN06	1797.1344	SW02	361.2250
VN07	1502.5667	SW03	237.5784
VN08	1502.3177	SW04	84.2413
VN09	1245.3663		

*1 For VNR-NP, the value of Nadir telescope is shown.

*2 Thuillier et al., The Solar Spectral Irradiance from 200 to 2400 nm as measured by the Solspec Spectrometer from the Atlas and Eureca Missions, Solar Physics, 214 (1): 1-22, May 2003.

4.1.3.3 **Level1 Product Granule ID Definition**

Granule ID means the code that enables to uniquely identify the earth observation satellite data. The file name of product is appended the extension ".h5" that indicates HDF5 file after Granule ID. Table 4-3 shows the granule ID assignment rules for Level1 product. Table 4-4 and Table 4-5 show the granule ID setting values.

Table 4-3 Level1 Product Granule ID

ID	Scene ID																			Product ID																					
Byte	1	2	3	4	5	6	7	8	9	10	11	12	13	14	15	16	17	18	19	20	21	22	23	24	25	26	27	28	29	30	31	32	33	34	35	36	37	38	39	40	41
GID	G	C	1	S	G	1	_	Y	Y	Y	Y	M	M	D	D	H	H	m	m	s	P	P	P	S	S	_	L	L	x1	x2	_	K	K	K	m	r	_	a	p	p	p
Example	G	C	1	S	G	1	_	2	0	1	1	1	1	1	3	2	3	4	5	A	0	1	2	0	6	_	1	B	S	G	_	I	R	S	N	K	_	z	0	0	1
Parameter	Satellite (fix)			Sensor (fix)			_	Year				Month		Day		Hour		min		sec	Path*2			Scene *3		_	Level *4		Type *5*6		_	subsystem *7			mode*8	resolution*9	_	algorithm ver.*10	parameter ver. *11		
								Observation start UT*1																																			

Table 4-4 Level1 Product Granule ID Setting Value

No.	GID	Item	Details	Note
*1.	YYYYMMDD HHmms	Observation start UT	Set the ideal start time of product. As there is some overlap before and after product, it does not match with the time of product start line (UTC time) The number of seconds is expressed by single alphabet.	Table 4-5
*2.	PPP	Path	Set the path number. Setting value: 1 to 485	See 4.1.3.3 (1)
*3.	SS	Scene	Set the scene number. Setting value: 1 to 24	See (2)
*4.	LL	Level	Set the processing level. Case of L1A: 1A Case of L1B/L1B (Low resolution resampling) : 1B	―
*5.	x1	Type	Fix to S (standard product)	―
*6.	x2	Type	Set the processing type for each operation. Case of standard processing (global): G Case of near-real time processing (around Japan): L Case of near-real time processing (global): N	See 4.1.3.3 (3)
*7.	KKK	subsystem	Set the type of observation data. Case of VNR-NP: VNR Case of VNR-PL: POL Case of IRS (SWIR+TIR): IRS	―
*8.	m	mode	Set the type of daytime/nighttime observation. [Standard product] Case of daytime observation (Day): D Case of nighttime observation (Night): N [Calibration product] Solar calibration: S Internal lamp calibration: L Electrical calibration: E Maneuver: M	To link to VNR sensor's ON/OFF, it may not match with the ground surface status (Daytime/Nighttime) in calibration mode or irregular observation. See 4.1.3.3 (4).
*9.	r	resolution	Set the resolution. K: 1000 m L: 1000 m (Low resolution resampling) Q：250 m Case of IRS, there additional exist four types: H, Y, X, and M. See Table 4-6.	See 4.1.3.3 (5)
*10.	a	algorithm ver.	Set the algorithm version. Setting value: 0 to 9, A t Z.	―
*11.	ppp	parameter ver.	Set the parameter version. Setting value: 000～999.	―

Table 4-5 Symbols for Seconds in Level1 Product Granule ID

Symbol for number of seconds	Number of seconds
A	00≦sec＜03
B	03≦sec＜06
C	06≦sec＜09
D	09≦sec＜12
E	12≦sec＜15
F	15≦sec＜18
G	18≦sec＜21
H	21≦sec＜24
J	24≦sec＜27
K	27≦sec＜30
L	30≦sec＜33
M	33≦sec＜36
N	36≦sec＜39
P	39≦sec＜42
Q	42≦sec＜45
R	45≦sec＜48
S	48≦sec＜51
T	51≦sec＜54
U	54≦sec＜57
V	57≦sec＜60
W	60≦sec＜61

(1) Path Number

The path is defined as the satellite passes from the ascending node to the North pole, the South pole and then reaches the ascending node again, and the path number increases toward the west at the adjacent orbit interval. The recurrent period of GCOM-C is 34 days, and the number of orbits is 485. Figure 4-3 to Figure 4-5 show the orbit of path per 30.

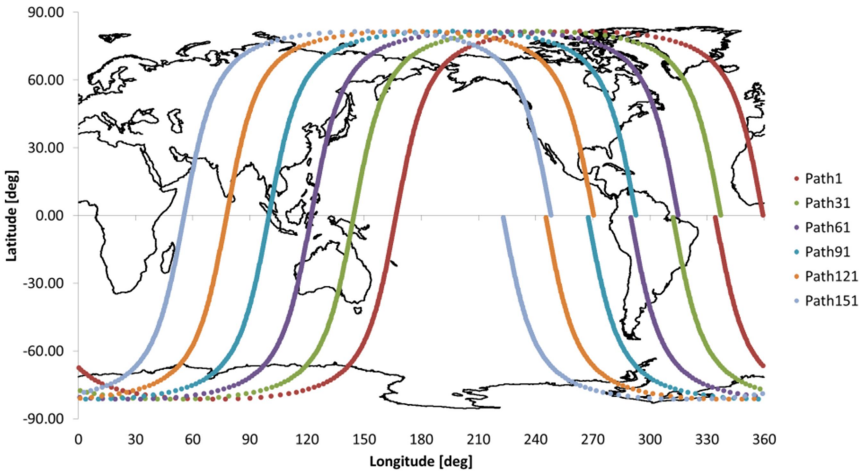

Figure 4-3 GCOM-C Path Definition (Path 1 to 151)

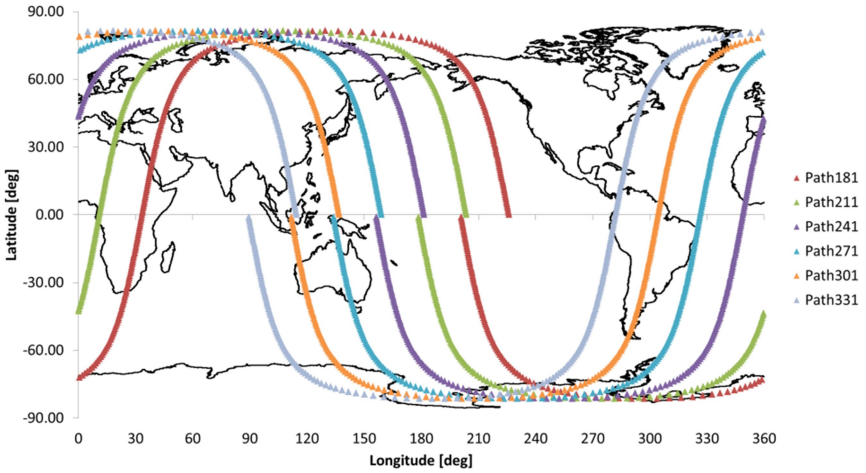

Figure 4-4 GCOM-C Path Definition (Path 181 to 331)

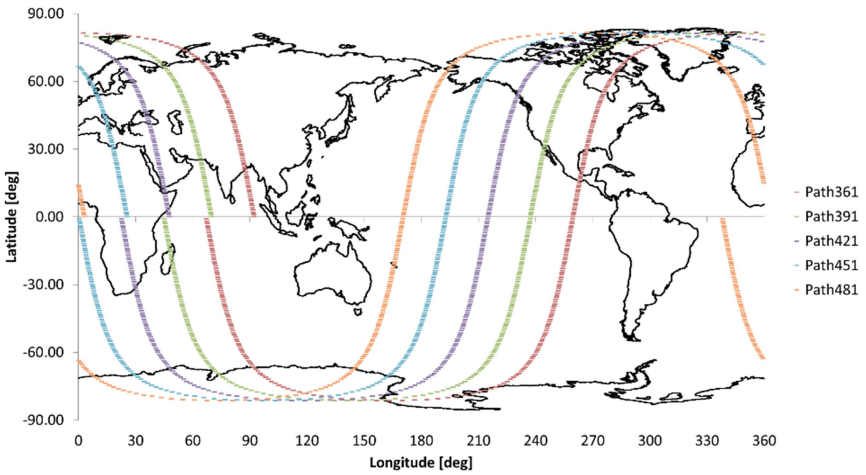

Figure 4-5 GCOM-C Path Definition (Path361 to 481)

(2) Scene Number

The scene is defined the unit of Level1 processing. In VNR-NP and IRS, a scene is the range of 1/24 of the orbit. After passing the ascending node, the scene with the earliest observation time is numbered 01, and the scene number is increased by 1 for each of the following scenes in sequence. When a scene is divided into multiple product, since those products are originally one scene, multiple product with the same scene number with different observation times are generated.

In VNR-PL, a scene is defined as the range including the whole daytime observation region within one orbit. Therefore, the scene number is fixed to 00.

(3) Standard/Near-real time Processing

The near-real time product is generated placing the highest priority to the compliance to the delivery time requirement, and therefore, it may be different from the range of scene generation in standard processing. The lists of near-real time products are shown in 3.5.2

(4) Daytime/Nighttime

In basic observation pattern, SGLI keeps observing the data of VNR and IRS in daytime. In nighttime, VNR observation is stopped, and SWIR of IRS is switched ON/OFF depending on the observing regions. However, TIR of IRS keeps observing regardless of day/night.

During the period that observation is stopped, no product is generated in principle. However, in cases such as that either one of TIR or SWIR is stopped, the observation suspension is short, or the timing of observation start is slightly off between VNR and IRS, the missing value is stored to the corresponding data within a product.

The basic concept of SGLI operation during daytime and nighttime is provided in 2.2.4

(5) Spatial Resolution

Since SGLI observes by switching the spatial resolution, the resolution identifications in granule ID are shown in Table 4-6. In particular, SWIR and TIR data are stored in one product for IRS, the ID identification is varied depending on the combinations of the spatial resolution.

Table 4-6 Spatial Resolution Identification

Product Type	VNR-NP Product	VNR-PL Product	IRS Product		
Resolution Symbol	Resolution	Resolution	SW01,02,04 Resolution	SW03 Resolution	TIR Resolution
K	1 km	1 km	1 km	1 km	1 km
			OFF		1 km
			1 km	1 km	OFF
H	—	—	1 km	1 km	500 m
			OFF		500 m
Y	—	—	1 km	1 km	250 m
X	—	—	1 km	250 m	1 km
M	—	—	1 km	250 m	500 m
Q	250 m	—	1 km	250 m	250 m
			OFF		250 m
			1 km	250 m	OFF
L	1 km (Low resolution resampling)	—	1 km	1 km (Low resolution resampling)	1 km (Low resolution resampling)
			1 km	1 km (Low resolution resampling)	1 km
			1 km	1 km	1 km (Low resolution resampling)

4.1.4 **Level2 Product**

The Level 2 product is processed using Level1B and Level2 product of upstream of the processing flow as the input and are stored the geophysical variables. The types of Level2 product are shown in Table 4-7 and Table 4-8, and the types of statistic products of Level2 products are shown in Table 4-9.

Table 4-7 List of Level2 Product (1/2)

Level2	Parameter	Generation Unit	Temporal Statistics 01D : 1 day 08D : 8 days 01M : 1 month	Product ID	Resolution K : 1 km H : 500 m Q : 250 m F : 1/24 deg C : 1/12 deg		
Ocean	Normalized water leaving radiance Photosynthetically available radiation Atmosphere correction parameter	Scene	-	NWLR	K	Q	
	Chlorophyll-a concentration Total suspended matter concentration Colored dissolved organic matter	Scene	-	IWPR	K	Q	
	Sea surface temperature	Scene	-	SST	K	H	Q
Cryosphere	Okhotsk sea-ice distribution	Scene	-	OKID	K	Q	
	Snow and Ice cover extent	Tile	01D	SICE	K	Q	
	Snow surface properties	Tile	01D	SIPR	K	Q	
Land	Top of atmosphere radiance	Tile	01D	LTOA	K	Q	
	Land atmospheric corrected reflectance	Tile	01D	RSRF	Q		
	Vegetation index	Tile	01D	VGI_	Q		
	Leaf area index Fraction of absorbed PAR	Tile	01D	LAI_	Q		
	Above-ground biomass Vegetation roughness index	Tile	01D	AGB_	Q		
	Land surface temperature	Tile	01D	LST_	Q		

Table 4-8 List of Level2 Product (2/2)

Level2	Parameter	Generation Unit	Temporal Statistics 01D : 1 day 08D : 8 days 01M : 1 month	Product ID	Resolution K : 1 km H : 500 m Q : 250 m F : 1/24 deg C : 1/12 deg		
Atmosphere	Cloud flag	Tile	01D	CLFG	K	Q	
	Cloud properties	Tile	01D	CLPR	K		
	Aerosol by Non-Polarization	Tile	01D	ARNP	K		
	Aerosol by Polarization	Tile	01D	ARPL	K		
Atmosphere (Global)	Top of atmosphere radiance (global)	Global	01D	LTOA	F		
	Top of atmosphere radiance with clear pixels (global)	Global	01D	LCLR	F		
	Cloud flag (global)	Global	01D	CLFG	F		
	Cloud properties (global)	Global	01D	CLPR	F		
	Aerosol by Non-Polarization (global)	Global	01D	ARNP	F		
	Aerosol by Polarization (global)	Global	01D	ARPL	F		

Table 4-9 List of Level2 Statistical Product

Level2 Statistics	Parameter	Generation Unit	Temporal Statistics 01D : 1 day 08D : 8 days 01M : 1 month		Product ID						Resolution K : 1 km H : 500 m Q : 250 m F : 1/24 deg C : 1/12 deg
Cryosphere (Statistics)	Snow and Ice cover extent (statistic)	Tile	08D	01M	SICE						K
	Snow and ice surface temperature (statistic)	Tile	08D	01M	SIPR						K
	Snow grain size of shallow layer (statistic)	Tile	08D	01M	SGSL						K
Land (Statistics)	Top of atmosphere radiance (statistic)	Tile	08D	01M	LTOA						Q
	Land atmospheric corrected reflectance (statistic)	Tile	08D	01M	RV01 *1	RV02 *1	RV03 *1	RV04 *1	RV05 *1	RV06 *1	Q
					RV07 *1	RV08 *1	RV09 *1	RV10 *1	RV11 *1	RS01 *2	Q
					RS02 *2	RS03 *2	RS04 *2	RT01 *2	RT02 *2	GEOV *6	Q
					GEOI *6	RN08 *5	RN11 *5	RP01 *4	RP02 *4	GEOP *6	Q
	Normalized vegetation index (statistic)	Tile	08D	01M	NDVI						Q
	Enhanced vegetation index (statistic)	Tile	08D	01M	EVI_						Q
	Shadow index (statistic)	Tile	08D	01M	SDI_						Q
	Leaf area index (statistic)	Tile	08D	01M	LAI_						Q
	Fraction of absorbed PAR (statistic)	Tile	08D	01M	FPAR						Q
	Above-ground biomass (statistic)	Tile	08D	01M	AGB_						Q
	Vegetation roughness index (statistic)	Tile	08D	01M	VRI_						Q
	Land surface temperature (statistic)	Tile	08D	01M	LST_						Q

*1 RVxx : VNR-NP Band xx Reflectance
*2 RSxx : IRS-SWIR Band xx Reflectance
*3 RTxx : IRS-TIR Band xx Reflectance
*4 RPxx : VNR-PL Band xx Reflectance
*5 RNxx : Reflectance of VNR-NP Band xx co-registered for VNR-PL
*6 GEO : Geometry(V:VNR-NP, I:IRS, P:VNR-PL)

4.1.4.1 **Level2 Product Generation Unit**

As shown in Table 4-7 and Table 4-8, the generation unit of Level2 product is scene, tile, or global. The scene product definitions are same as Level1 product shown in 4.1.3.3 (2).

The product storing the global range by EQA (sinusoidal equal area) projection shown in Figure 4-6 is defined as a global product and each region divided by grids is defined as a tile. The tile and global products are generated in the satellite's direction of the ascending and descending respectively. The latitude/longitude to each pixel of the tile can be calculated as below:

For the tile whose latitude/longitude (lat,lon) is to be calculated, the pixel number of the pixel in vertical direction (top => bottom) is defined as lin, and that in horizontal direction (left => right) is defined as col. The pixel number of the upper left pixel within a tile is defined as (0,0).

e.g.) Case of resolution 250 m [Image size 4800 x 4800 pixel, tile number v05h29]

- $lin_{tile} = 4800$: Number of pixels in vertical direction in a tile (corresponds to 250 m)
- $col_{tile} = 4800$: Number of pixels in horizontal direction in a tile (corresponds to 250 m)
- $vtile = 5$: Tile number in vertical direction
- $htile = 29$: Tile number in horizontal direction
- $vtile_{num} = 18$: Total number of tiles in vertical direction
- $htile_{num} = 36$: Total number of tiles in horizontal direction
- NL : Total number of pixels from south pole to north pole
- NP_0 : Total number of pixels in east-west direction at the equator

$d = 180.0/lin_{tile}/vtile_{num}\ [deg/pixel]$

$NL = 180.0/d$ (from S-pole to N-pole)

$NP_0 = 2 \times NINT[180.0/d]$ (from 180W to 180E)

$lin_{total} = lin + (vtile \times lin_{tile})$

$col_{total} = col + (htile \times col_{tile})$

The latitude/longitude (lat,lon) are as follows:

$$lat = 90.0 - (lin_{total} + 0.5) \times d$$

$$NP_i = NINT[NP_0 \times cos(lat)]$$

$$lon = 360.0/NP_i \times (col_{total} - NP_0/2 + 0.5)$$

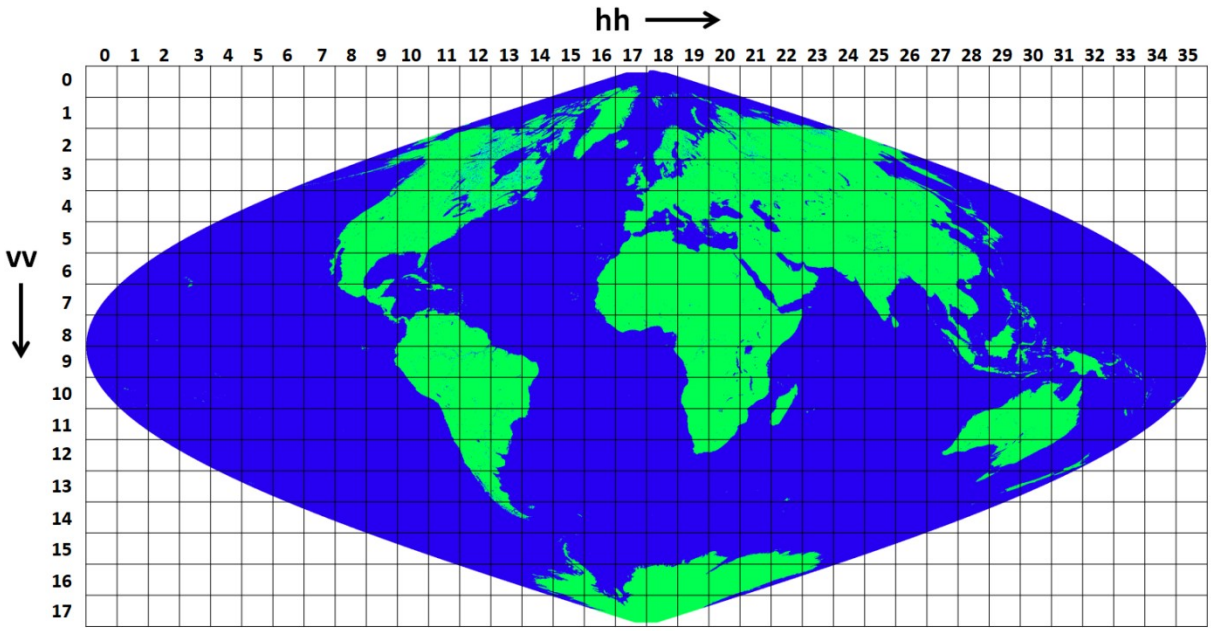

Figure 4-6 EQA (sinusoidal equal area) projection

4.1.4.2 **Level2 Product Granule ID Definition**

Table 4-10 and Table 4-11 show the granule ID assignment rule for Level2 product (scene) and Level2 product (tile and global), respectively. In addition, the setting values are shown in Table 4-12 and Table 4-13 respectively.

Near-resl time Level2 product (tile) name is defined by adding sequence value to granule ID (Granule ID_nnn.h5, nnn is three digit integer). Multiple products with the same granule ID are created in the case of observing the same tile more than once a day. Sequence value is assigned in the order observed from 000 and it is possible to distinguish these products.

Table 4-10 Level2 Product (Scene) Granule ID

ID	Scene ID																				Product ID																									
Byte	1	2	3	4	5	6	7	8	9	10	11	12	13	114	15	16	17	18	19	20	21	22	23	24	25	26	27	28	29	30	31	32	33	34	35	36	37	38	39	40	41			
GID	G	C	1	S	G	1	_	Y	Y	Y	Y	M	M	D	D	H	H	m	m	s	P	P	P	S	S	_	L	L	x1	x2	_	K	K	K	K	r	_	a	p	p	p			
Example	G	C	1	S	G	1	_	2	0	1	1	1	1	1	3	2	3	4	5	6	0	1	2	0	6	_	L	2	S	G	_	S	S	T	D	K	_	1	0	0	1			
Parameter	Satellite (fix)			Sensor (fix)			_	Year			Month	Day		Hour		min		sec		Path *1			Scene *1		_	Level *2		Type *1		_	Subsystem *3				Resolution*1	_	algorithm ver.*1		parameter ver. *1					
								Observation start UT*1																																								

Table 4-11 Level2 Product (Tile/Global) and Level3 Product Granule ID

ID	Scene ID																					Product ID																									
Byte	1	2	3	4	5	6	7	8	9	10	11	12	13	114	15	16	17	18	19	20	21	22	23	24	25	26	27	28	29	30	31	32	33	34	35	36	37	38	39	40	41			
GID	G	C	1	S	G	1	_	Y	Y	Y	Y	M	M	D	D	m	t	t	t	_	g	A	A	A	A	_	L	L	x1	x2	_	K	K	K	K	r	_	a	p	p	p			
Example	G	C	1	S	G	1	_	2	0	1	1	1	1	1	3	D	0	1	D	_	A	0	0	0	0	_	L	2	S	G	_	C	L	F	G	Q	_	1	0	0	1			
Parameter	Satellite (fix)			Sensor (fix)			_	Year			Month	Day		A/D*2	Process time unit *3		_	Mapping*4	Area tile no. *5			_	Level *6	Type *7*8		_	Subsystem *9				Resolution*10	_	algorithm ver.*11		parameter ver. *12										
								Observation start UT*1																																								

Table 4-12 Level2 Product (Scene) Granule ID Setting Value

No.	GID	Parameter	Description	Remarks
*1.	See Table 4-4 Level1 Definition			
*2.	LL	Level	Set the processing level: L2	―
*3.	KKKK	subsystem	Set the product ID.	See Table 4-7 for product ID

Table 4-13 Level2 Product (Tile/Global) and Level 3 Product Granule ID Setting Value

No.	GID	Parameter	Description	Remarks
*1.	YYYYMMDD	Observation start UT	Set the observation start time. UTC time system, round down to minute.	―
*2.	m	A/D	Set the satellite's direction. Ascending : A Descending : D	―
*3.	ttt	Process time unit	Period of statistic data 1 day : 01D 8 days : 08D 1 month : 01M	―
*4.	g	Mapping	Map projection EQA (1- dimension) : X EQA : A EQR : D PS-N : N PS-S : S Tile : T	―
*5.	AAAA	Area tile no.	Tile number vvhh vv: Vertical direction number (00 to 17) hh: Horizontal direction number (00 to 35)	―
*6.	LL	Level	Set the processing level L2 : L2 L3Bin statistic : 3B L3Map : 3M	―
*7.	x1	Type	Fixed to S (standard product).	―
*8.	x2	Type	Set the type of processing for each operation. Case of standard processing (global): G Case of near-real time processing (around Japan): L Case of near-real time processing (global): N	―
*9.	KKKK	subsystem	Set the product ID.	See Table 4-7, Table 4-8, and Table 4-9 for product ID.
*10.	r	resolution	Set the resolution. Case of 1000 m: K Case of 250 m: Q Case of 1/24 deg: F Case of 1/12 deg: C	―
*11.	a	algorithm ver.	Set the algorithm version. Setting value: 0 to 9, A to Z.	―

*12.	ppp	parameter ver.	Set the parameter version. Setting value: 000 to 999.	－

4.1.5 **Level3 Product**

The Level3 product uses Level2 products as input and calculates the temporal statistics and spatial statistics of various geophysical variables. Table 4-14 shows the types of L3 products.

Table 4-14 List of Level3 Product (1/2)

	Parameter	Generation Unit	Temporal Statistics 01D : 1 day 08D : 8 days 01M : 1 month			Projection 3B : EQA 3M : EQR PS : Polar Stereo			Product ID						Resolution F : 1/24 deg C : 1/12 deg
Ocean (L3)	Normalized water leaving radiance	Global	01D	08D	01M	3B	3M		L380	L412	L443	L490	L530	L565	F
									L670						
	Photosynthetically Available radiation	Global	01D	08D	01M	3B	3M		PAR_						F
	Atmospheric correction parameter	Global	01D	08D	01M	3B	3M		T670	T865					F
	Chlorophyll-a concentration	Global	01D	08D	01M	3B	3M		CHLA						F
	Total suspended matter concentration	Global	01D	08D	01M	3B	3M		TSM_						
	Colored dissolved organic matter	Global	01D	08D	01M	3B	3M		CDOM						F
	Sea surface temperature	Global	01D	08D	01M	3B	3M		SST_						F
Cryosphere (L3)	Snow and Ice cover extent	Global/Polar region	01D	08D	01M	3B	3M	PS	SICE						F
	Snow and ice surface Temperature	Global/Polar region	01D	08D	01M	3B	3M	PS	SIST						F
	Snow grain size of shallow layer	Global/Polar region	01D	08D	01M	3B	3M	PS	SGSL						F
Land (L3)	Land atmospheric corrected reflectance	Global	01D	08D	01M	3B	3M		RV01 *1	RV02 *1	RV03 *1	RV04 *1	RV05 *1	RV06 *1	F
									RV07 *1	RV08 *1	RV09 *1	RV10 *1	RV11 *1	RS01 *2	
									RS02 *2	RS03 *2	RS04 *2	RT01 *3	RT02 *3	GEOV *6	
									GEOI *6	RN08 *5	RN11 *5	RP01 *4	RP02 *4	GEOP *6	
									SNZV *7	SLZV *8	RLAV *9	SNZP *7	SLZP *8	RLAP *9	
									SNZI *7	SLZI *8	RLAI *9				
	Normalized vegetation index	Global	01D	08D	01M	3B	3M		NDVI						F
	Enhanced vegetation index	Global	01D	08D	01M	3B	3M		EVI_						F

Table 4-15 List of Level3 Product (2/2)

	Parameter	Generation Unit	Temporal Statistics 01D : 1 day 08D : 8 days 01M : 1 month			Projection 3B : EQA 3M : EQR PS : Polar Stereo			Product ID						Resolution F : 1/24 deg C : 1/12 deg
Land (L3)	Shadow index	Global	01D	08D	01M	3B	3M		SDI_						F
	Leaf area index	Global	01D	08D	01M	3B	3M		LAI_						F
	Fraction of absorbed PAR	Global	01D	08D	01M	3B	3M		FPAR						F
	Above-ground biomass	Global	01D	08D	01M	3B	3M		AGB_						F
	Vegetation roughness index	Global	01D	08D	01M	3B	3M		VRI_						F
	Land surface temperature	Global	01D	08D	01M	3B	3M		LST_						F
Atmosphere (L3)	Classified cloud fraction	Global	01D	08D	01M	3B	3M		CFR1	CFR2	CFR3	CFR4	CFR5	CFR6	C
									CFR7	CFR8	CFR9	CFRA	CFRH	CFRM	
									CFRL						
	Cloud top temperature	Global	01D	08D	01M	3B	3M		CLTT						C
	Cloud top height	Global	01D	08D	01M	3B	3M		CLTH						C
	Water cloud optical thickness	Global	01D	08D	01M	3B	3M		COTW						C
	Water cloud effective radius	Global	01D	08D	01M	3B	3M		CERW						C
	Ice cloud optical thickness	Global	01D	08D	01M	3B	3M		COTI						C
	Aerosol optical thickness over ocean	Global	01D	08D	01M	3B	3M		AOTO						C
	Aerosol optical thickness over land (near ultraviolet)	Global	01D	08D	01M	3B	3M		AOTL						C
	Aerosol angstrom index over ocean	Global	01D	08D	01M	3B	3M		AAEO						C
	Aerosol angstrom index over land (near ultraviolet)	Global	01D	08D	01M	3B	3M		AAEL						C
	Aerosol optical thickness over land (polarized)	Global	01D	08D	01M	3B	3M		AOTP						C
	Aerosol angstrom index over land (polarized)	Global	01D	08D	01M	3B	3M		AAEP						C
	Single scattering albedo over land	Global	01D	08D	01M	3B	3M		ASSA						C

*1 - *6 : Same as Table 4-9

*7 SNZ : Sensor Zenith Angle (V:VNR-NP, I:IRS, P:VNR-PL)

*8 SLZ : Solar Zenith Angle (V:VNR-NP, I:IRS, P:VNR-PL)

*9 RLA : Relative Azimuth Angle (V:VNR-NP, I:IRS, P:VNR-PL)

4.1.5.1 **Level3 Product Generation Unit**

As shown in Table 4-14 and Table 4-15, the Level3 products is projected to EQA and EQR (equirectangular), or PS (polar stereographic). Figure 4-7 shows the definition of EQA projection (1-dimension), Figure 4-8 shows the definition of EQR projection, and Figure 4-9 shows the definition of PS projection.

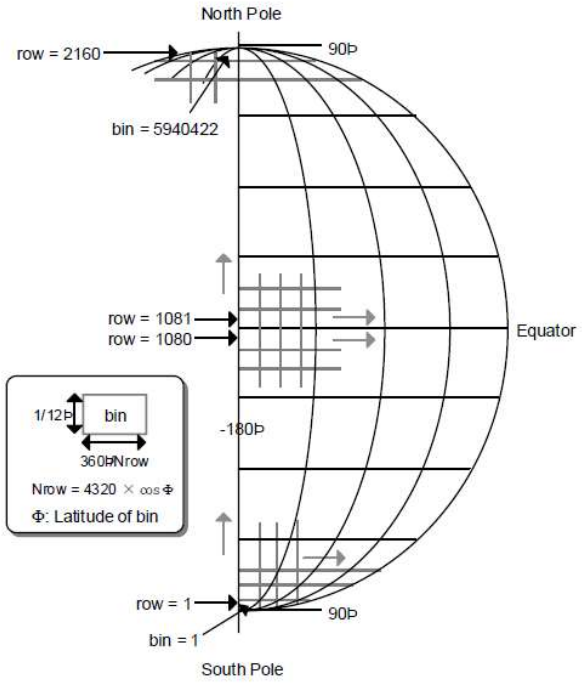

In the above figure, if latitude of a row center is Φ, the number of binned grids including the row is calculated from the following equation.
Number of binned grids (Nrow) = [4320 x cos Φ] (where, [ ] means half adjust)
Ex. (Number of binned grids included in a row): raw 1→ 3 grids, row 2→ 9 grids ‥ row 1080→ 4320 grids ‥ row 2160 → 3 grids

Figure 4-7 Definition of Level3 Product EQA projection (1-Dimension)

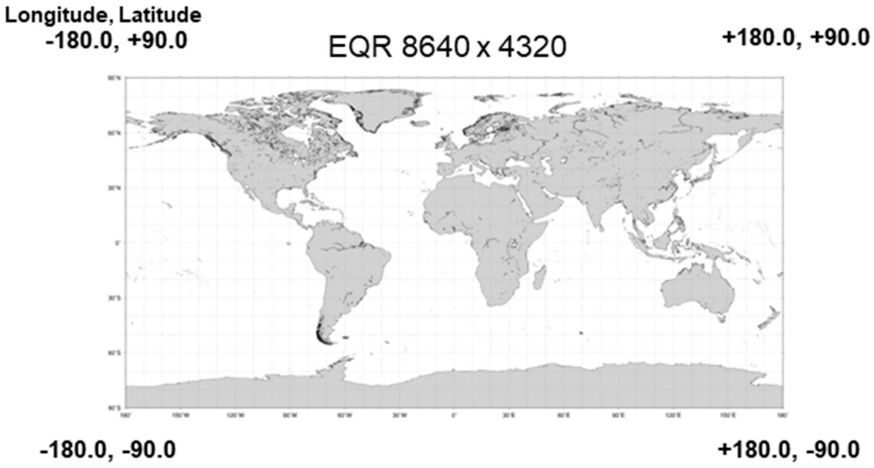

Figure 4-8 Definition of Level3 Product EQR projection

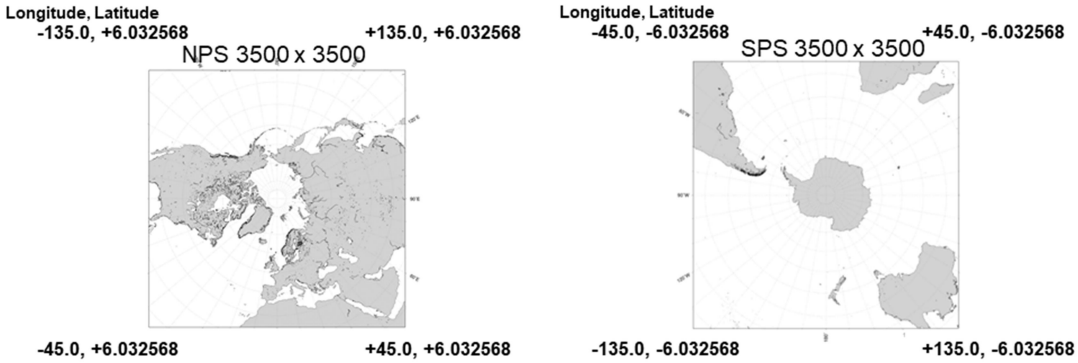

Figure 4-9 Definition of Level3 Product PS projection

4.1.5.2 **Level3 Product Granule ID Definition**

The definition of Level3 product granule ID is shown in Table 4-11, and the product ID is shown in Table 4-14 and Table 4-15.

4.2 Level1 Processing Algorithms

4.2.1 Precondition

SGLI observes four data shown in Table 4-16 using each sensor.

Table 4-16 Brief Overview of SGLI Sensor

No.	Sensor	Number of Channels	Description of Observation Data
1.	VNR-NP	11 ch	Observation of the strength of lights reflected or absorbed by atmosphere and land surface by NP sensor (non-polarized).
2.	VNR-PL	2 ch (3 polarizers)	Observation of the polarization status of lights reflected or absorbed by atmosphere and land surface by PL sensor (polarized).
3.	IRS SWIR	4 ch	Observation by SWIR (Short wavelength Infrared) of IRS.
4.	IRS TIR	2 ch	Observation by TIR (Thermal Infrared) of IRS.

The brief overview of Level1 processing is provided in Table 4-17, and the processing flow of each sensor is shown in Figure 4-9 to Figure 4-13. Please refer to ATBD (Algorithm Theoretical Basis Documents) and Level1 Implementation Processing Document for more details of each process.

Table 4-17 Brief Overview of Level1 Process

No.	Process	Brief Description	Remarks
1	Preprocessing	・Depacketing from RAW data ・Engineering value conversion ・Data check ・Check for loss ・Calculation of geometric information	—
2	Radiometric information calculation	・Calculation of radiometric parameter (Gain/Offset)	—
3	Radiometric correction	・Calculation of radiance (radiometric correction)	—
4	Conversion to Level1B reference coordinate	・Calculation of conversion coefficient to convert to Level1B reference coordinate	—
5	Level1A geometry information calculation	・Calculation of observation time of L1A line ・Calculation of latitude/longitude information of each pixel (WGS84 coordinate system)	—
6	Stray light correction	・Stray light correction ・Stray light flag calculation	IRS-TIR excluded
7	Stripe noise correction	・If there is any stripe noise or radiometric gap between telescope of VNR-NP, remove such stripe.	—
8	Re-replacement of radiance to Level1B reference coordinate	・Replacement of radiance after stray light correction process to Level1B reference coordinate.	—
9	Second Stripe noise correction	・Removal of stripe noise that remained after radiometric and No. 7 corrections.	Implement after launch as needed.
10	Stokes vector calculation	・Conversion to stokes vector.	VNR-PL only
11	Land-water flag calculation	・Calculation of land-water ratio of footprint of each pixel.	—
No.	Processing	Brief Description	Remarks
1	Resampling to low resolution product	・Resampling of high resolution (250 m or 500 m) product to low resolution (1 km) product	VNR-PL excluded

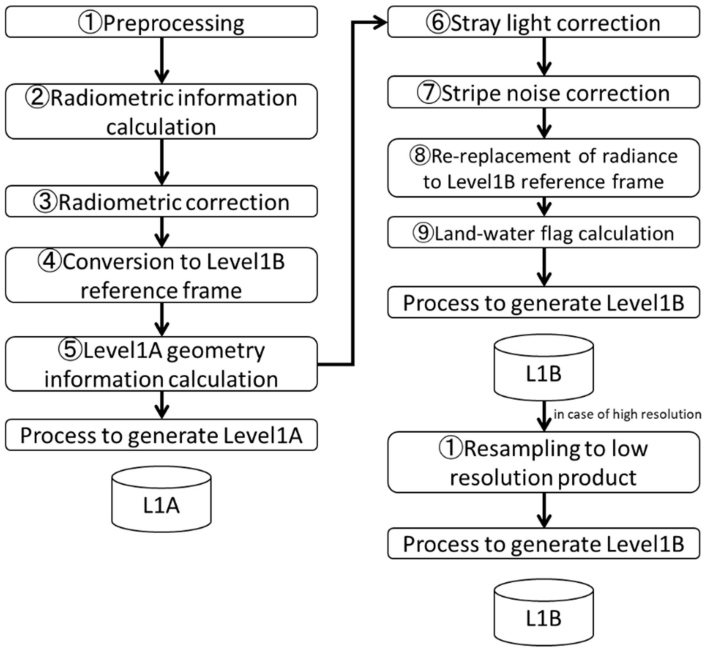

Figure 4-10 VNR-NP Level1 Processing Flow

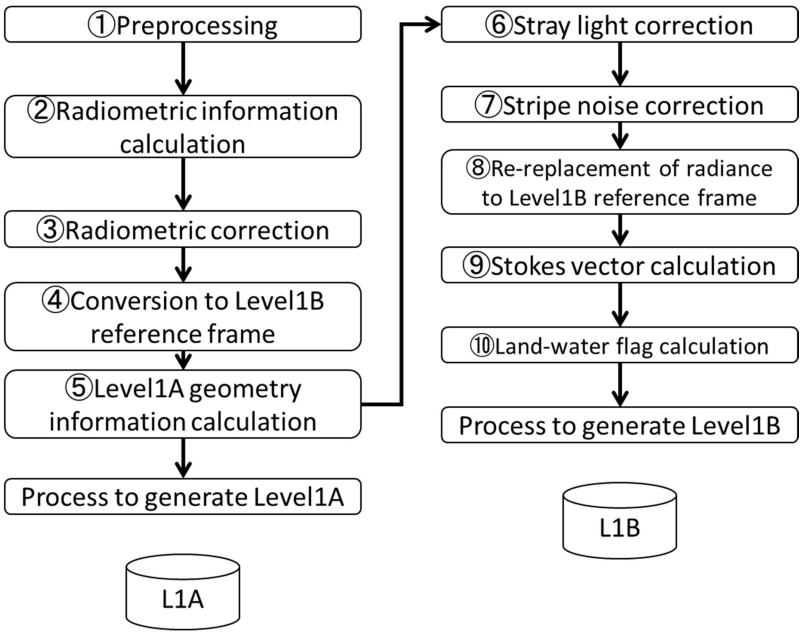

Figure 4-11 VNR-PL Level1 Processing Flow

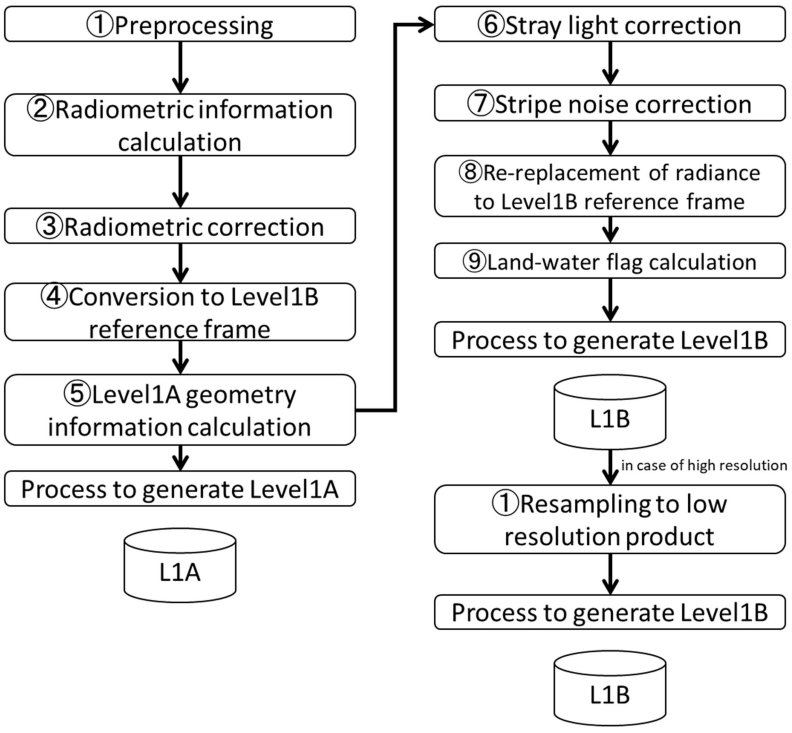

Figure 4-12 IRS-SWIR Level1 Processing Flow

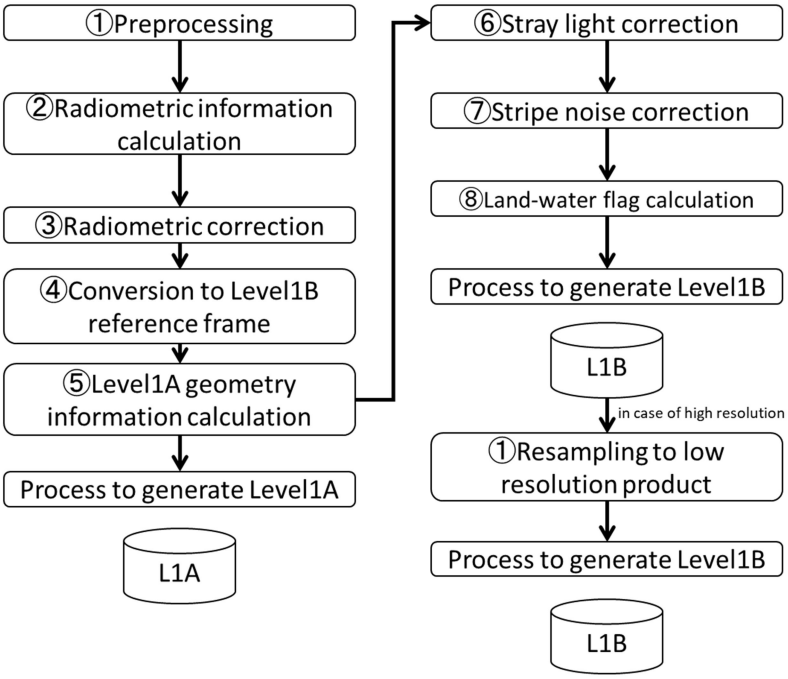

Figure 4-13 IRS-TIR Level1 Processing Flow

4.2.2 **Level1 Processing**

4.2.2.1 **Preprocessing**

Input in Level1A processing of normal processing is ASD or Level0 data (mission data, real-time PCD telemetry) file. Preprocessing consists of multiple processes. Preprocessing inputs the orbit and attitude data to calculate geometry information, corrects the observation time in each scene and distinguishes the calibration product. Table 4-18 shows the overview of preprocessing.

In case of re-processing, instead of ASD data or Level0 data, the data equivalent to ASD (Level0 data) is extracted from the Level1A product to conduct the preprocessing.

Table 4-18 Overview of Preprocessing

No.	Process	Overview of Process
1	ASD input	Obtains mission data packet or real-time PCD packet from ASD file or Level0 data file and performs the following processing. ・Align packets and delete duplicate
2	Observation time calculation	Corrects or converts the time included in the mission data packet or real-time PCD packet obtained by ASD input process as follows. ・Convert GPS time to TAI93 time system ・Correction of DMS time ・Calculation of observation time
3	Calibration product discrimination	Distinguishes the observation data from the calibration data from the mission data packet obtained by ASD input process.
4	PCD information extraction	Extracts converted PCD data (orbit/ attitude information) from the real-time PCD packet.
5	ASD information extraction	Extracts the data stored in Level1A product in re-processing, and restores the packet of mission data or real-time PCD auxiliary data.
6	Mission data product conversion	Puts the mission packet data obtained by ASD input process into the format of each scan and extracts necessary information. ・Checks the observation data packet for loss, and generates packet lost information. ・Interpolates the lost observation time of scan. ・Extracts and calculates various information included in mission (observation) data packet and stores it in Raw_data, Ancillary_data of Level1 product. ・Interpolates tilt angle.
7	Scene trimming	Trims data at specified scene start time or scene end time.
8	Orbit data calculation	Calculates the satellite position and velocity that corresponds to attitude determination time.
9	Attitude data calculation	Calculates the attitude data of attitude determination time.
10	Geometry information calculation	Calculates following values using geometry information and earth orientation parameter. ・Solar azimuth angle in satellite coordinate system ・Solar zenith angle in satellite coordinate system ・Lunar azimuth angle in satellite coordinate system ・Lunar zenith angle in satellite coordinate system ・The angle between lunar direction vector and satellite Y-axis (IRS only)

4.2.2.2 **Radiometric Information Calculation**

The radiometric information is calculated for each sensor. Figure 4-14 shows the schematic diagrams of VNR-NP, VNR-PL, and IRS-SWIR processing (left) and IRS-TIR processing (right).

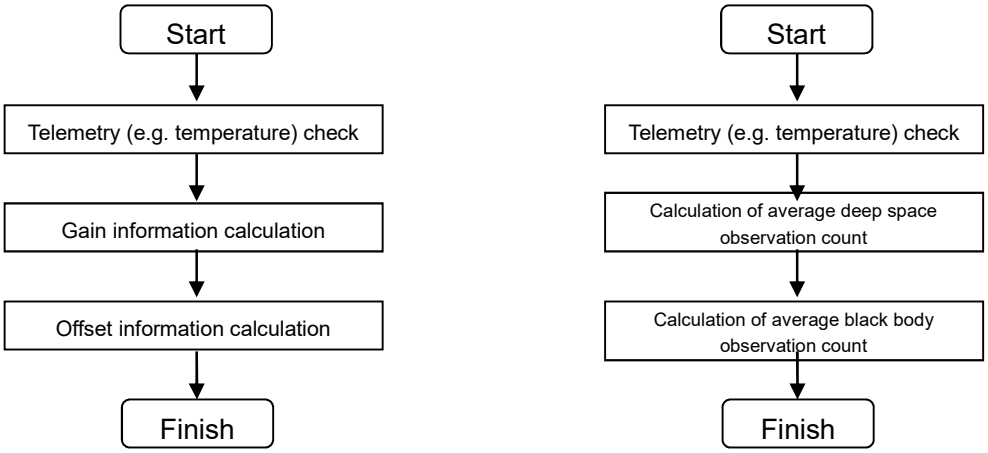

Figure 4-14 Radiometric Information Calculation: (left) NP/PL/SWIR, (right) TIR

(1) VNR-NP, PL

(a) Telemetry Check

Limit Check is performed to ASP (Analog Signal Processor) temperature and CCD temperature converted to count values, and the lines judged to be abnormal are not used for processing. The temperatures ($\overline{T^{ASP}}, \overline{T^{CCD}}$) in normal lines are used to calculate the temperature-dependent radiometric parameters.

(b) Gain Information Calculation

The total gain G_{total} is calculated for each telescope/band/pixel using the base gain G_0 characterized by pre-launch ground test, electrical shutter correction coefficient ΔG_{shutt}, temperature-dependency correction coefficient ΔG_{Temp}, and gain aging parameter ΔG_{period}.

$$\left\{[G_{total}]_{n_{poly}}\right\}_{k,ch,r,s,p} = [G_0]^{n_{poly}}{}_{k,ch,r,p} \cdot [\Delta G_{shutter}]_{k,ch,r,s,p} \cdot \left[\Delta G_{Temp}\right]_{k,ch,r,p} \cdot \left[\Delta G_{period}\right]_{k,ch,r,p}$$

Here, k is telescope, ch is band, r is resolution, s is scan, p is pixel, and $poly$ is polynomial order. Those parameters are updated according to the on-orbit calibration result.

(c) Offset Information Calculation

VNR sensors are performed multiple offset corrections. VNR sensors have pre/post pixels for offset correction. The pre/post Optical Black (OB) pixels near the observation pixels are shielded and structurally unexposed, and Scan pixels outside of OB structurally have only CCD without photodiode (PD). The sequence of pixel is shown in Table 4-19 and Table 4-20.

Using these Scan/OB pixels, Scan/OB offset correction value $DN_{obs}^{Scan/OB}$ is calculated line by line.

Table 4-19 Sequence of Pixels for VNR-NP Observation

VNR-NP	Blank	pre Scan	pre OB	dummy	OBS pixel	dummy	post OB	pre Scan	Blank
pixel	1-20	21-37	38-45	46	【1500 pixel (250 m)】 【375 pixel (1 km)】	47	48-55	56-91	73-92

Table 4-20 Sequence of Pixels for VNR-PL Observation

VNR-PL	pre Scan	pre OB	dummy	OBS pixel	dummy	post OB	pre Scan
pixel	1-34	35-44	45-46	【857 pixel (1 km)】	47-48	49-58	59-92

As the other offset correction, Dark Signal Non-Uniformity (DSNU) correction is performed for variation in pixel direction. $DN_{dsnu-offset}$ is held as a table and is updated according to the result of on-orbit calibration. The total offset value DN_{offset} is calculated as below.

$$\left[DN_{offset}\right]_{k,ch,r,s,p} = \left[DN_{obs}^{Scan/OB}\right]_{k,ch,r,s} + \left[DN_{dsnu-offse}\right]_{k,ch,r,p} + \left[DN_{period}\right]_{k,ch,r,p}$$

(2) IRS-SWIR

(a) Telemetry Check

Limit Check is performed SWIR focal plane temperature, ASP temperature, and pre-amplifier temperature, and the scans judged to be abnormal are not used for processing. The temperatures in normal lines are used to calculate the temperature-dependent radiometric parameters.

(b) Gain Calculation

The total gain G_{total} is calculated using the base gain G_0 characterized by pre-launch ground test, temperature-dependent correction coefficient ΔG_{Temp}, and gain aging parameter ΔG_{period}. The temperature-dependent correction coefficient ΔG_{Temp} consist of gain functions that depend respectively on detector temperature $\overline{T^{DET}}$, ASP temperature $\overline{T^{ASP}}$, and pre-amplifier temperature T^{PRE}

$$\left\{\left[G_{total}\right]_{n_{poly}}\right\}_{ch,r,l,s} = \left[G_0\right]^{n_{poly}}{}_{ch,r,l} \cdot \left[\Delta G_{Temp}\right]_{ch,r,s} \cdot \left[\Delta G_{period}\right]_{ch,r,l}$$

Here, ch is band, r is resolution, s is scan, l is line, and $poly$ is polynomial order. Those parameters are updated according to the on-orbit calibration result. The relationship between a line and pixel in IRS is shown in Figure 4-15.

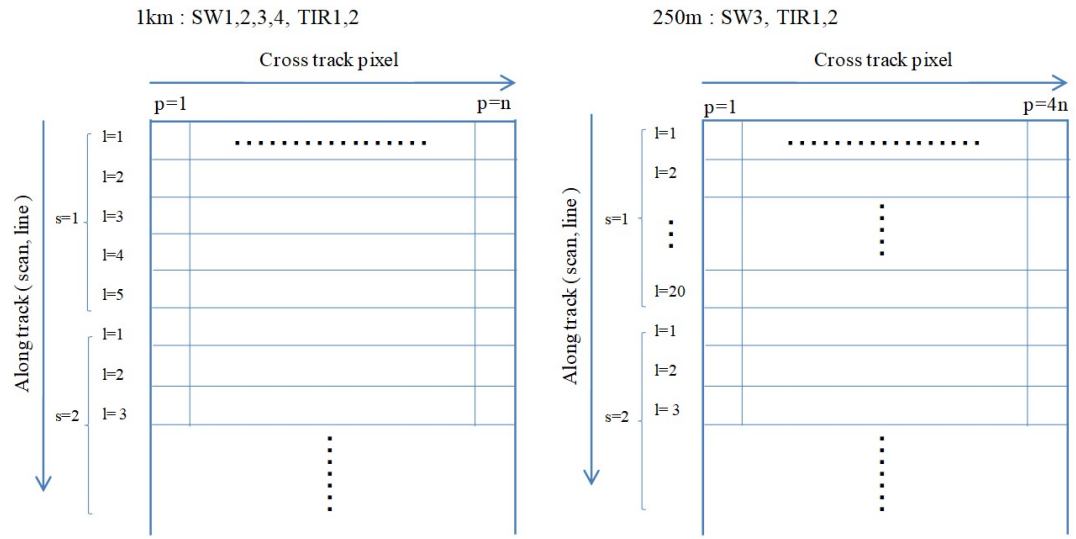

Figure 4-15 Relationship between IRS Lines and Pixels

(c) Offset Information Calculation

Using the deep space data observed per scan, the offset value DN_{offset} is calculated. The deep space data $\overline{DN_{DS}}$ is averaged over several pre/post scans to remove noises. ΔDN_{offset} is the correction parameter.

$$\left[DN_{offset}\right]_{ch,r,s,l} = \left[\overline{DN_{DS}}\right]_{ch,r,s,l} + \left[\Delta DN_{offset}\right]_{ch,r,l}$$

(d) Non-linearity Correction

Due to the leak current affected by ASP temperature, non-linearity correction is performed to DN value.

$$\left[DN_{obs\_nlc}\right]_{ch,r,s,l,p} = \left[DN_{obs}\right]_{ch,r,s,l,p} - \left[Leak_{obs}\right]_{ch,r,l}$$
$$\left[DN_{offset\_nlc}\right]_{ch,r,s,l} = \left[DN_{offset}\right]_{ch,r,s,l} - \left[Leak_{offset}\right]_{ch,r,l}$$

(3) IRS-TIR

(a) Telemetry Check

The average temperature $\left[\overline{T_{BB}}\right]_s$ is calculated for the black body temperature. In addition, limit check is performed on the temperature around black body, and considering the view factor analysis of calibration black body, weighted temperature $\left[\overline{T_{env}}\right]_s$ is calculated.

(b) Calculation of Average Deep Space Count

Using the deep space data observed per scan, the offset value DN_{offset} is calculated. The deep space data $\overline{DN_{DS}}$ is averaged over several pre/post scans to remove noises. $[\Delta DN_{DS}]_{tm,ch,r,l}$ is the correction parameter for average deep space observation count value.

$$\left[\overline{DN_{DS\_C}}\right]_{tm,ch,r,s,l} = \left[\overline{DN_{DS}}\right]_{tm,ch,r,s,l} + \left[\Delta DN_{DS}\right]_{tm,ch,r,l}$$

Here, *tm* is TDI mode, ch is band, r is resolution, s is scan and l is line.

(c) Calculation of Average Black Body Count

Similar to the deep space data, the black body data $\overline{DN_{BB}}$ is averaged over several pre/post scans to remove noises. $[\Delta DN_{BB}]_{tm,ch,r,l}$ is the correction parameter for average black body observation count.

$$\left[\overline{DN_{BB\_C}}\right]_{tm,ch,r,s,l} = [\overline{DN_{BB}}]_{tm,ch,r,s,l} + [\Delta DN_{BB}]_{tm,ch,r,l}$$

4.2.2.3 **Radiometric correction**

Using the radiometric information obtained in 4.2.2.2 the spectral radiance is calculated.

(1) VNR-NP, PL

The spectral radiance $[L]_{k,ch,r,s,p}$ is calculated from the following formula using the observed count $[DN_{obs}]_{k,ch,r,s,p}$ and the calculated gain and offset.

$$[L]_{k,ch,r,s,p} = \sum_{n=0}^{4}\{[G_{total}]_n\}_{k,ch,r,s,p} \cdot \left([DN_{obs}]_{k,ch,r,s,p} - \left[DN_{offset}\right]_{k,ch,r,s,p}\right)^n$$

(2) IRS-SWIR

The spectral radiance $[L]_{ch,r,s,l,p}$ is calculated from the following formula using the observed count $\left[DN_{obs\_nlc}\right]_{ch,r,s,l,p}$ and the calculated gain and offset.

$$[L_{SWI}]_{ch,r,s,l,p} = \sum_{n=0}^{4}\{[G_{total}]_n\}_{ch,r,l,p} \cdot \left(\left[DN_{obs\_nlc}\right]_{ch,r,s,l,p} - \left[DN_{offset\_nlc}\right]_{ch,r,s,l}\right)^n$$

(3) IRS-TIR

The non-linearity of TIR is corrected by offset adjustment function $[e]_{tm,ch,r,l}$.

$$[DN_{obs}{}']_{tm,ch,r,l} = [DN_{obs}]_{tm,ch,r,l} - [e]_{tm,ch,r,l}$$
$$\overline{[DN_{DS}{}']_{tm,ch,r,l}} = \overline{[DN_{DS\_C}]_{tm,ch,r,l}} - [e]_{tm,ch,r,l}$$
$$\overline{[DN_{BB}{}']_{tm,ch,r,l}} = \overline{[DN_{BB\_C}]_{tm,ch,r,l}} - [e]_{tm,ch,r,l}$$

TIR spectral radiance is calculated by the following formula using the nonlinearity correction and two-point calibration formula.

$[\kappa_{BB}]_{tm,ch}$ indicates the black body radiation factor. $\mathrm{B}(\lambda,T)$ is the Planck function of temperature T [K].

$$L_{TIR} = \frac{\sum_{n=0}^{4}\{[\beta']_n\}_{tm,ch,r,l} \cdot \left\{\left([DN_{obs}{}']_{tm,ch,r,l}\right)^n - \left(\overline{[DN_{DS}{}']_{tm,ch,r,l}}\right)^n\right\}}{\sum_{n=0}^{4}\{[\beta']_n\}_{tm,ch,r,l} \cdot \left\{\left(\overline{[DN_{BB}{}']_{tm,ch,r,l}}\right)^n - \left(\overline{[DN_{DS}{}']_{tm,ch,r,l}}\right)^n\right\}}$$
$$\cdot \left\{[\kappa_{BB}]_{tm,ch} \cdot \bar{B}(\overline{T_{BB}} + 273.15) + [\sigma]_{ch} \cdot \bar{B}(\overline{T_{env}} + 273.15)\right\}$$
$$\bar{B}(T) = \int_{\lambda_{min}}^{\lambda_{max}} R'(\lambda)B(\lambda,T)d\lambda$$

$$R'(\lambda) = \frac{R(\lambda)}{\int_{\lambda_{min}}^{\lambda_{max}} R(\lambda)d\lambda}$$

$$B(\lambda, T) = \frac{2hc^2}{\lambda^5} \cdot \frac{1}{e^{\frac{hc}{\lambda k}} - 1}$$

Here, β' is non-linearity correction coefficient and σ is effective emissivity of background emission

4.2.2.4 **Conversion to Level1B reference coordinate**

(1) Calculation of Latitude and Longitude

Figure 4-16 shows the outline of calculation of latitude and longitude of observation points.

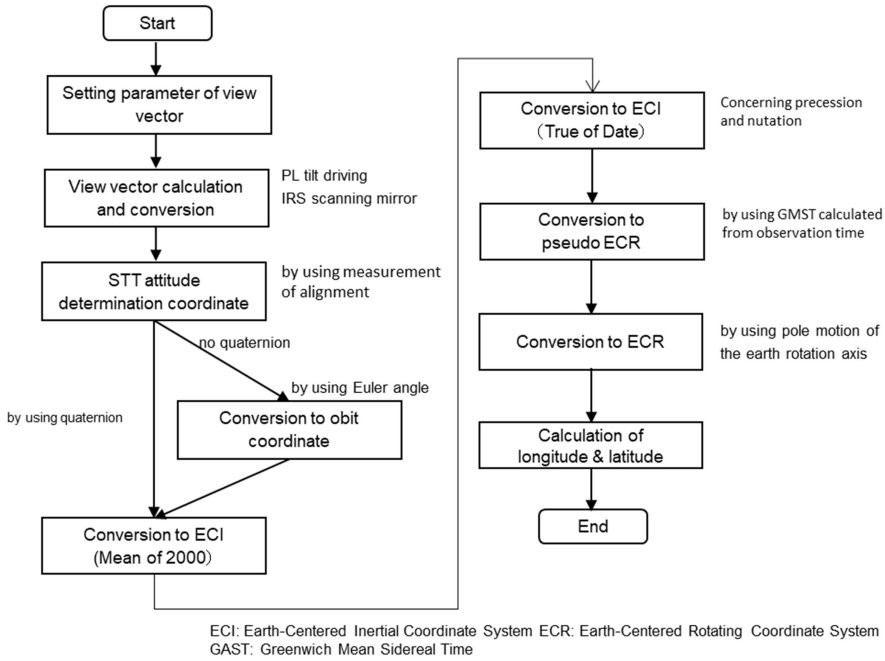

Figure 4-16 Processing Flow of Calculation of Latitude and Longitude

(a) View Vectors Calculation and Conversion

The view vectors of each pixel in the base coordinate of radiometer are calculated using the geometry function $Geo_{\_opt}$ given to each sensor. Since VNR (NP, PL) optical systems have a wide view angle and many pixels on the focal plane, $Geo_{\_opt}$ is geven by the high-dimensional function of the pixel number. In addition, since PL is tilt-driven, the tile angle rotation matrix must be considered. On the other hand, IRS (SWIR, TIR) have a narrow view angle and a small number of pixels on the focal plane. However, considering the reflection by rotary scanning mirror, the view vectors are calculated.

(b) Conversion to STT Attitude Determination Coordinate System

The view vectors in the base coordinate of radiometer obtained in (a) are converted to the

view vectors in STT attitude determination coordinate system using the pointing alignment matrix. The pointing alignment matrices consist of fixed bias, long-term bias variation component, and orbital fluctuation component by thermal distortion.

(c) Conversion to ECI (Mean of J2000)

Using the quaternions contained in real-time PCD, the view vectors in STT coordinate are converted to Earth-Centered Inertial Coordinate System (ECI). However, since quaternions are sampled at 10Hz, that are interpolated at the instant imaging timing. In addition, if the quaternion is not available, the vectors are converted to the orbit coordinate system using the attitude error angle at the instant imaging timing and converted to ECI using the satellite position and velocity vector.

(d) Conversion to ECI（True of Date）

The vectors in ECI (J2000) are converted to ECI (True of Date) by calculating the precession and nutation using the instant imaging timing and earth orientation parameter.

(e) Conversion to Pseudo ECR

The vectors in ECI (True of Date) are converted to the pseudo Earth-Centered Rotating Coordinate System (ECR) using Greenwich mean sidereal time.

(f) Conversion to ECR

The vectors in the pseudo ECR are converted to the ECR using the polar motion parameter.

(g) Calculation of Latitude and Longitude

Using the view vector u^{ECR}, view vector origin r_O^{ECR}, and satellite position r_{SAT} in ECR, the latitude and longitude of observation point are calculated. Figure 4-17 shows the schematic diagram of the process.

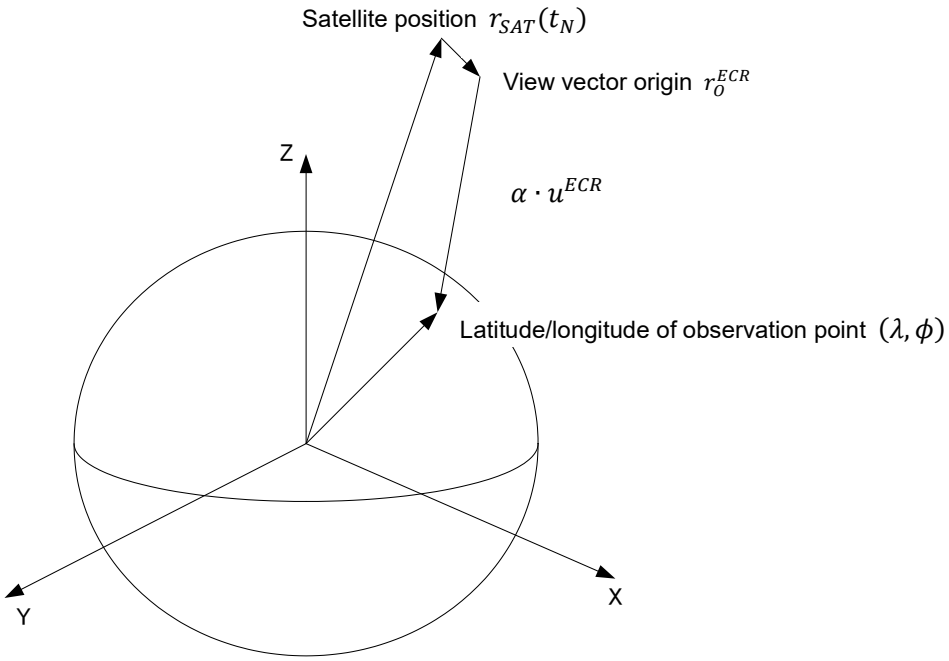

Figure 4-17 Schematic Diagram: Calculation of Latitude/longitude of Observation Point

(2) Conversion to Level1B reference coordinate

As Level1B reference coordinate to which Level1A pixel is projected, a virtual frame in which a push bloom CCD line sensor is arranged on the virtual cylindrical plane centered on the satellite orbit is defined as Level1B reference coordinate system (Figure 4-18).

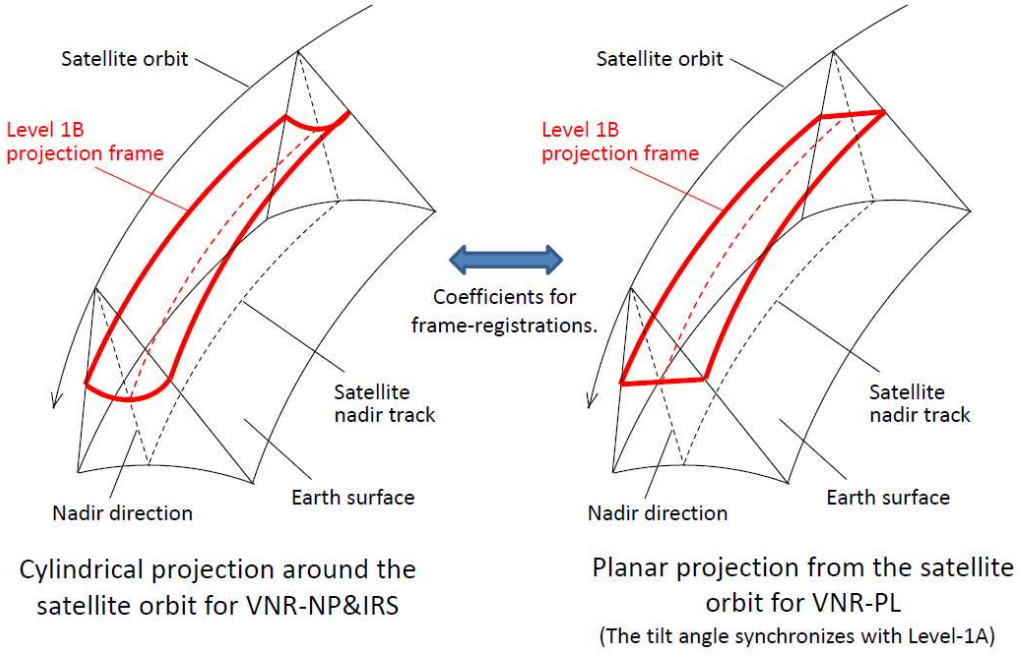

Figure 4-18 Definition of Level1B Reference Coordinate

In the conversion process to Level1B reference coordinate, Level1A pixel addresses

corresponding to the pixel addresses in Level1B coordinate are calculated by the convergence calculation, and the radiance value of Level1A is transferred in Level1B coordinate. These address relation are expressed as the coefficients of approximate polynomial. In addition, these coefficients are stored in Level1B product.

4.2.2.5 **Calculation of Level1A Geometry Information**

The latitude and longitude information of Level1A are obtained, just as 4.2.2.4 using the correspondence relationship between Level1A and Level1B pixel addresses. However, unlike 4.2.2.4 this process uses the coefficients of approximate polynomial to Level1B for each line of Level1A. These coefficients are given to each telescope in case of VNR-NP and stored in Level1B product.

4.2.2.6 **Stray Light Correction**

The stray light is a part of light that passes through the optical path different from the usual by the characteristics of hardware within the sensor. Figure 4-19 shows the image of occurrence of the stray light. The stray light correction means the process to remove such stray light with the software. When the light enters a pixel, the degree of occurrence of stray light in adjacent areas can be measured by pre-launch ground test. It is able to consider that SGLI observation images are the convolution of optical transfer function of SGLI stray light and true observation images, therefore, if the transfer function of SGLI stray light can be measured in advance, it is able to remove stray lights from SGLI observation images by applying deconvolution to observed image on-orbit.

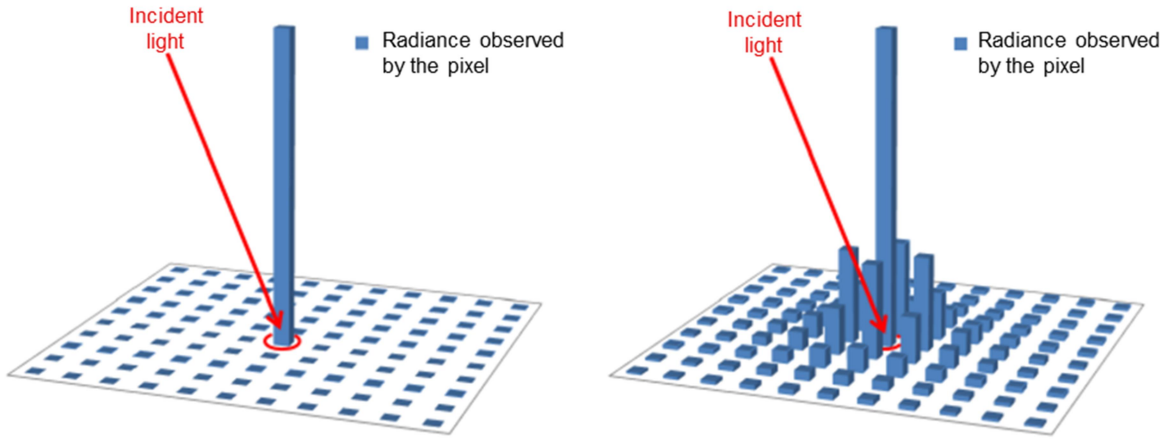

Figure 4-19 Ideal Observation Value (left) and Observation Value with Stray Light (right)

There are two types of stray light correction: the correction performed in Level1A coordinate system (on-orbit observation image) and the correction performed on a coordinate system after the simplified geometric correction (ground test coordinate system for VNR and view vector

coordinate system of SRU for IRS). First, the stray light corrections are performed in Level1A coordinate system, and then the simplified geometric corrections are performed for the FFT calculation area divided in CT direction in Level1A coordinated system, and the instant images at t=t_0 are generated. The stray light sources at t=t_0 are moved due to the rotation of earth at t=t_0+∆t. Therefore, if the stray light corrections are performed in Level1A coordinate system, except the stray light generated near the pixels on focal plane, the deviation of stray light source affect the correction accuracy. Therefore, the instant images observed at the satellite position at t=t_0 are generated. These processes are called the simplified geometric correction. Subsequently, the stray light corrections are performed to the instant image to obtain stray light correction amount ∆L for each pixel. These stray light correction amount ∆L images are performed to convert to L1A coordinate system by the inverse simplified geometric correction. These ∆L images are appended the original image. For more details about stray light types in each sensor, coordinate system to conduct correction, and correction processes, please see Algorithm Theoretical Basis Documents and Level1 Implementation Processing Document.

4.2.2.7 **Stripe noise correction**

In the image after radiometric correction, the stripe noise caused by photo response non-uniformity or radiometric gap between telescopes of VNR-NP may be remained. Therefore, the correction processes to remove the stripe noise are implemented. For more details, please refer to Level1 Implementation Processing Document.

4.2.2.8 **Land-water flag calculation**

The process searches for land and water flag source information included in the footprint, and the percentage of the land area in the footprint is obtained.

4.2.2.9 **Calculation of Stokes Vector (VNR-PL)**

Using the observed data of 2 telescopes x 3 channels (polarizer: + 60 ° [S09], 0 ° [S10], - 60 ° [S11]) of VNR-PL, stokes vector (I, Q, U components) for 2 telescopes are calculated. There are two types for the calculated models: a simplified model or a model to correct optical polarization properties.

(1) Simplified Model

$$\text{Stokes vector } \vec{S}_{n,s,p} = \begin{bmatrix} I \\ Q \\ U \end{bmatrix}_{n,s,p} = A_{n,p} \begin{bmatrix} L_{n,S09,s,p} \\ L_{n,S10,s,p} \\ L_{n,S11,s,p} \end{bmatrix}$$

The data analysis matrix A is obtained from $M_{POL,band}$ that is obtained by removing gain component from the Mueller matrix.

$$A_{n,p} = \begin{bmatrix} 1 & cos(2\phi_{n,S09}) & sin(2\phi_{n,S09}) \\ 1 & cos(2\phi_{n,S10}) & sin(2\phi_{n,S10}) \\ 1 & cos(2\phi_{n,S1\ }) & sin(2\phi_{n,S11}) \end{bmatrix}^{-1}$$

n: Band

ch: three polarizer: + 60 ° [S09], 0 ° [S10], - 60 ° [S11]

s: scan number (line number)

p: pixel number

$L_{n,ch,s,p}$: Spectral radiance (Level1B reference coordinate)

$\phi_{n,S09}$: Azimuth angle of transmission angle of polarization filter in S09

(2) Model to Correct Optical Polarization Properties

The data analysis matrix A is obtained from the Mueller matrix of light collection optical system M_{LEN}, and Mueller matrixes of polarized azimuth angle of polarization filter and optical depolarization component $M_{POL,band}$.

$$A = \begin{pmatrix} 1 & (1-a_{P,09})\cos 2(\phi_l+\phi_{09}) & (1-a_{P,09})\sin 2(\phi_l+\phi_{09}) \\ 1 & (1-a_{P,10})\cos 2(\phi_l+\phi_{10}) & (1-a_{P,10})\sin 2(\phi_l+\phi_{10}) \\ 1 & (1-a_{P,11})\cos 2(\phi_l+\phi_{11}) & (1-a_{P,11})\sin 2(\phi_l+\phi_{11}) \end{pmatrix}^{-1}$$

The data analysis matrix A in which the matrix components are parameterized is as follows. Nine components ($n_{11,09}$ to $n_{13,11}$) of inverse matrix are sensor calibration parameters.

$$A_{n,p} = \begin{pmatrix} n_{n,p,11,09} & n_{n,p,12,09} & n_{n,p,13,09} \\ n_{n,p,11,10} & n_{n,p,12,10} & n_{n,p,13,10} \\ n_{n,p,11,11} & n_{n,p,12,11} & n_{n,p,13,11} \end{pmatrix}^{-1}$$

ϕ_l: Polarization rotation angle of light collection optical system

Since $n_{11,09}$ to $n_{13,11}$ are parameters at pixel number i of CCD, it is necessary to refer to the conversion coefficient to the pixel number on Level1A address.

In addition, since $\vec{S}_{n,s,p}$ is the stokes vector at coordinate observed by PL sensor, the vector is converted to scattering plane coordinate. The angle (α) between the normal vector at scanning plane and the normal vector at scattering plane coordinate is used to coordinate transformation matrix.

$$\vec{S}_{n,s,p\_scattering\_plane} = \begin{pmatrix} 1 & 0 & 0 \\ 0 & \cos 2\alpha & -\sin 2\alpha \\ 0 & \sin 2\alpha & \cos 2\alpha \end{pmatrix} \vec{S}_{n,s,p}$$

The Level1B product is stored stokes vector $\vec{S}_{n,s,p\_scattering\_plane}$, spectral radiance $L_{n,ch,s,p}$ and the coefficient of formula to convert to Level1A address (4.2.2.4).

4.2.2.10 **Resampling to low resolution product**

In sensors except VNR-PL, Level1B high resolution observation (250-500 m) products are resampled to generate low resolution (1 km) Level1B product. The scene products before and after the L1B high resolution scene product to be processed are input at the same time. Those products are to be used for compensation if any part of the overlap of the target product is missing. The resampling method depends on the data set properties such as averaging process and extraction of representative values.

4.3 **Level2 & Level3 Processing Algorithm**

The general descriptions of higher level processing algorithms of land, atmosphere, ocean, cryosphere, and statistical processing are provided in 4.3.1 through 4.3.4 respectively. For more details, please refer to Algorithm Theoretical Basis Documents (ATBD) of each algorithm. Level2 & Level3 processing ATBD is available at the following URL:
https://suzaku.eorc.jaxa.jp/GCOM_C/data/product_std.html

4.3.1 **Land Algorithm**

For land algorithm, as Level2 processing, there is a precise geometric correction processing that is a process to generate tile data in the Sinusoidal projection. In addition, there are five standard algorithms specialized in retrieving the physical variable of land from the tile data.

4.3.1.1 **Precise Geometric Corrected Radiance Algorithm**

(1) As the tile product of precise geometric corrected top of atmosphere (TOA) radiance, it corrects the parallax due to postural change or altitude using the parameter PGCP with positional variation estimated using GCP, and stores the image projected onto the grid of EQA projection centered on 0-degree longitude.

(2) General Description of Algorithm

The precise geometric corrected TOA radiance product consists of multiple numbers of algorithms. The general description of individual algorithm is provided below. In addition, the overall processing flow is shown in Figure.

a. Geometric Orientation Algorithm

Using the Level1B for each path of VNR/IRS and GCP_Info (GCP measurement data) as input, it obtains orientation elements of VNR and IRS respectively by orientation calculation, and stores the orientation element with orientation residual data of each GCP in the PGCP file.

b. Ortho Mosaic Algorithm

Using the Level1B of VNR/IRS/POL, PGCP and DEM as input, the map of Level1B address corresponding to the horizontal position of each tile grid and altitude are generated by geometric projection processing which takes into account the orientation element error of PGCP. Using the level-1B address map, it sets the level-1B image data and geometric data (such as sensor angle, solar angle) to each grid of the tile. In the case of the overlap of several paths, the data with smaller sensor zenith angle is prioritized. The tiles at 1 km resolution are generated by the conversion (4 x 4 averaging) of 250 m resolution tiles data.

c. GCP Matching

Using the Level1B positional information (latitude and longitude data) as input, the image of SGLI and AVNIR-2 (reference) are resampled to the matching image of the same resolution. The algorithm extracts characteristic points form SGLI image automatically, and by the matching process using Normalized Cross-Correlation, extracts the tie point with AVNIR-2 as GCP. It calculates the latitude and longitude from AVNIR-2 geometric information data, adds the height from DEM, and outputs "GCP_info" as GCP (image address, latitude, longitude and height) automatic measurement data.

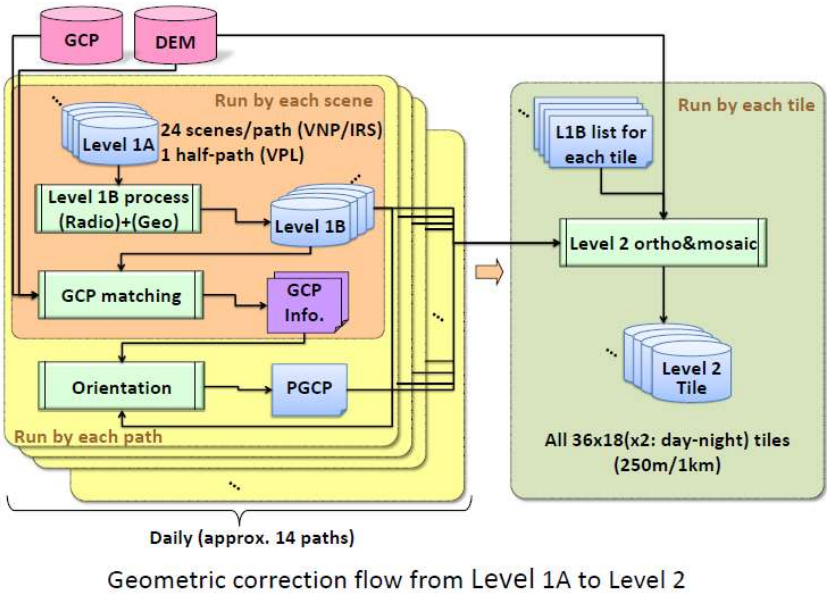

Geometric correction flow from Level 1A to Level 2

Figure 4-20 Overall Flow of Precise Geometric Corrected Radiance Algorithm

4.3.1.2 Land Atmospheric Correction Algorithm

(1) Product Definition

The product is the atmospherically corrected reflectance equivalent to that of the land surface removing the effect of scattering/absorption of light caused by gas molecules and aerosol particles in the atmosphere, and in case of 8-day or 1month product, directional dependence of the reflectance is corrected.

(2) General Description of Algorithm

The algorithm uses TOA radiance (reflectance) data of the daytime as input, corrects the scattering/absorption by atmospheric molecules and aerosol, and outputs the ground level reflectance.

By using tile data of multiple days as input, it outputs the reflectance under the satellite and solar geometric condition on a target date of processing taking into account the land surface BRDF.

4.3.1.3 **Vegetation Index Algorithm**

(1) Product Definition

The product consists of the Normalized Difference Vegetation Index (NDVI), Enhanced Vegetation Index (EVI), and ShaDow Index (SDI). NDVI and EVI are indices indicating the coverage or activeness of vegetation, and SDI is an index indicating the ratio of shadow of vegetation using spectrum information.

(2) General Description of Algorithm

NDVI is calculated by the formula (near infrared – red) / (near infrared + red), and the larger the value becomes, the larger the vegetation density. EVI is calculated by the formula G x (near infrared – red) / (near infrared + C1 x red – C2 x blue + L), where G, C1, C2, L are constant numbers, and it provides higher sensitivity compared to NDVI where vegetation is dense. SDI is the "fraction of shadow generated by conformation of vegetation (areal occupation within a pixel)" and is estimated with regression equation as functions of the solar incident angle and the reflectance at a shortwave infrared band, the coefficients of which are determined based on in-situ observations.

4.3.1.4 **Leaf Area Index/ Fraction of Absorbed Photosynthetically Active Radiation Algorithm**

(1) Product Definition

The product consists of Leaf Area Index (LAI) and Fraction of Absorbed Photosynthetically Active Radiation (FAPAR). LAI is the total area (m^2/m^2) of one side of all leaves of plants per unit area of ground, and this product estimates LAI of upper layer vegetation (crown for forest area, low trees and plants for non-forest area). FAPAR is, among the incident light of the spectrum region absorbed by plants photosynthetically (wavelength: 400-700 nm), the percentage absorbed by the crown (leaves on trees).

(2) General Description of Algorithm

a. Derivation of the Relation between LAI, FAPAR and Reflectance (NDVI) (for Each Land Cover)

For each land cover, the algorithm generates a lookup table (LUT) indicating the relationship between LAI, FAPAR, land surface reflectance and crown reflectance using FLiES that performs 3-dimensional radiative transfer simulations, in relation to arbitrary solar zenith angle, satellite zenith angle and relative azimuth angle. In the simulations, a tuning with the in-situ data is performed using forest stand structure (number of trees, crown shape, crown height for instance) that represents each land cover, reflectance/transmittance of individual leaves, and soil reflectance. In addition, NDVI is calculated with RED/NIR reflectances in the algorithm.

b. Calculation of Land Surface Reflectance of Satellite's Nadir Direction (the value when the satellite zenith angle becomes the minimum during the past 8 days)

Using SGLI observation data for the past 8 days including the observations day, the SGLI data of the day on which the satellite zenith angle became the minimum (the satellite elevation became the highest) is selected for each pixel.

c. Estimation of LAI/FAPAR from Bi-directional NDVI (Calculated form Land Surface Reflectance)

By making use or the bi-directional observation capability, which is one of the unique characteristics of SGLI, LAI/FAPAR is estimated using the reflectances at nadir view direction (VN08 and VN11) and reflectances at slant view direction (PI01 and PI02).

4.3.1.5 **Above-Ground Biomass Algorithm**

(1) Product Definition

The product consists of above-ground biomass (AGB) and vegetation roughness index (VRI). AGB is the volume of aboveground biomass shown in dry weight (t/ha), and VRI is the index expressing 3D structural information of vegetation (the unevenness changes in spatial distribution of canopy density) extracted from the "the dependence of observed radiance on the observing angle" obtained by multi-angle observations.

(2) General Description of Algorithm

Using the reflectance data (at satellite's nadir and slant viewing directions) as input, the algorithm outputs AGB derived based on LUT which indicates the relationship between the spectral reflectance of canopy and AGB. SGLI non-polarization data at red and near infrared bands (VN08, VN11) are used for reflectance at nadir view direction, whereas the data of the polarization telescope (PI01 (red) and PL02 (near infrared)) are used for reflectance at slant view direction. In generation of LUT, the bi-directional reflectance simulator BiRS is used. The forest structure model to be input to BiRS is generated based on the in-situ data such as canopy in shadow area, canopy in sunny area, and layout of trees. AGB is calculated using

the existing land cover classification product for each land cover type.

a. Calculation of Relationship between AGB, VRI and Reflectance (for 8 types of land cover)

Using BiRS, LUT which makes the relationship between RED and NIR reflectances (at nadir and slant view direction), AGB and VRI are generated for each land cover type of GlobCover dataset (the LUT is also functions the arbitrary zenith angle, satellite zenith angle, relative azimuth angle).

b. Estimation of AGB and VRI Using Bi-directional ground surface reflectance

The algorithm determines the estimates of AGB and VRI using the reflectance at satellite's nadir direction (VN08 and VN11) and reflectance at slant direction (PI01 and PI02) at the geometric condition of the SGLI observation.

4.3.1.6 **Land Surface Temperature Algorithm**

(1) Product Definition

The product consists of the land surface temperature (LST) and emissivities at the two split-window bands (TI01 and TI02).

(2) General Description of Algorithm

Using the geometric corrected TOA radiance data as input, the algorithm estimates the land surface temperature and land surface emissivities simultaneously by semi-analytical approach based on the radiative transfer simulation at two thermal infrared bands and the Split-Window method. This enables to obtain the land surface temperature taking into account the temporal fluctuation of land surface emissivity. The radiative transfer code is developed and implemented for the speed up the processing.

4.3.2 Atmosphere Algorithm

Atmosphere algorithm uses the tile data as input, and there is a process to generate global products of TOA radiance and four standard algorithms specialized in retrieving physical variables of the atmosphere.

4.3.2.1 Global Top of Atmosphere Radiance/Clear Region Composition Algorithm

(1) Product Definition

Using observation data of a target day, the algorithm generates a global EQA product (1/24 deg) of TOA radiance (LTOAF) and that TOA radiance using only clear pixels (eliminating cloudy pixels) (LCLRF)

(2) General Description of Algorithm

Using the Level1B (1 km) products of target day as input, the algorithm generates a global

TOA radiance product. This output product becomes the input to cloud flag and cloud properties algorithm. In addition, using the TOA radiance tile (1 km) products and cloud flag (1 km) products of a target day as input, it generates the composite of global TOA radiance with only clear pixel (cloudy pixel removed). This output product becomes the input to non-polarized/polarized aerosol algorithm.

4.3.2.2 Cloud Flag Algorithm

(1) Product Definition

The product consists of two flags. One is the cloud flag that indicates the existence of cloud within the pixel and the other is the cloud phase flag that indicates whether the cloud particles are water or ice. Both flags are generated from both daytime and nighttime observation data with global coverage. In addition, the cloud flag becomes the input of cloud properties/ non-polarized aerosol/ polarized aerosol/ clear region composition algorithm.

(2) General Description of Algorithm

The cloud identification algorithm CLAUDIA (Cloud and Aerosol Unbiased Decision Intellectual Algorithm) performs multiple threshold tests using the TOA radiance (reflectance/radiance temperature) and their difference or ratio to calculate the confidence level for each threshold test (0.0: cloud – 1.0: clear) and then integrates the calculated confidence level to generate the final clear confidence level as output. Since the selection of the threshold tests is arbitrary, the algorithm has versatility regarding channel configuration of satellite sensors. In addition, even when the data include partially missing, the clear confidence level can be calculated as far as more than one threshold test is performed. Therefore, there is robustness in the processing. The cloud phase identifies whether the cloud particle is water or ice using brightness temperatures at infrared bands.

4.3.2.3 Cloud Properties Algorithm

(1) Product Definition

The product consists of water-cloud optical thickness, effective radius, ice-cloud optical thickness, cloud top temperature, and height, and International Satellite Cloud Climatology Project (ISCCP) cloud type that are defined by the relationship between cloud optical thickness and cloud-top atmosphere pressure and the morphological cloud type. The cloud optical thickness and effective radius of cloud particle are retrieved only from daytime observation data, and the cloud-top temperature and height, and ISCCP cloud type are from both daytime and nighttime data.

(2) General Description of Algorithm

The cloud properties algorithm utilizes the Comprehensive Analysis Program for Cloud

Optical Measurements (CAPCOM), which has been developed for the previous GLI mission and now customized for the SGLI channel characteristics, and provides functions of estimation of ice cloud properties and the classification of ISCCP cloud types as additional new products of SGLI. In addition, the calculation of radiative transfer is speeded up using LUT, and the out-of-band response around the wavelength of 1.6 μm at SW4 (2.21 μm) is taken into account by the radiative transfer calculation.

The simulations of light scattering by ice particle are performed assuming Voronoi particle model for ice particle shape. In addition, ISCCP cloud type classification is performed based on the relationship between the cloud optical thickness and cloud-top atmosphere pressure.

4.3.2.4 Non-polarized Aerosol Algorithm

(1) Product Definition

The aerosol properties over the ocean consist of the optical thickness of aerosol, angstrom exponent and aerosol type estimated based on the visible and near infrared reflectance. In addition, the aerosol properties over the land consist of aerosol optical thickness, angstrom exponent and single scattering albedo estimated based on the near ultraviolet reflectance.

(2) General Description of Algorithm

A common aerosol optical model is used for the retrieval over ocean and land, and the model is determined based on the skyradiometer observation data. While fixing the particle shape, real part of complex refraction index and size distributions of large and small particle, the fraction of small particle and complex refraction index (in terms of SSA) are assumed to be variable. For retrieval, the algorithm estimates an aerosol parameter suitable to the SGLI observation, and outputs aerosol optical thickness, angstrom exponent and single scattering albedo.

4.3.2.5 Polarized Aerosol Characteristics Algorithm

(1) Product Definition

The product consists of aerosol optical thickness, angstrom exponent and single scattering albedo over the land estimated from the polarized observation data.

(2) General Description of Algorithm

The algorithm uses non-polarized observation at 380 nm band (VN01) and polarized observation at 670 nm and 870 nm bands (PL01, PL02) to estimates the aerosol optical thickness, angstrom exponent and single scattering albedo over the land. By referring to previously generated LUT based on the radiative transfer calculation, the estimation process is speeded up.

4.3.3 Ocean Algorithm

The ocean algorithm uses the Level1B product (scene) as input, and there are total of three standard algorithms specialized in the physical variables of the ocean.

4.3.3.1 Sea Surface Temperature Algorithm

(1) Product Definition

The algorithm calculates the bulk temperature [°C] of sea surface (including cloud detection).

(2) General Description of Algorithm

The sea surface temperature is estimated by approximately solving the infrared radiative transfer equation (LUT is used for implementation). Clear/cloud is estimated from VN8 and SW2 (only for daytime), T1, and T2 data with a method combined of threshold based tests and a method based on Bayesian inference. Derived cloud probability, that statistically connects to quality of determined SSTs, is used for the decision of the quality level (QL) of retrieved SST.

4.3.3.2 Ocean Atmosphere Correction Algorithm

(1) Product Definition

The product consists of the normalized water-leaving radiance (NWLR), atmosphere correction parameter (ACP) and photosynthetically available radiation (PAR). NWLR [W/m^2/sr/μm] is the upwelling radiance just above the sea surface, ACP is the aerosol optical thickness $\tau_a$used to estimate effects of atmospheric scattering, and PAR [Ein/m^2/day] is the photon flux density within the visible wavelength range (400 to 700 nm) over the ocean which is potentially available to marine plants for photosynthesis.

(2) General Description of Algorithm

The algorithm uses the Level1B product of the radiance observation in daytime region as input, corrects for the atmosphere molecule, aerosol, sun-glitter, white cap and Bidirectional Reflectance Distribution Function (BRDF), and outputs NWLR. ACP is estimated during the aerosol reflectance correction processing in the algorithm. PAR is estimated by simplifying the solar light incident on the sea surface into two elements: "atmospheric molecule + aerosol" and "cloud + sea surface".

4.3.3.3 In-water properties Algorithm

(1) Product Definition

The product consists of chlorophyll-*a* concentration (CHLA), Total suspended matter concentration (TSM) and Colored dissolved organic matter (CDOM). CHLA [mg/m^3] is the concentration of the green pigment in phytoplankton in sea surface layer, TSM [g/m^3] is the

dry weight of suspended matter in a unit volume of surface water which is the sum of organics such as phytoplankton and inorganics such as soil and CDOM [m^{-1}] is defined as the light absorption coefficient of organics dissolved in surface water.

(2) General Description of Algorithm

CHLA is estimated using the ratio of the remote sensing reflectance between the blue and green bands. When the estimated concertation is lower than a threshold, the algorithm further applies a difference of the spectral remote sensing reflectance. TSM is estimated by an empirical relationship between a remote sensing reflectance ratio and TSM. For CDOM, the absorption index is derived firstly from an inherent optical property model, and then the light absorption coefficient of dissolved organic matter is estimated using an empirical relationship with the index.

4.3.4 Cryosphere Algorithm

The cryosphere algorithm uses tile data as input, and there are in total two standard algorithms specialized in the retrievals of snow/ice cover extents and snow physical variables. The local product of sea-ice distribution for Okhotsk Sea is derived from the Level1B radiance data (scene) using the same algorithm for the retrieval of snow and ice cover extents.

4.3.4.1 Snow and Ice Cover Extent Algorithm

(1) Product Definition

The product consists of the Snow and Ice Cover Extent product (SICE) covering on global and Okhotsk sea-Ice Distribution product (OKID) targeting on the Sea of Okhotsk, northern of Japan. It distinguishes snow, ice, cloud and several types of ground surface focusing on the cryospheric region based on the difference in reflectance characteristics by ground surface varieties.

(2) General Description of Algorithm

By using the observed reflectance and brightness temperature, the algorithm performs several threshold tests including normalized difference snow index (NDSI) test, single band threshold test, and two band test with dynamic threshold, to discriminate cloud and surface type cover types (snow, sea-ice, bare land), and outputs the identified flag.

① The threshold tests of NDSI are performed to determine snow region, non-snow region and cloud region.

② As single band reflectance test, multiple tests are performed using the threshold of reflectance of visible/near infrared range to determine cloud region. The clear pixels are used to discriminate ground surface types

③ As two band test with dynamic thresholds, since the reflectance of snow is varied as the grain size changes due to morphological change of ice particles, LUT is generated in consideration of that effect on the SW4 and SW3 reflectances. Using the threshold determined based on the generated LUT, snow and cloud region are determined.

4.3.4.2 Snow ice physical properties Algorithm

(1) Product Definition

As snow and ice physical properties product (SIPR) in snow cover over land and sea-ice region, snow grain size of shallow layer (SGSL) and snow and ice surface temperature (SIST) in clear sky region are retrieved.

(2) General Description of Algorithm

It estimates snow and ice physical properties by three steps: forward radiative transfer model, neural network training, and nonlinear optimal estimation. In the estimation of optical properties of snow grain, as the particle shape model, non-spherical Voronoi particle, which is closer to the real snow grain compared with the spherical shape or hexagonal column shape used in the former GLI algorithm, is used to estimate scattering properties precisely. Using the optical properties derived with the Voronoi particle shape model, radiative transfer of atmosphere-snow system is calculated using the discrete-ordinate radiative transfer (DISORT) model for cases with various grain sizes to estimate the relationship between snow grain size and radiance. To estimate the snow grain size from the radiance, their relationship is learned as a nonlinear function using the neural network training, and the snow grain size of shallow layer is estimated based on the observed radiance by nonlinear optimal estimation method. The snow and ice surface temperature is estimated by the split window method. Considering that the snow surface emissivity varies depending on the observation angle, parameters for the Split-Window method are changed in accordance with the observation conditions to estimate the temperature.

4.3.5 Statistic Processing Algorithm

The statistics processings of Level2 are temporal statistic and mosaic per 8-day or 1-month. The spatial resolutions of the input tile products are kept the same. The statistics processings of Level3 are spatial and temporal statistic per 8-day or 1-month. The spatial resolution of output is 1/12 or 1/24 degree.

4.3.5.1 Level2 Tile Statistic Algorithm

(1) Product Definition

It generates the temporal statistic product of Level2 land/cryosphere tile product.

(2) General Description of Algorithm

Using the Level2 product of land and cryosphere (Daily, Tile, 250 m or 1 km resolution) as input, it calculates and outputs the temporal statistics of 8-days or 1-month. The region definition and spatial resolutions of the output product are kept those of input data.

The statistics values stored to product are average (AVE), root-mean-square (RMS), maximum value (MAX), minimum value (MIN), number of input data (Ninput), number of data used (Nused), date of observation (Date), and quality flag (QA_flag).

4.3.5.2 Level2 Tile Top of Atmosphere Radiance Mosaic Algorithm

(1) Product Definition

It generates the mosaic (clear region composite) product of Level2 tile product of precise geometric corrected TOA radiance.

(2) General Description of Algorithm

Using the Level2 tile product of precise geometric corrected TOA radiance (Daily, Tile, 250m resolution) as input, the clear region mosaic data for 8-days or 1-month is stored in the output product. The region definition and spatial resolutions of the output product are kept the input data. Maximum absolute NDVI composite method is used for mosaicking process. In this method output data store the TOA radiance of a single observation day on which the value of |NDVI-α| becomes the maximum during the temporal interval (8-day or 1-month). Here, α is a tuning parameter.

4.3.5.3 Level2 Tile BRDF-corrected Land Reflectance Algorithm

(1) Product Definition

The product stores temporal statistics of the atmospheric corrected reflectance with the correction of its directional dependence.

(2) General Description of Algorithm

Using the Level2 atmospheric corrected land surface reflectance tile product (Daily, Tile, 250 m resolution) as input, BRDF correction is performed for the land surface in clear region using data of multiple days, and the reflectance equivalent to that at nadir view direction is stored in the output product. The region definition and spatial resolutions of the output product are kept the input data. In 8-day and 1-month processing, the land surface reflectance data of the past 24 days (including the last day of the 8-days) and that of the past 1-month, respectively are fitted to generate appropriate BRDF models with the correction coefficients.

4.3.5.4 Level3 Global Spatial Binning Algorithm

(1) Product Definition

It generates the Level3 daily spatial binning statistics product (EQA) by reducing the spatial resolution of the Level2 product.

(2) General Description of Algorithm

Using the Level2 products (Daily, Tile-250 m and 1 km [land and cryosphere], Scene-1 km [ocean], Global Bin-1/24 deg [atmosphere]) as input, the algorithm outputs and stores the statistics of geophysical variables in the spatial resolution 1/24 deg grid (land, cryosphere and ocean) or 1/12 deg grid (atmosphere). The statistics values stored in the output product are average (AVE), root-mean-square (RMS), maximum value (MAX), minimum value (MIN), number of input data (Ninput), number of data used (Nused), date of observation (Date), and quality flag (QA_flag).

4.3.5.5 Level3 Global Temporal Binning Algorithm

(1) Product Definition

It generates the Level3 8-day or 1-month temporal binning statistics product (EQA).

(2) General Description of Algorithm

Using the Level3 spatial binning product (Daily, Global Bin-1/24 deg [land, cryosphere and ocean] or 1/12 deg [atmosphere]) as input, the algorithm outputs and stores 8-day or 1-month statistics. The statistics values stored in the output product are average (AVE), root-mean-square (RMS), maximum value (MAX), minimum value (MIN), number of input data (Ninput), number of data used (Nused), date of observation (Date), and quality flag (QA_flag).

4.3.5.6 Level3 Global Map Algorithm

(1) Product Definition

It generates the Level3 map-projected statistics products projected to the equirectangular (EQR) grid for all products and also projected to polar stereographic (PS) projection only for cryosphere products

(2) General Description of Algorithm

Using the Level3 spatial/temporal binning statistics products (Global Bin-1/24 deg [land/cryosphere/ocean], Global Bin-1/12 deg [atmosphere]) as input, the algorithm projects the statistics to the EQR (PS in case of cryosphere). The statistics values stored in the output product are average (AVE) and quality flag (QA_flag).

4.4 **Product Formats**

The details of SGLI Level1 and Level2 & Level3 product formats are available at G-Portal.

- SGLI Level 1 Product Format Description
- SGLI Higher Level Product Format Description

4.5 **Data Calibration and Validation**

GCOM-C calibration and validation guarantee the quality and reliability of GCOM-C/SGLI standard products through a series of calibration and validation activities including pre-launch ground test, sensor model development, on-orbit calibration data evaluations and accuracy evaluation results of geophysical variables. Figure 4-21 shows the outline of calibration and validation schedule.

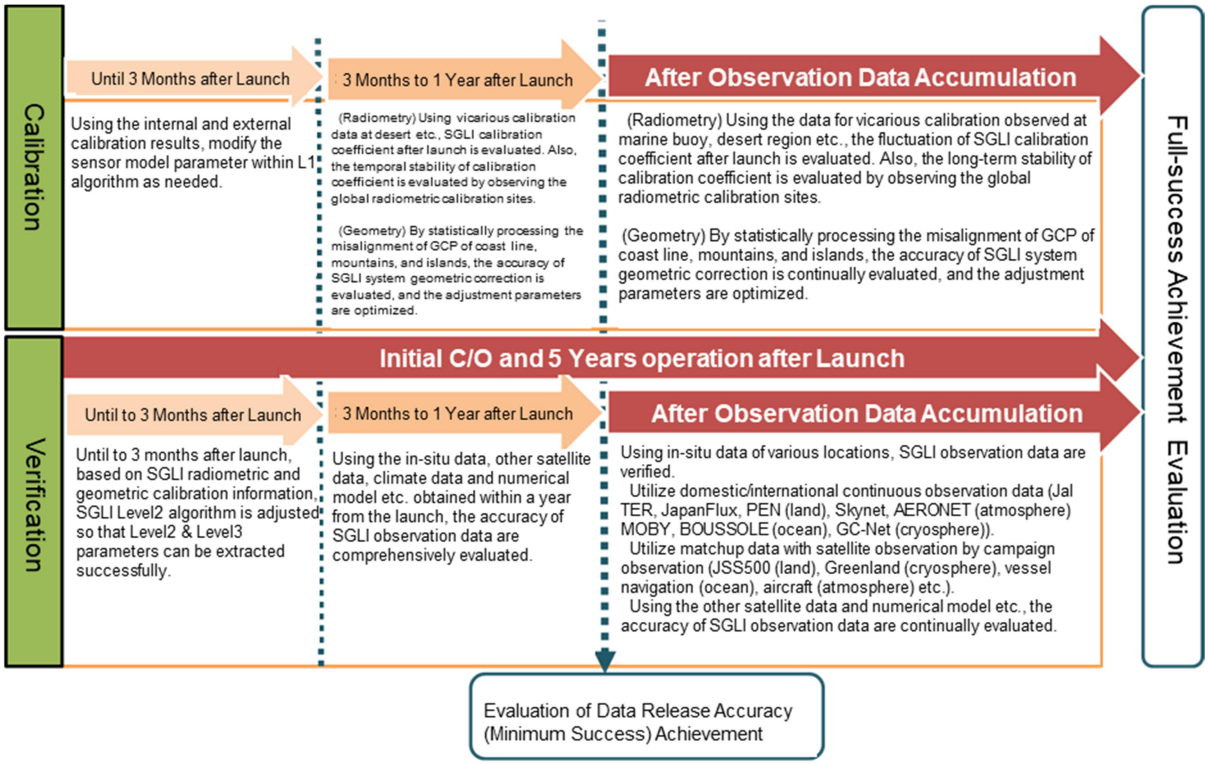

Figure 4-21 Outline of SGLI Calibration and Verification Schedule

4.5.1 **Calibration**

4.5.1.1 **Calibration Phase**

The schedules in each phase from pre-launch are shown below.

(1) Sensor Performance Evaluation Phase (pre-launch)

This phase identifies sensor properties associated with calibration, conducts ground test and analysis, and examines corrective methods as needed. Based on the results of these examinations, the coefficient of the sensor model for radiometric and geometric correction are determined and the values are inputed to Level1 processing algorithms as the pre-launch initial value.

(2) Initial Checkout Phase (Launch to Launch + 3M)

This phase obtains the on-orbit calibration data of solar diffuser, internal lamp, black body and initial images to evaluate the healthiness of various functions of satellite and sensor (earth observation and calibration function etc.). In addition, the maneuver observation functions obtain the data for the evaluation of lunar calibration or β angle dependency of diffuser. The geometry calibration evaluates GCP to stabilize the geometry accuracy at an early stage of initial calibration and validation phase.

(3) Initial Calibration and Validation Phase (Launch + 3M to Launch 12M)

This phase conducts solar calibration, internal lamp calibration, deep space calibration, lunar calibration, electrical calibration, and GCP evaluation periodically to perform regular check of the sensor performance and trend evaluation. The phase also conducts image evaluation, vicarious calibration, and cross-calibration to estimate sensor characteristic necessary for the product creation. For Level1 product data release, the results of those calibrations are reflected to algorithms.

(4) Regular Evaluation Phase (from Launch + 12M and later)

This phase regularly evaluates the on-orbit calibration, and the product accuracy is continuously assured by reflecting the calibration result to the algorithm as needed. Particularly, regarding the temporal fluctuation of sensor sensitivity, detailed analysis of the effect of β angle in solar calibration, the effect of lunar age in lunar calibration and the vicarious calibrations are performed in combination.

4.5.2 **Validation**

4.5.2.1 **Product Validation**

The variation is performed to evaluate the accuracy of geophysical variables products, and it is conducted by comparison with the in-situ data obtained by in-situ observation. The

accuracy evaluation of SGLI Level2 & Level3 products is conducted by comparing the target accuracy defined for each mission phase with in-situ data, other satellites data, and the numerical model data etc.

Table 4-21 to Table 4-26 describe the target accuracy and validation method for each phase. The calibration and validation monitor systems are developed to automate the series of processing from data obtaining to matchup analysis of SGLI observation value and parameters.

Table 4-21 Overview of SGLI Level2 & Level3 products Verification Method（1/6）

Cate -gory	Product [Definition・Unit]	Accuracy[*1]		Cal/Val Method
Common	Satellite-observed radiance (Level1B) Def.: Satellite-observed radiances which are radiometrically and geometrically corrected with inter-band registration. Calibration information is added. Unit: $W/m^2/sr/\mu m$	Release (Data release threshold)	5% (absolute[*1]) geometric accr.<1pixel	Accuracy of radiance is evaluated as RMS error based on vicarious calibration, on-board calibrations with solar diffuser and blackbody and so on. Geometrical accuracy is evaluated using GCP as RMS error of pixel position after systematic geometric correction.
		Standard	except TIR: 5%(abs.[*1]), 1% (relative) TIR: 0.5K (@300K) geometric accr.<0.5pixel	Accuracy of radiance is evaluated as RMS error based on vicarious calibration, on-board calibrations with solar diffuser and blackbody, and maneuver operations for moon calibration and inter-band calibration (yaw-direction maneuver). Geometrical accuracy is evaluated using GCP as RMS error of pixel position after systematic geometric correction.
		Goal	Except TIR: 3%(abs.[*1]), 0.5% (relative) TIR: 0.5K (@300K) geometric accr.<0.3pixel	
Land	Precise geometric corrected radiance (LTOA) Def.: This product contains 1) PGCP parameters which indicate geometric biases estimated using GCP, and 2) radiance images which are projected to sinusoidal projection plane with the center longitude of 0 degree after the correction of the geometric biases using the PGCP. Unit: W/m2/sr/μm	Release	<1pixel	Accuracy of precise geometric correction is evaluated as RMS error of pixel position using GCPs.
		Standard	<0.5pixel	
		Goal	<0.25pixel	
	Land atmospheric corrected reflectance (RSRF) Def.: Land surface reflectance corrected for the effects of atmospheric scattering and absorption. Correction of directional anisotropic effects are also made for 8-day and monthly composite products. Unit: none	Release	0.3 (<=443nm), 0.2 (>443nm) (scene)[*L1]	RMS error between satellite-derived reflectances and ground truth measurements is estimated at a region where aerosol optical thickness at 500nm is less than 0.25.
		Standard	0.1 (<=443nm), 0.05 (>443nm) (scene)[*L1]	RMS error between satellite-derived reflectances and ground truth measurements is estimated.
		Goal	0.05 (<=443nm), 0.025 (>443nm) (scene)[*L1]	
	Vegetation index (VGI) Def.: Indices indicating vegetation cover and activity such as NDVI and EVI Unit: none	Release	Grass land：25% (scene), Forest：20% (scene)	RMS error is evaluated comparing SGLI-derived VI with in-situ measured VI derived from spectroradiometer data at JaLTER, JapanFlux, PEN, Yatsuga-take tower site etc. and also with other satellite VI products.
		Standard	Grass land: 20% (scene), Forest：15% (scene)	RMS error is evaluated comparing SGLI-derived VI with in-situ measured VI derived from spectroradiometer data at JaLTER, JapanFlux, PEN, Yatsuga-take tower site etc.
		Goal	Grass land：10% (scene), Forest: 10% (scene)	

Table 4-22 Overview of SGLI Level2 & Level3 products Verification Method（2/6）

Cate -gory	Product [Definition・Unit]	Accuracy*1		Cal/Val Method
Land	Above-ground biomass (AGB) Def.: Dry weight of above-ground vegetation Unit: t/ha	Release	Grass land：50%, Forest：100%	RMS error is evaluated comparing SGLI-derived AGBIO with in-situ measured AGBIO at JaLTER, JapanFlux, PEN, Yatsuga-take tower site etc. (derived from direct measurements of dry weight of grass at grass land, indirect estimation with allometry equation as functions of tree diameter at brest height (DBH) and tree height, or 3-D laser scanner measurements at forest), and also with AGBIO derived from other satellites, existing database and literature value.
		Standard	Grass land：30%, Forest：50%	RMS error is evaluated comparing SGLI-derived AGBIO with in-situ measured AGBIO at JaLTER, JapanFlux, PEN, Yatsuga-take tower site etc.
		Goal	Grass land：10%, Forest：20%	
	Vegetation roughness index (VRI) Def.: An index indicating plant vertical structure observed from multi-angle directions. Unit: none	Release	Grass land・Forest：40% (scene)	RMS error is evaluated comparing SGLI-derived VRI with in-situ measured VRI at JaLTER, JapanFlux, PEN, Yatsuga-take tower site etc. (derived from spectoral reflectance data acquired using tower and RC helicopter and so on).
		Standard	Grass land・Forest：20% (scene)	
		Goal	Grass land・Forest：10% (scene)	
	Shadow index (SI) Def.: An index indicating shadow fraction of vegetation area inferred from spectral reflectance. Unit: none	Release	Grass land・Forest：30% (scene)	RMS error is evaluated comparing SGLI-derived VRI with in-situ measured SI at JaLTER, JapanFlux, PEN, Yatsuga-take tower site etc. (derived from spectoral reflectance data acquired using tower and RC helicopter and so on), or comparing with SI inferred from data of other satellite high spatial resolution optical sensor as an aid.
		Stan- dard	Grass land・Forest：20% (scene)	
		Goal	Grass land・Forest：10% (scene)	
	Fraction of absorbed PAR (FAPAR) Def.: Fraction of photosynthetically active radiation absorbed by vegetation Unit: none	Release	Grass land：50%, Forest：50%	RMS error is evaluated comparing SGLI-derived FAPAR with in-situ measured FAPAR at JaLTER, JapanFlux, PEN, Yatsuga-take tower site etc. (derived from data of PAR meter or spectroradiometer data measuring upward and downward PAR at forest canopy and floor.), and with other satellite FAPAR products.
		Standard	Grass land：30%, Forest：20%	RMS error is evaluated comparing SGLI-derived FAPAR with in-situ measured FAPAR at JaLTER, JapanFlux, PEN, Yatsuga-take tower site etc. (derived from data of PAR meter or spectroradiometer data measuring upward and downward PAR at forest canopy and floor.).
		Goal	Grass land：20%, Forest：10%	

Table 4-23 Overview of SGLI Level2 & Level3 products Verification Method（3/6）

Cate -gory	Product [Definition・Unit]	Accuracy[*1]		Cal/Val Method
Land	Leaf area index (LAI) Def.: The sum of the one sided green leaf area per unit ground area. Unit: none	Release	Grass land：50%, Forest：50%	RMS error is evaluated comparing SGLI-derived LAI with in-situ measured LAI at JaLTER, JapanFlux, PEN, Yatsuga-take tower site etc. (derived from data of litter trap or LAI-2000 and spectroradiometer data measuring downward radiant flux etc. at forest floor.), and also with LAI of other satellite, database and literature value.
		Standard	Grass land：30%, Forest：30%	RMS error is evaluated comparing SGLI-derived LAI with in-situ measured LAI at JaLTER, JapanFlux, PEN, Yatsuga-take tower site etc. (derived from data of litter trap or LAI-2000 and spectroradiometer data measuring downward radiant flux etc. at forest floor.).
		Goal	Grass land：20%, Forest：20%	
	Land surface temperature (LST) Def.: Temperature of terrestrical land surface. Unit: Kelvin	Release	Less than 3.0K (scene)	RMS error is evaluated comparing SGLI-derived LST with in-situ measured radiation temperature at the bare ground and forest surface with uniform land cover and also comparing with other satellite LST products.
		Standard	Less than 2.5K (scene)	RMS error is evaluated comparing SGLI-derived LST with in-situ measured LST and also comparing with LST calculated from ground weather station(GTS etc.) measurement data considering the injection rate.
		Goal	Less than 1.5K (scene)	
Atmosphere	Cloud flag (CLFG) Def.: Cloud discrimination flag including the classification of cloud type and phase (liquid/solid). Unit: none	Release	10% (comparison with sky-camera binary image)	Classification error is evaluated comparing SGLI derived CLFG with skycamera images.
		Standard	Evaluated as the cloud fraction products.	Same as the classified cloud fraction.
		Goal	Evaluated as the cloud fraction products.	Same as the classified cloud fraction.
	Classified cloud fraction(CLFR) Def.: Cloud fractions for 9 cloud types which are classified based on the ISCCP classification rule. Unit: percent	Release	20% (as solar radiation)[*A1]	Overall classification error is evaluated comparing SGLI derived solar radiation which is monthly average for every 0.1 degree global grid with in-situ measured solar radiation, skycamera images, and existing cloud fraction climate datasets such as ISCCP(the International Satellite Cloud Climatology Project).
		Standard	15%(as solar radiation)[*A1]	
		Goal	10%（as solar radiation)[*A1]	
	Cloud top temp/height (CLTTH) Def.: Temperature and height of cloud top layer. Unit: Kelvin for temperature, km for height	Release	1K [*A2]	The release criterion shown in the left column indicates a threshold for SGLI TIR band brightness temperature by which the ability to sense cloud top temperature is evaluated indirectly. The accuracy of TIR band is assessed through the product evaluation process of sea surface temperature etc. Also confirmed is the consistency of SGLI derived cloud top temperature with object analysis data of air temperature profile and cloud top height with climate over ocean in daytime.
		Standard	3K [*A3] /2km [*A3]	RMS error is evaluated comparing SGLI derived CLTTH with those derived from airbone and satellite borne lidar, sounder and radiometer etc. for uniform liquid clouds with moderate optical thickness.
		Goal	1.5K [*A3] /1km[*A3]	

Table 4-24 Overview of SGLI Level2 & Level3 products Verification Method（4/6）

Cate -gory	Product [Definition・Unit]	Accuracy[*1]		Cal/Val Method
Atmosphere	Water-cloud optical thickness & effective radius (CLOTER_W) Def.: Optical thickness and effective radius of water cloud droplets Unit: none for thickness, μm for radius	Release	10%/30% (optial thickess/radius) [*A4]	RMS error is evaluated comparing SGLI derived CLOTER_W with those from other satellite sensors for clouds of mid- to low latitude regions (monthly average).
		Standard	100% (as cloud liquid water[*A6])	RMS error is evaluated comparing cloud liquid water converted from SGLI derived CLOTER_W with those measured with microwave radiometer on the ground.
		Goal	50% [*A5] /20% [*A6]	Overall RMS error is evaluated comparing SGLI derived CLOTER_W with those derived from microwave radiometer and skyradiometer (for optical thickness) and other satellite sensors (both param.).
	Ice-cloud optical thickness (CLOT_I) Def.: Optical thickness of ice cloud. Unit: none	Release	30% [*A4]	RMS error is evaluated comparing SGLI derived CLOT_I with those from other satellite sensors for clouds of mid- to low latitude regions (monthly average). .
		Standard	70% [*A6]	RMS error is evaluated comparing SGLI derived CLOT_I with those from skyradiometers at ground observation network and other satellite sensors.
		Goal	20 % [*A6]	
	Aerosol over the ocean (ARNP) Def.: Optical thickness, Ångström exponent, and classification of aerosol over ocean estimated using visible and near infrared band. Unit: none	Release	0.1(monthly ave. of τa_670, 865) [*A7]	Overall RMS error is evaluated comparing SGLI derived ARV with those from other satellite sensors and climate datasets based on the past satellite observations (monthly average).
		Standard	0.1(scene's τa_670, 865)[*A7]	RMS error is evaluated comparing SGLI derived ARV with those from other satellite sensors and shipborne in-situ observations (AERONET/Maritime Aerosol Network).
		Goal	0.05(scene's τa_670, 865)	
	Land aerosol by near-UV (ARNP) Def.: Optical thickness and light absorption coefficient of aerosol over land estimated using near-ultraviolet band. Unit: none	Release	0.15(monthly ave. ofτa_380) [*A7]	RMS error is evaluated comparing SGLI derived ARU with those from skyradiometers at ground observation network (Skynet, Aeronet) and other satellite sensors.
		Standard	0.15(scene's τa_380) [*A7]	
		Goal	0.1(scene's τa_380)	
	Aerosol by Polarization (ARPL) Def.: Optical thickness, Ångström exponent, and classification of aerosol estimated using polarization bands. Unit: none	Release	0.15(monthly ave. of τa_670, 865) [*A7]	RMS error is evaluated comparing SGLI derived ARP with those from skyradiometers at ground observation network (Skynet, Aeronet) and other satellite sensors for fine mode particles.
		Standard	0.15(scene's τa_670, 865) [*A7]	
		Goal	0.1(scene's τa_670, 865)	

Table 4-25 Overview of SGLI Level2 & Level3 products Verification Method（5/6）

Cate -gory	Product [Definition・Unit]	Accuracy*1		Cal/Val Method
Ocean	Normalized water leaving radiance (NWLR) Def.: The upwelling radiance just above the sea surface. Unit: W/m^2/str/um or 1/sr	Release	60% (443~565nm)	RMS error is evaluated comparing SGLI derived NWLR with in-situ optical measurements conducted during simultaneous ship observations campaign and also comparing with other satellite products.
		Standard	50% (<600nm) 0.5W/m2/str/um (>600nm)	RMS error is evaluated comparing SGLI derived NWLR with in-situ optical measurements conducted during simultaneous ship observations campaign.
		Goal	30% (<600nm) 0.25W/m2/str/um (>600nm)	
	Atmospheric correction param.(ACP) Def.: Aerosol optical properties for the atmospheric correction over ocean. Unit: none	Release	80% (τa_865)	RMS error is evaluated comparing SGLI derived aerosol optical thickness with those from in-situ measurements using radiometers during simultaneous ship observations campaign and also comparing with other satellite sensors.
		Standard	50% (τa_865)	RMS error is evaluated comparing SGLI derived aerosol optical thickness with those from in-situ measurements using radiometers during simultaneous ship observations campaign.
		Goal	30%	
	Photosynthetically Available Radiation (PAR) Def.: Photon flux density within the visible wavelength range (400 to 700 nm) over ocean which is potencially available to plant for photosynthesis. Unit: Ein/m^2/day or mol photons/m^2/day	Release	20% (10km/month)	RMS error is evaluated comparing SGLI derived monthly averaged PAR with those derived from mooring buoy such as NDBC, TAO/TRITON etc. as solar radiation or PAR.
		Standard	15% (10km/month)	
		Goal	10% (10km/month)	
	Chlorophyll-*a* concentration (CHLA) Def.: Concentration of the green pigment in phytoplankton in sea surface layer. Unit: mg/m^3	Release	-60~+150% (open sea)	RMS error is evaluated comparing SGLI derived CHLA with those derived from sea water samples by fluorescence method or HPLC analysis and also with other satellite products.
		Standard	-60~+150%	RMS error is evaluated comparing SGLI derived CHLA with those derived from sea water samples by fluorescence method or HPLC analysis.
		Goal	-35~+50% (open sea), -50~+100% (coastal)	
	Total Suspended Matter concentration (TSM) Def.: Dry weight of suspended matter in a unit volume of surface water which is the sum of organics such as phytoplankton and inorganics such as soil. Unit: g/m^3	Release	-60~+150% (open sea)	RMS error is evaluated comparing SGLI derived TSM with those derived from sea water samples by filtration method and also with other satellite products.
		Standard	-60~+150%	RMS error is evaluated comparing SGLI derived TSM with those derived from sea water samples by filtration method.
		Goal	-50~+100%	
	Colored dissolved organic matter (CDOM) Def.: Light absoption coefficient of organics dissolved in surface water. Unit: 1/m	Release	-60~+150% (open sea)	RMS error is evaluated comparing SGLI derived CDOM with those derived from sea water samples by optical measurements and also with other satellite products.
		Standard	-60~+150%	RMS error is evaluated comparing SGLI derived CDOM with those derived from sea water samples by optical measurements.
		Goal	-50~+100%	

Table 4-26 Overview of SGLI Level2 & Level3 products Verification Method（6/6）

Cate -gory	Product [Definition・Unit]	Accuracy[*1]		Cal/Val Method
Ocean	Sea surface temperature (SST) Def.: Temperature of sea surface. Unit: °C	Release	0.8K (daytime only)	Overall RMS error is evaluated comparing SGLI derived SST with those derived from other satellite sensors and also comparing with those from GTS, internet distribution buoy measurements and ship measurements (iQuam etc.) in daytime.
		Standard	0.8K	Overall RMS error is evaluated comparing SGLI derived SST with those derived from other satellite sensors and also comparing with those from GTS, internet distribution buoy measurements and ship measurements (iQuam etc.).
		Goal	0.6K	
Cryosphere	Snow and Ice covered area (SICA) Def.: The extent of global snow and ice cover. Unit: none	Release	10% (comparison with other satellite products)	Overall RMS error is evaluated comparing SGLI derived SICA with other satellites' same products and climate of related geophysical parameters derived from the past observations.
		Stan- dard	7%	Overall RSM error is evaluated comparing SGLI derived SICA with those derived from moderate and high spatial resolution satellite sensors and also with snow and ice cover information obtained at ground stations etc.
		Goal	5%	
	Okhotsk sea-ice distribution (OKID) Def.: The extent of sea ice in Okhotsk Sea. Unit: none	Release	10% (comparison with other satellite products)	Overall RSM error is evaluated comparing SGLI derived OKID with other satellites' same products and climate of related geophysical parameters derived from the past observations.
		Standard	5%	Overall RSM error is evaluated comparing SGLI derived OKID with those derived from moderate and high spatial resolution satellite sensors and also with ice information obtained at ship etc.
		Goal	3%	
	Snow and ice surface Temperature (SIST) Def.: Temperature of snow and ice surface. Unit: Kelvin	Release	5K (comparison with other satellite products and meteorological measurements)	Overall RMS error is evaluated comparing SGLI derived SIST with those from other satellite sensors, air temperatures from GTS and ice buoys, and climate datasets derived from the past observations.
		Stan- dard	2K	RMS error is evaluated comparing SGLI SIST with those from in-situ radiometer measurements and snow pit works, air temperatures from GTS and ice buoys.
		Goal	1K	
	Snow grain size of shallow layer (SNGSL) Def.: Grain size of snow ice particle in shallow layer derived mainly from SGLI 865nm band reflectance. Unit: μm	Release	100%(evaluated with climate of temperature-snow grain size relationship)	Overall error is evaluated comparing SGLI derived SNGSL with other satellites' products and climate derived from the past observations.
		Standard	50%	RMS error is evaluated comparing SGLI SNGSL with those from in-situ radiometer measurements and snow pit works. And also consistentcy is confirmed with other satellite product as an aid.
		Goal	30%	

Common note：

*1 The "release threshold" is minimum levels for the first data release at one year from launch. The "standard" and "research" accuracies correspond to full- and extra success criteria of the mission respectively. Accuracies are shown by RMSE basically.

Land note:

*L1 Defined with land reflectance~0.2, solar zenith<30deg, and flat surface. Release threshold is defined with AOT@500nm less 0.25

Atmosphere note:

*A1 Comparison with in-situ observation on monthly 0.1-degree
*A2 Vicarious val. on sea surface and comparison with objective analysis data
*A3 Inter comparison with airplane remote sensing on water clouds of middle optical thickness
*A4 Release threshold is defined by vicarious val with other satellite data (e.g., global monthly statistics in the mid-low latitudes)
*A5 Comparison with cloud liquid water by in-situ microwave radiometer
*A6 Comparison with optical thickness by sky-radiometer (the difference can be large due to time-space inconsistence and large error of the ground measurements)
*A7 Estimated by experience of aerosol products by GLI and POLDER

Chapter 5 **Data Providing Service**

In principle, GCOM-C/SGLI products are provided through G-Portal (Globe Portal System: https://gportal.jaxa.jp/gpr/). G-Portal is a portal system to provide all earth observation satellite data processed at/provided by JAXA, and GCOM-C/SGLI standard products and near-real time products are provided through this system to users via internet. For details such as data search or ordering of GCOM-C/SGLI products, please refer to G-Portal User's Manual.

https://gportal.jaxa.jp/gpr/assets/mng_upload/COMMON/upload/GPortalUserManual_en.pdf

5.1 **Product Provision Policy**

GCOM-C products are available to users shown in 5.1.1 For details of the right or usage condition of GCOM-C data, please refer to "GCOM-C Data Distribution Policy."

5.1.1 **User Categories**

Users are categorized into alliance organizations or general users as shown below. The data categories available for users are shown in Table 5-1.

(1) Alliance Organizations

Organization and researcher contributing to calibration and validation of GCOM-C/SGLI and research of climate change.

Organization and researcher adopted in research announcement (RA)

Organization owning weather forecast and climate model.

Organization verifying the utility of using the information of fishing, oceanographic condition and sea route management etc.

(2) General Users

General users other than the above.

Table 5-1 Provision of GCOM-C/SGLI Products

	Level1A Product	Level1B Product	Level2 Product	Level3 Product
Alliance organization	Standard	Standard / Near-real time	Standard /Near-real time	Standard
General user (*)	Standard	Standard	Standard	Standard

(*) JAXA screens the application for "special user" submitted by a user and makes near-real time products available for the users JAXA approves.

5.1.2 **Product Provision Procedure**

G-Portal has a storage area from which users can obtain the latest data. The storage area and the storage period of the latest product and near-real time product are shown in Table

5-2. The storage period may be modified for each product. In addition, the access authority of near-real time products is as shown in Table 5-1. Products outside of the storage period can be obtained by order within the range of generation management. Ordered products such as trimming/format conversion etc. are also provided via G-Portal.

Table 5-2 G-Portal Product Storage Area/Storage Period (Real time Storage)

<table>
<tr><th colspan="2">Product</th><th>G-Portal Storage Area</th><th>Storage Period</th></tr>
<tr><td colspan="2">Standard Level1A</td><td rowspan="6">For latest product</td><td>31 days</td></tr>
<tr><td colspan="2">Standard Level1B</td><td>31 days</td></tr>
<tr><td rowspan="3">Standard Level2</td><td>Scene</td><td>31 days(*1)</td></tr>
<tr><td>Tile</td><td>Entire period</td></tr>
<tr><td>Global</td><td>Entire period</td></tr>
<tr><td colspan="2">Standard Level3</td><td>Entire period</td></tr>
<tr><td colspan="2">Near-real time level1B</td><td rowspan="2">For near-real time product</td><td>7 days</td></tr>
<tr><td colspan="2">Near-real time level 2</td><td>7 days</td></tr>
</table>

(*1) Some types of the scene produdts are stored over an entire period.

5.1.3 Processing Version

JAXA releases GCOM-C/SGLI data after maintaining the algorithm of GCOM-C continuously and carrying out trial process and calibration/validation using SGLI data. The version 1 of processing algorithms is given GCOM-C/SGLI product are released. After the first data release, the algorithm version will be updated every 1.5 years for better product accuracy.

Upon re-processing along with such upgrade, products with different processing version may be generated in the same sensor/period/obsevation area. Since the products processed by the latest algorithm are provided as a general rule (refer to 5.1.4 for generation management), it is necessary to pay attention to the processing version when obtaining and referring to data. Each processing version can be identified by the product version given to the file name (granule ID). Please refer to Table 4-3, Table 4-10, and Table 4-11 for granule ID.

5.1.4 Generation Management of Products

Only 1-generation management, which is the latest generation management, is the basic concerning GCOM-C products of G-Portal. However, GCOM-C re-processing is planned for every predetermined period backward and thus there is a period in which the second generation exists in a phased manner.

5.1.5 **Terms of Use**

For the details of data provision policy and handling of personal information of G-Portal,

please refer to JAXA's site policy (http://www.jaxa.jp/policy_j.html).

5.2 **User Tool**

SGLI user tool is provided for users. The user tool is distributed for free of charge basically, and individual user support for the tool is not provided as the online help etc. is prepared. The tool is available at G-Portal. Table 5-3 shows the overview of the user tool functions. Please refer to "SGLI User Tool Instruction Manual" for more details.

Table 5-3 SGLI User Tool Function

Function	Description
Image Display	Obtains observation data and latitude/longitude information from SGLI products, and displays the image on the screen by the projection method corresponding to the product.
Zoom In/Out/Transfer	Zooms in/out the specified point in the image displayed on the map.
Data triming	To the image displayed on the map, outputs the area specified by mouse operation in the supported file format by using the format conversion function.
Format Conversion	Outputs the data of the specified area of the product displayed on the map in the following file formats: ・Binary format ・CSV format ・KML (KMZ) format ・Image format (JPEG, TIFF, BMP, PNG) ・GeoTiff format ・NetCDF format ・HDF5 format
Movie File Conversion	Obtains SGLI product and outputs as a movie file (AVI format/KML (KMZ) format /MPEG2 format).
Annotation Display	Displays the meta information stored in the product displayed on the map. Also, displays the product information (channel, observation time; only for a case of single channel display) and latitude/longitude (and observation value) at the position of the image specified by mouse operation at the bottom frame of the screen.
Help	By menu operation, displays the document describing the user tool operation and FAQ.
Batch Processing Function	Records the operation by the user tool and outputs it as the command history and executes the command as a batch processing by reading and executing the command history.

5.3 **I/O Toolkit**

SGLI product I/O toolkit (SGTK：SGLI Toolkit) is provided for users to enable the use of C language or Fortran language programs. SGTK is used for easy access to SGLI product data of HDF. This tool is available at G-Portal. For details of installation and usage, please refer to "SGLI product I/O Toolkit Instruction Manual".

Annex 1 Acronyms

Acronyms	Description
ALOS	Advanced Land Observing Satellite
AMSR2	Advanced Microwave Scanning Radiometer 2
ADEOS	ADvanced Earth Observing Satellite
ADEOS-Ⅱ	ADvanced Earth Observing Satellite -Ⅱ
AOCS	Attitude and Orbit Control Subsystem
APID	Application Process IDentifier
ASD	APID Sorted Data
ASP	Analog Signal Processor
AT	Along Track
ATBD	Algorithm Theoretical Basis Documents
AVNIR-2	Advarced Visible Near Infrared Radiometer 2
BiRS	Bi-directional Reflectance Simulator
BRDF	Bidirectional Reflectance Distribution Function
CAPCOM	Comprehensive Analysis Program for Cloud Optical Measurements
CCD	Charge Coupled Device
CCE	Cooler Control Electronics
CDA	Cooler Dewar Assembly
CLAUDIA	CLoud and Aerosol Unbiased Decision Intellectual Algorithm
CT	Cross Track
DEM	Digital Elevation Model
DISORT	DIScrete Ordinate Radiative Transfer
DM	Deployment Monitor subsystem
DSNU	Dark Signal Non-Uniformity
DSP	Digital Signal Processor
EearthCARE/CPR	Earth Clouds, Aerosols and Radiation Explorer/Cloud Profiling Radar
ELU	ELectronic Unit
EORC	Earth Observation Research Center
EPS	Electrical Power Subsystem
EQA	sinusoidal EQual Area
EQR	EQuiRectangular
ESA	Earth Sensor Assembly
EVI	Enhanced Vegetation Index
FAPAR	Fraction of Absorbed Photosynthetically Active Radiation

FFT	Fast Fourier Transform
FLiES	Forest Light Environmental Simulator
GCOM	Global Change Observation Mission
GCOM-C	Global Change Observation Mission - Climate
GCOM-W	Global Change Observation Mission - Water
GCP	Ground Control Point
GEOSS	Global Earth Observation System of Systems
GLI	GLobal Imager
GN	Ground Network system
GOSAT	Greenhouse gases Observing SATellite
GOSAT-2	Greenhouse gases Observing SATellite-2
GPM/DPR	Global Precipitation Measurement/Dual-frequency Precipitation Radar
G-Portal	Globe Portal system
GPS	Global Positioning System
GPSR	GPS Receiver
GTS	Global Telecommunication System
HCE	Heater Control Electronics
HDF	Hierarchcal Data Format
HK	House Keeping
HPLC	High Performance Liquid Chromatography
IFOV	Instantaneous Field Of View
IOP	Inherent Optical Properties
IPCC	Intergovernmental Panel on Climate Change
IRS	InfraRed Scanning radiometer
IRS-ELU	IRS Electronic Unit
IRS-SRU	IRS Scanning Radiometer Unit
ISCCP	International Satellite Cloud Climatology Project
I-ASP	IRS Analog Signal Processor
I-DSP	IRS Digital Signal Processor
JAXA	Japan Aerospace Exploration Agency
KSAT	Kongsberg Satellite Services AS
LAI	Leaf Area Index
LED	Light Emitting Diode
LST	Land Surface Temperature
LUT	Look-Up Table
MDHS	Mission Data Handling Subsystem
MDR	Mission Data Recorder

MLI	Multi Layer Insulation
MODIS	MODerate resolution Imaging Spectrometer
NAP	Non-algae particles
NASA	National Aeronautics and Space Administration
NASA/GSFC	NASA Goddard Space Flight Center
NDBC	National Data Buoy Center
NDSI	Normalized Difference Snow Index
NDVI	Normalized Difference Vegetation Index
NIR	Near InfraRed
NP	Non Polarized
NP-ASP	Non Polarized Analog Signal Processor
OB	Optical Black
OCTS	Ocean Color Temperature Scanner
PCD	Payload Correction Data
PD	Photo Diode
PDL	Solar Array Paddle Subsystem
PGCP	Precise Geometric Correction Parameter
PL	PoLarized
PL-ASP	PoLarized Analog Signal Processor
POL	POLarization
PS	Polar Stereographic
RA	Research Announcement
RCS	Reaction Control Subsystem
RMS	Root Mean Square
SDI	ShaDow Index
SGLI	Second-generation Global Imager
SMCU	Scan Motor Control Unit
SNR	Signal to Noise Ratio
SRU	Scanning Radiometer Unit
SSA	Single Scattering Albedo
SST	Sea Surface Temperature
STR	Structure Subsystem
STT	Star Tracker
SWIR	Short Wave InfraRed
S-ANT	S-band Antenna
TAI	International Atomic Time
TCS	Thermal Control Subsystem

TIR	Tharmal InfraRed
TT&C	Telemetry, Tracking and Command Subsystem
UT	Universal Time
UTC	Coordinated Universal Time
VNR	Visible and Near Infrared Radiometer
VNR-ELU	VNR ELectronic Unit
VNR-SRU	VNR Scanning Radiometer Unit
VRI	Vegetation Roughness Index
V-DSP	VNR Digital Signal Processor
WGS84	World Geodetic System 1984
X-ANT	X-band ANTenna

Annex 2 Related Information

Annex 2.1 Bibliography

(1) GCOM-C Climate Change Observation Satellite (Briefing document) (Japanese)
(2) SGLI Level 1 Product Format Description
(3) SGLI Higher Product Format Description
(4) SGLI Algorithm Theoretical Basis Documents (Japanese)
(5) SGLI Level 1 Implementation Processing Document (Japanese)
(6) Level 2 & Level 3 Algorithm Theoretical Basis Documents
(7) SGLI User Took Instruction Manual
(8) G-Portal Earth Observation Data and Information System User Manual
(9) GCOM-C Data Distribution Policy
(10) SGLI Products I/O Toolkit Instruction Manual
(11) SGLI Characrerization Guide (Japanese)

Annex 2.2 Relevant Website

■ JAXA's site

(1) JAXA website

http://global.jaxa.jp/

(2) Global Change Observation Mission – Climate "SHIKISAI" (GCOM-C) Webpage

http://global.jaxa.jp/projects/sat/gcom_c/

(3) GCOM-C/EORC

https://suzaku.eorc.jaxa.jp/GCOM_C/index.html

■ Overseas Site

(1) HDF Homepage

http://www.hdfgroup.org/

Annex 2.3 Contact Inforation

Please contact the following for data provision and user handbook information.

2-1-1, Sengen, Tsukuba-city, Ibaraki 305-8505, Japan
National Research and Development Agency Japan Aerospace Exploration Agency
Earth Observation Data and Information System (G-Portal) Support Office
E-mail：z-gportal-support[*]ml.jaxa.jp
(Note) Please change [*] to @.